2016-06-01

Glutamic Acid Resorcinarene-based Molecules and Their Application in Developing New Stationary Phases in Ion Chromatography

Tayyebeh Panahi
Brigham Young University

Glutamic Acid Resorcinarene-Based Molecules and Their Application in Developing New Stationary Phases in Ion Chromatography

Tayyebeh Panahi

A dissertation submitted to the faculty of
Brigham Young University
in partial fulfillment of the requirements for the degree of

Doctor of Philosophy

Roger G. Harrison, Chair
John D. Lamb
David V. Dearden
Richard K. Watt
Matt A. Peterson

Department of Chemistry and Biochemistry

Brigham Young University

June 2016

ABSTRACT

Glutamic Acid Resorcinarene-Based Molecules and Their Application in Developing New Stationary Phases in Ion Chromatography

Tayyebeh Panahi
Department of Chemistry and Biochemistry, BYU
Doctor of Philosophy

Resorcinarenes can be functionalized at their upper and lower rims. In this work, the upper rim of a resorcinarene was functionalized with glutamic acids and the lower rim was functionalized with either methyl or undecyl alkyl groups. The cavitands were characterized by nuclear magnetic resonance (NMR), mass spectrometry (MS), UV-vis spectroscopy, dynamic light scattering (DLS) and electron microscopy. The binding of resorcinarene with amine guests was studied in DMSO by UV-vis titration. The obtained binding constants (K values) were in the range of 12,000-136000 M^{-1}. The resorcinarenes were shown to form aggregates in a variety of solvents. The aggregates were spherical as confirmed by DLS, SEM and TEM experiments. Dynamic light scattering (DLS) experiments revealed the size of the aggregates could be controlled by cavitand concentration, pH, and temperature.

The resorcinarene with undecyl alkyl group were adsorbed onto 55% cross-linked styrene-divinylbenzene resin to prepare a new stationary phases for ion chromatography (IC) columns. The new column packing material was applied in determination of uremic toxins and water contaminants. The new IC column afforded separation of the five uremic toxins : guanidinoacetic acid, guanidine, methylguanidine, creatinine, and guanidinobenzoic acid in 30 minutes. Detection and quantification of uremic toxins helps diagnose kidney problems and start patient care. Gradient elutions at ambient temperature with methanesulfonic acid (MSA) as eluent resulted in detection levels in water from 10 to 47 ppb and in synthetic urine from 28 to 180 ppb. Trace levels of creatinine (1 ppt) were detected in the urine of a healthy individual using the columns.

The new IC stationary phase separated cationic pharmaceuticals including a group of guanidine compounds in surface water. Detection limits in the range of 5 - 32 μg L^{-1} were achieved using integrated pulsed amperometric detection (IPAD) for guanidine (G), methylguanidine (MG), 1,1-dimethylbiguanidine (DMG), agmatine (AGM), guanidinobenzoic acid (GBA) and cimetidine (CIM). Suppressed conductivity (CD) and UV-vis detection resulted in limits of detection similar to IPAD, in the range of 1.7 - 66 μg L^{-1}, but were not able to detect all of the analytes. Three water sources, river, lake, and marsh, were analyzed and despite matrix effects, sensitivity for guanidine compounds was in the 100 μg L^{-1} range and apparent recoveries were 80-96 %. The peak area precision was 0.01 - 2.89% for IPAD, CD and UV-vis detection.

Keywords: resorcinarene, binding constant, aggregates, ion chromatography, uremic toxins, detection limit, guanidines, separation

ACKNOWLEDGEMENTS

During my time at Brigham Young University, I have had the opportunity to work with some extremely talented and magnificent colleagues. I would first like to thank Dr. Roger G. Harrison for accepting me into his lab and providing me with the guidance, mentorship, motivation and support. I would also like to thank Dr. John Lamb for his generosity in providing guidance and necessary resources for conducting part of this research. I would also like to thank my committee members for their time, willingness to mentor and advising me on specific projects: Dr. David Dearden, Dr. Richard Watt and Dr. Matt Peterson. I am also very appreciative of the material, financial support and technical cooperation and friendship from Thermofisher Scientific Inc. Especially, I acknowledge Chris Pohl and Andy Woodruff.

I would like to thank everyone that has helped me with my studies. Undergraduate students who devoted a lot of time in the lab and helped me through my projects especially Holly Anderson, Douglas Weaver, and Spencer Krieger. I would also like to thank everyone who helped me outside of the laboratory: Dr. Wood for giving me the opportunity to be a teaching assistant for different classes and laboratories; Michael Standing and Dr. Jeffrey Farrer at the Electron Microscopy Facility, for helping me with the microscopes. I would also like to thank the Department of Chemistry and Biochemistry and BYU Graduate Studies for honoring me with several awards including a graduate research fellowship award that helped fund my research.

I would like to thank my family for their support over the past few years. My husband, Nima Momtahan, for his unconditional love, support, and resolute understanding during the long, and instable hours spent in the lab. My parents, Mohammad-Reza and Shahla, and my siblings,

Reza, Sona and Hamid, for their love and understanding of my strange schedule, which often caused me to be out of contact for a long while.

In the end, I would like to thank The Church of Jesus Christ of Latter-day Saints, which supports BYU financially and spiritually. BYU, throughout the university has provided me the perfect atmosphere for growing spiritually and maturing mentally and I appreciate that.

TABLE OF CONTENTS

LIST OF FIGURES

LIST OF TABLES

LIST OF SCHEMES

Chapter 1 Resorcinarene-Based Molecules and Their Application to Ion Chromatography

Abstract

The synthesis of resorcinarene-base molecules and their application in ion chromatography techniques are reviewed in this chapter. Macrocyclic resorcinarene molecules are synthesized by condensation of resorcinol (1,3-dihydroxybenzene) and different aldehydes. Resorcinarenes can be modified with various substituents on their upper and lower rims to provide specific functionality and selectivity. These various derivatives have applications in supramolecular recognition, nanoscale reaction containment, catalysis, chiral NMR shift agents, and chromatographic separations, as well as drug encapsulation, protection, and delivery. The stationary phase of different separation techniques such as HPLC, GC, and IC can be modified by resorcinarene derivatives. Two classes of IC columns including cation and anion exchange were designed and applied in separation of transition metals, biological compounds and pharmaceuticals. Electrochemical and conductivity detectors have been used widely in analysis of pharmaceutical and biological compounds with IC. The broad applications of resorcinarene-based molecules show that they are a promising class of compounds. Therefore, synthesis and their separation applications are explored.

Keyword: Resorcinarene; Derivatives; Separation; Ion chromatography; Detectors.

1. Introduction

A resorcinarene is a macrocyclic molecule that arises from the condensation of resorcinol (1,3-dihydroxybenzene) and various aldehydes.[1] Resorcinarenes have been used industrially since the 1930s, when the products of resorcinol-aldehyde condensation reactions were found to

enhance the resistance of adhesives and paste.[2] Later, in the 1940s, Niederl and Vogel published several studies using elemental analysis techniques on the condensation reaction between aliphatic aldehydes and resorcinol, which resulted in the proposed cyclic tetrameric structure in Figure 1 (R_1 = alkyl).[3] Full characterization of the resorcinarene molecule was accomplished by Högberg and coworkers later in the 1980s using X-ray crystallography and NMR spectroscopy.[1,4] In 1982, Cram and his coworkers, gave the name cavitand to this class of the compounds[5]; this name came from the concave cavity shape of the molecule, which was sufficiently large to accommodate other molecules and ions.

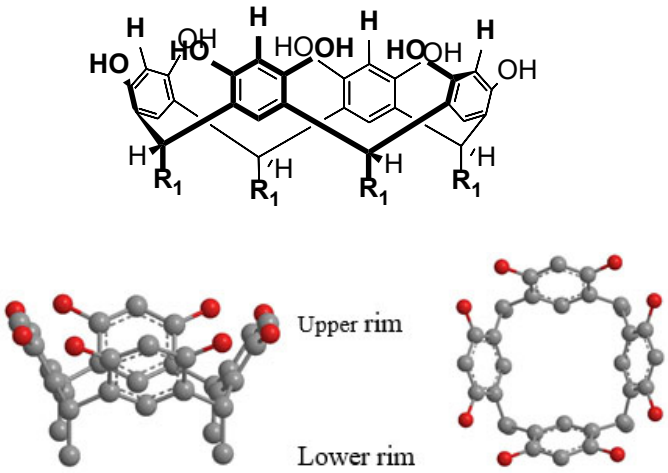

Figure 1 (a) Structure of the first synthesized resorcinarene[3]; molecular models of resorcinarene (b) side view; (c) top view. R_1 = alkyl.

Hydroxyl groups on the upper rim of the resorcinarenes make them vulnerable to electrophilic aromatic substitution reactions. In addition, the adjustable ring size and changeable lower rim have assisted chemists in designing a wide range of resorcinarene derivatives. These various derivatives have applications in supramolecular recognition, nanoscale reaction

containment, catalysis, chiral NMR shift agents, and chromatographic separations, as well as drug encapsulation, protection, and delivery.[6–11]

Most of the earliest cavitands were shallow, bowl-shaped structures and prepared from resorcinarenes through alkylation, silylation, or a one-step derivatization with the aryl group of the phenolic hydroxyls.[12–14] These cavitands were limited by their dimensions (ca. 9.0 Å wide and 3.0 Å deep) and were only able to interact with small molecules. However, due to the simplicity of their synthesis, they have been used extensively in many areas. For example, a shallow water-soluble cavitand was used (Figure 2, a and b) as an efficient catalyst for the hydrolysis of esters of phosphate acids[15] (a) and inverse phase-transfer[16] (b). The phase-transfer catalyst can carry out the Mannich-type reactions in water without the need for any added surfactants or organic solvents.[16] The resorcinarene derivative can afterward be recovered in aqueous solution and recycled after the simple extraction of the water-insoluble products.

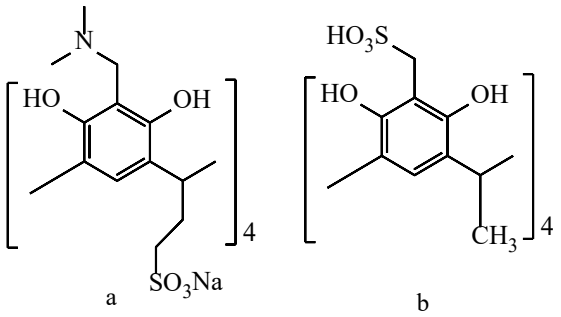

Figure 2 Water-soluble calixarene sulfonic acid. Shallow resorcinarene cavitand as an efficient catalyst for the hydrolysis of esters of phosphate acids[15] (a) and inverse phase-transfer[16] (b).

There is a wide range of applications for shallow resorcinarenes with different functional groups on the upper rim or lower rim; we have limited this text to more recent applications. For instance, a recent report showed the application of a newly synthesized resorcinarene (tetra-methoxy resorcinarene tetra-hydrazide) as a reducing and capping agent for the synthesis of water-dispersible stable palladium nanoparticles.[17] These derivatives of resorcinarene hydrazide function as reducing and stabilizing agents.

Another type of shallow cavitand with interesting applications was introduced by Wenzel et al.[11,18,19] They synthesized a water-soluble shallow cavitand with a chiral functional group on the upper rim and a sulfonic group on the lower rim (the presence of an ionic group on the lower rim assists in enhancing the polarity of the cavitand in aqueous conditions). Using these shallow cavitand derivatives, they conducted successful studies in chiral recognition. The introduction of chirality to resorcinarene cavitands opened a new and important path in the separation of small, hydrophobic chiral molecules, which we describe later in more detail.

Later work built up the rims of the resorcinarene and deepened the cavities (a depth of ~8.0 Å). Deeper cavitands are capable of housing more sizable guests and have been extensively applied in host-guest studies. One method of synthesizing a deeper cavitand has been through the condensation of the resorcinarene hydroxyl groups with a 6,7-disubstituted-2,3-dichloroquinoxaline.[20] An alternative method involves the use of a simpler building block in the bridging reaction followed by extension of the rim through heterocyclic synthesis. The cavitands in Figure 3 (a) are usually prepared by bridging the resorcinarene hydroxyl groups with a preformed heterocycle, e.g., condensation with a 6,7- disubstituted-2,3-dichloroquinoxaline.

Even later, a deeper cavitand (Figure 3(b)) was introduced, obtained by reaction of octanitrocavitand with phenylenediamine units and condensation with 1,2-diketones. The

resulting fused pyrazines provide the deepened cavities. Acenaphthenequinone formed another type of deep cavitand, which was also utilized to construct helicates and extended surfaces.[21,22] (Figure 3 (c))

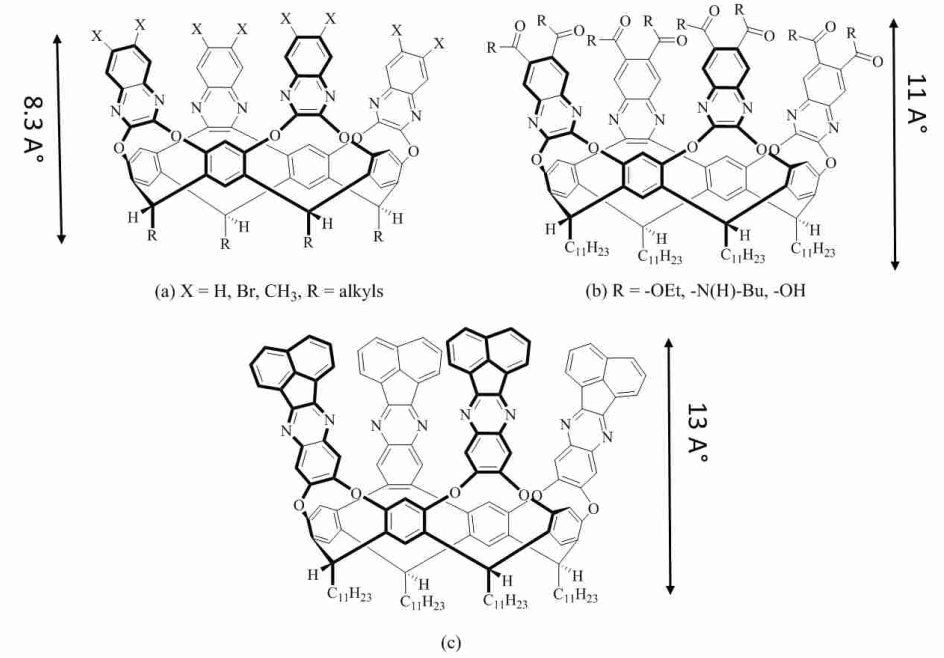

Figure 3 The structure of deepened cavitands, a: bridging with 6,7- disubstituted-2,3-dichloroquinoxaline, b) elongated with a reaction of octanitrocavitand with phenylenediamine units and condensed with 1,2-diketones c) bridging with acenaphthenequinone.[21,22]

Recently, another type of a deep cavitand with two major components, the resorcinarene scaffold and the quinoxoline panels, was introduced by our group.[23] The upper rim of a new resorcinarene molecule was elongated with four identical substituents of alanine and glycine groups, and the lower rim functionalized with methyl or undecyl alkyl chains. (Figure 4)

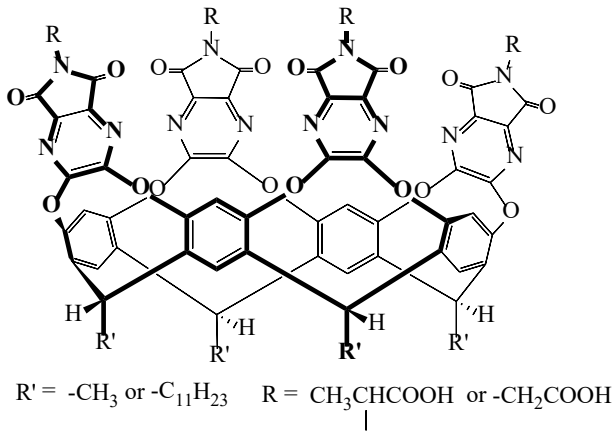

Figure 4 Alanine and glycine derivativatized resorcinarene molecule with methyl and undecyl chains at the lower rim.[23]

Another class of deep cavitand consists of capsules created by covalent or non-covalent binding between two or more resorcinarenes.[24–26] Encapsulation enables rigorous control of the environment and housing of molecules isolated from solvent at ambient temperatures in the liquid phase. In either conformation (cavitands or capsules) molecules in the confined space respond to the size, shape and chemical environment of the container. This provides a unique way for separation of small to large molecules from the solvent environment.

As mentioned earlier, introducing chirality to resorcinarene derivatives has been investigated by scientists during recent years. Chirality in resorcinarene derivatives is rare; however, it has been achieved by two primary methods. The first method, inherent chirality, refers to resorcinarene molecules with all achiral substituent groups in their structure.[27–29] One of the earliest C_4-symmetric inherently chiral resorcinarenes was obtained by substitution of one of the hydroxyl groups at each ring with a methoxy group to separate the enantiomers. Theses chiral hosts were shown to discriminate between enantiomeric guests (Figure 5).[30]

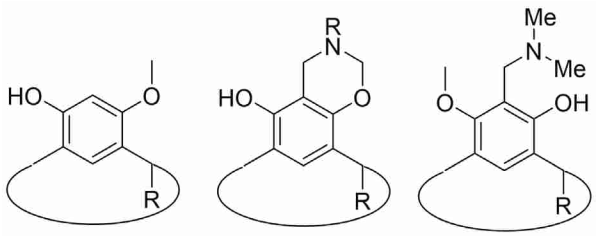

Figure 5 Inherently chiral C_4-symmetric resorcinarenes.[30]

The second method involves the attachment of one or more enantiomerically chiral groups to the molecule; this is the focus of our study.[23,31–33] Chiral groups are introduced on the upper rim or through substitution at the aryl hydrogen atom between the two hydroxyl groups of the resorcinarene bowl. Enantiomerically-pure groups have been bonded to shallow and deep cavitands to provide chirality and both cases showed successful chiral discrimination in reported research.[31-33]

One recent report on introducing chirality to shallow cavitands involves using eight fluorenylmethoxycarbonyl (Fmoc) derivatized alanine units surrounding the opening of the cavity. (Figure 6) The binding of pinanediol as a guest molecule was demonstrated with ^{1}H NMR, and the cavitand was shown to undergo a slow exchange of bound and unbound forms in acetone-d_6. Their studies showed the preference of chiral cavitand to bind to (-)-pinanediol rather than (+)-pinanediol, and the ^{1}H chemical shifts of the bound enantiomers were considerably different.[32]

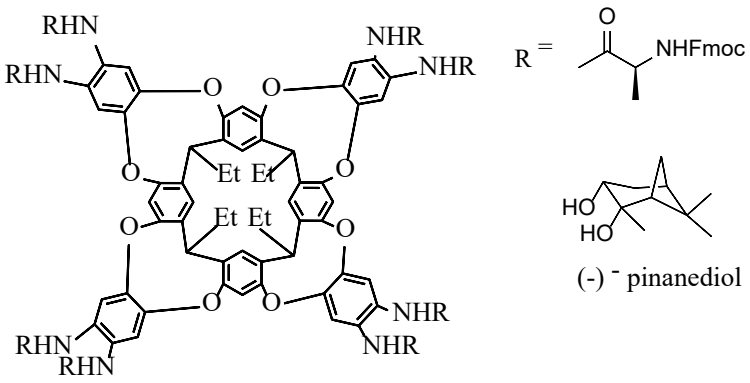

Figure 6 Chiral shallow cavitand and (-)-pinanediol. Chiral cavitand prefers to bind to (-)-pinanediol rather than (+)-pinanediol.[32] (Et = ethyl)

Another class of shallow cavitands with chiral functional groups on the upper rim was designed by Wenzel et al.[34] They introduced water-soluble shallow chiral cavitands, which have been widely used in chiral recognition among enantiomers (Figure 7). The sulfonate moiety on the bridging groups at the lower rim accounts for the water solubility. Chirality was achieved by binding L-proline (a), cis-4-hydroxy-D- (b), and -L-proline (c), trans-4- hydroxy-L-proline (d), and trans-3-hydroxy-L-proline (e) to the resorcinol rings. This water-soluble resorcinarene derivative was used as a chiral NMR solvating agent for a variety of compounds.

Optically pure chiral solvating agents are often used in NMR spectroscopy for the analysis of enantiomeric purity. Association of the enantiomers with the chiral solvating agent can involve noncovalent interactions such as hydrogen bonding, dipole-dipole interactions, and π-stacking between electron-rich and electron-deficient aromatic rings. Introducing a water-soluble chiral resorcinarene has opened a new path in the separation of small, hydrophobic chiral molecules. The affinity of the hydrophobic cavity enhances the binding and the successful separation of enantiomers in an aqueous environment.

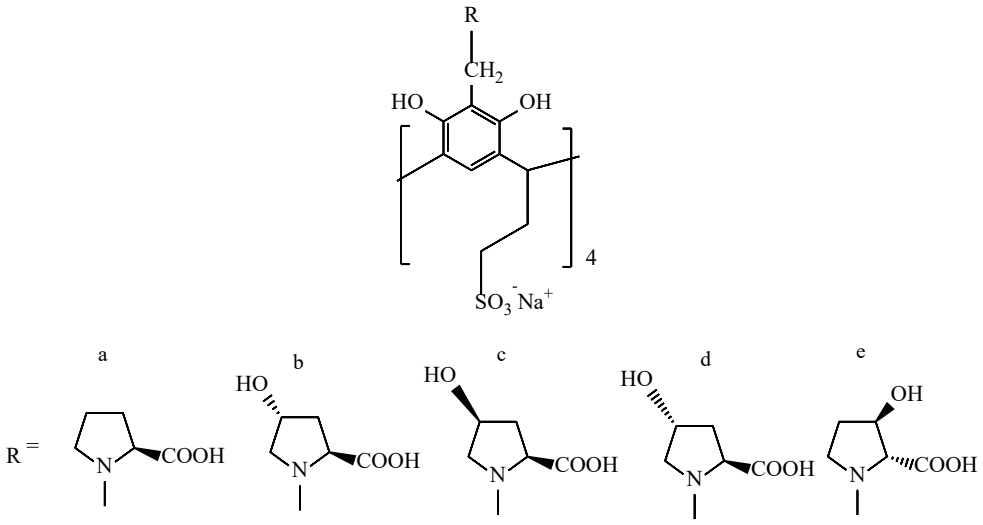

Figure 7 Water-soluble sulfonated calix[4]resorcinarenes derivatives. Chirality was achieved by bonding L-proline (a), cis-4-hydroxy-D-(b), and -L-proline (c), trans-4-hydroxy-L-proline (d), and trans-3-hydroxy-L-proline (e) to the resorcinol rings.[34]

Chirality on deeper cavitands has been achieved by bonding different enantiomerically pure compounds. Introduction of a chiral moiety through phthalimide units bridged through the hydroxyl groups of the resorcinol rings is another popular method in developing chiral resorcinarenes. Rebek et al. have studied a resorcinarene derivative with a deepened cavity in which phthalimide units bind through the hydroxyl groups of the resorcinol rings.[33] They successfully showed the enantiomeric differentiation of racemic trans-1,2-cyclohexanediol in m-xylene-d_{10}.

Our group used a similar method in the elongation of a resorcinarene molecule using phthalimide units to form a deep cavitand.[23] This cavitand was functionalized with enantiomerically pure alanine groups to introduce chirality. The presence of four carboxylic acids on the upper rim provides a potential binding site for amine groups. (Figure 4) A series of chiral amines containing a benzyl ring were chosen for binding studies. The chiral amines were

added to the acidified derivatives of the resorcinarene molecule and the signal of the amines was monitored. The changes in the chemical shift of the amines indicated the binding of chiral amines to the host molecule (resorcinarene derivatives).

Based on the polarimetry of the complexes, chiral recognition was reported for different substituents of the resorcinarene molecule. The amine substrates undergo rapid exchange and their resonances become deshielded in mixtures with the cavitand. The absence of significant shielding indicates that amine substrates are not encapsulated deep in the cavity. Instead, they undergo a neutralization reaction with the carboxylic acid group of the alanine and associate through dipole–dipole interactions. These newly designed deep resorcinarene molecules were characterized with different techniques such as nuclear magnetic resonance (NMR), mass spectrometry (MS), and the sustained *off*-resonance irradiation collision-induced dissociation (SORI-CID) technique in FTICR-MS.

2. Application of Resorcinarenes in Chromatography Techniques

The application of resorcinarenes in separation fields encompasses techniques such as high performance liquid chromatography (HPLC), gas chromatography (GC), electrokinetic chromatography (EKC), capillary electrophoresis (CE), and ion chromatography (IC) for the separation of a variety of organic and inorganic species.

2.1 High Performance Liquid Chromatography (HPLC)

Resorcinarenes have been applied to both the mobile phase and the stationary phase of HPLC.[35–40] Lipkowski et al. in 1998 used resorcinarene complexes in the mobile phase of reverse phase HPLC.[41] They showed the host–guest complexation of tetraalkylcalix[4] resorcinarene (the upper rim was modified with phosphoryl, sulfonyl and dialkylaminomethyl derivatives) with

some aromatic guests in the mobile phase. The formation of the inclusion complexes resulted in changes in the retention of aromatic guests and improved their separation.

In another example, application of resorcinarenes in HPLC techniques was reported by Pietraszkiewicz et al. in 1998, in which the RP-18 stationary phase was modified with calix[4]resorcinarene (Figure 8).[35] The lower rim of the resorcinarene molecule was derivatized with long alkyl chains, which provide enough hydrophobicity to attach to the hydrophobic surface of the resin; the resorcinarene derivative binds to the resin through hydrophobic interactions. The coated resin showed good separation of three pyrimidine bases including cytosine, uracil, and thymine.

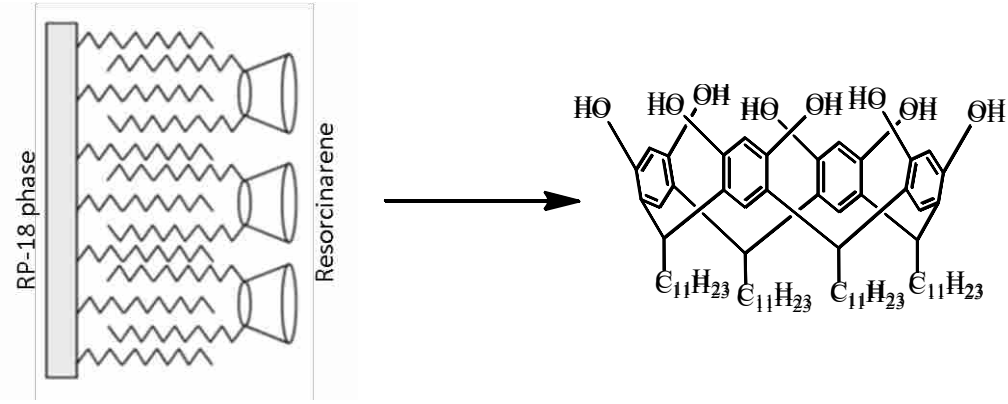

Figure 8 C-tetra-n-undecylcalix[4]resorcinarene coated RP-18 stationary phase.[35]

In 2005, Alexander Ruderisch et al. synthesized a novel silica-bonded stationary phase that was bonded covalently to a resorcinarene derivative (Figure 9).[38] They proposed a straightforward method to attach the resorcinarene to the surface of silica particles: The upper rim of the resorcinarene was modified with isopropyl isocyanate to form a polar interaction site, and the lower rim had long alkyl chains each containing a terminal double bond. The resorcinarene was then immobilized on the silica resin by a free radical-induced reaction on

mercaptopropyl-functionalized silica. The new stationary phase had improved hydrolytic stability under high aqueous conditions, higher efficiency for separation of polar analytes, and higher selectivity to low molecular weight acids.

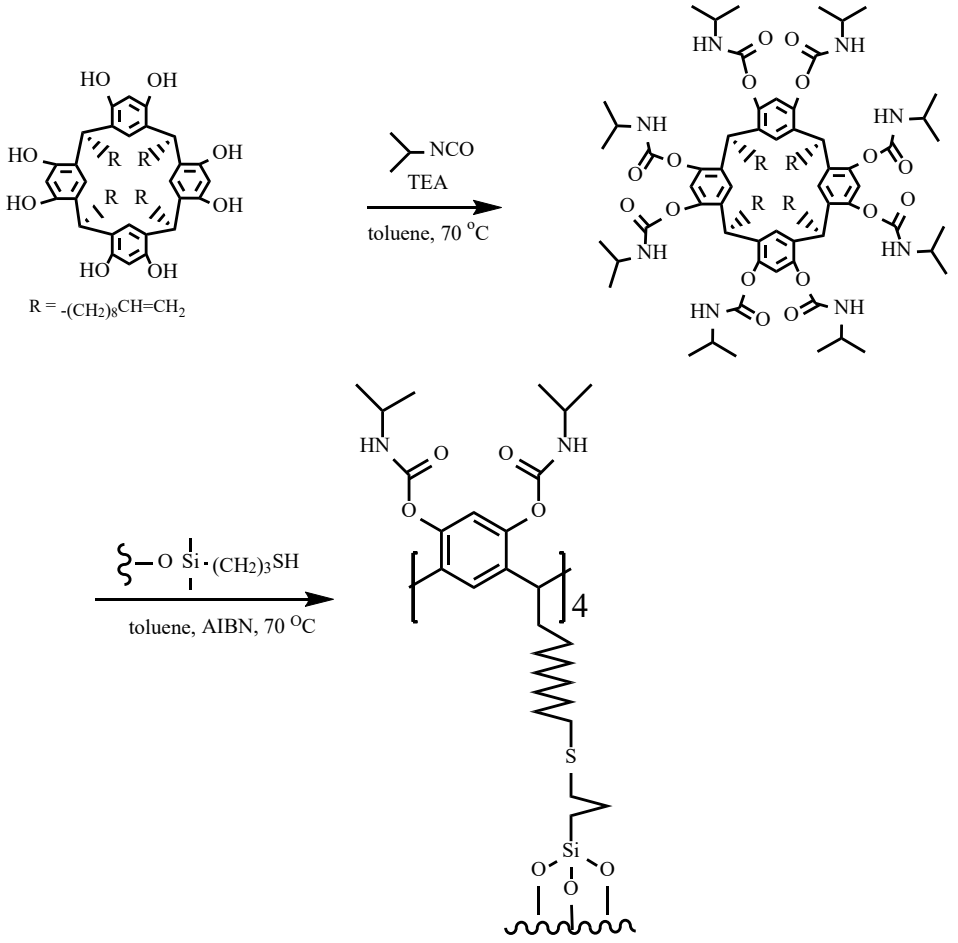

Figure 9 Synthetic pathway towards the silica-bonded and polar functionalized resorcinarene in RP-type stationary phase.[38]

More recently, in 2011, Huey Min Tan et al. showed the application of resorcinarene derivatives in the preparation of chiral stationary phases in HPLCs.[39] They synthesized two types of stationary phase, on which they immobilized two different derivatives of resorcinarene molecules. (Figure 10)

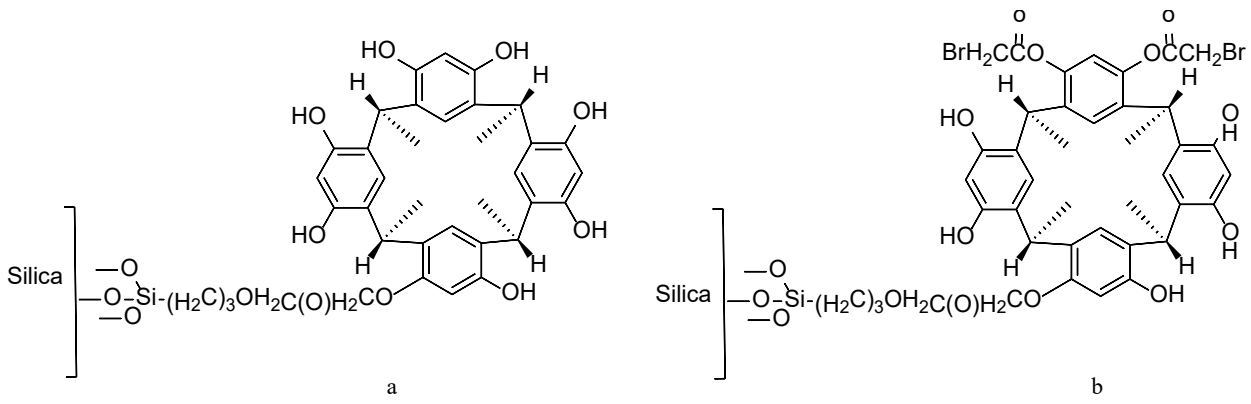

Figure 10 (3-(methylcalix[4]resorcinarene)-2-hydroxypropoxy)-propylsilyl-appended silica particles (MCR-HPS) [a] and bromoacetate-substituted MCR-HPS particles (BAMCR-HPS) [b] have been synthesized and used as chiral stationary phases for high-performance liquid chromatography (HPLC).[39]

Two newly developed stationary phases were studied for separation of several di-substituted benzenes and some chiral drug compounds. They examined both columns for separation of positional isomers of nitrophenol, using mixtures of methanol/water for the separation of isomers on both columns, and investigated the effect of methanol percentage on the separation efficiency.

Both columns were also applied to chiral separation. The BAMCR-HPS-packed column showed better chiral recognition; however, the separation efficiency was greatly influenced by the percentage of methanol. The optimum enantioseparation of 1-phenyl-1-propanol is shown in Figure 11using 4:1 MeOH/H_2O.

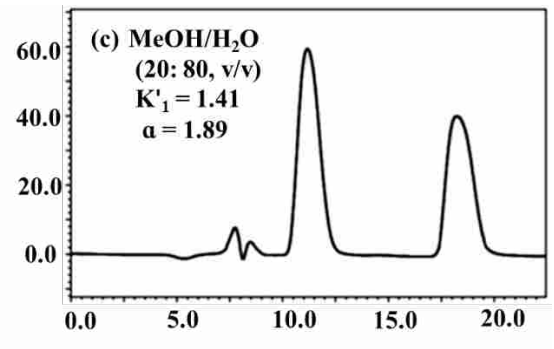

Figure 11 Enantioseparation of 1-phenyl-1-propanol on the BAMCR-HPS-packed column; the composition of mobile phase was MeOH/H_2O.[39]

In studies in 2014, Chamseddin et al. investigated calixarene- and resorcinarene-bonded stationary phases using modeling software.[42] They conducted a systematic evaluation of the applicability of DryLab (Molnár Institute, Berlin, Germany) to these types of stationary phases in the presence of conventional alkyl-bonded phases. Three types of resorcinarene-bounded stationary phases were modeled, including substituted benzene derivatives, 4-hydroxybenzoic acid esters and polycyclic aromatic hydrocarbons (Figure 12).

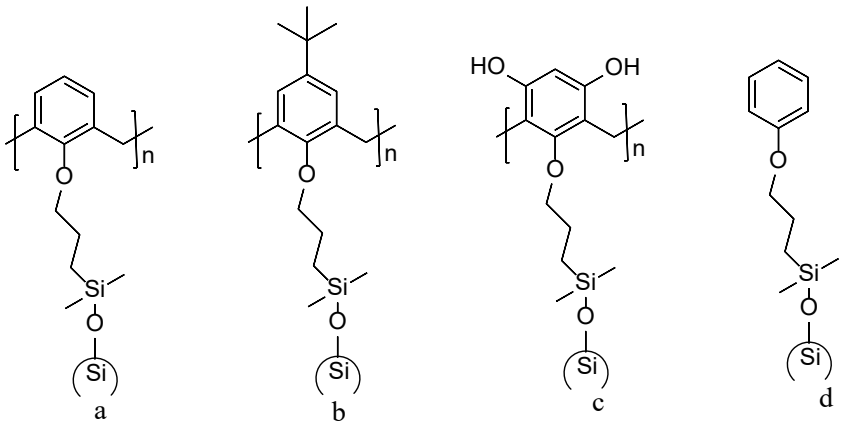

Figure 12 Resorcinarene derivatives attach to the silica stationary phase. Representative structures of stationary phases, a: calixarene A (AI: n = 4; AII: n = 6; AIII: n = 8), b: calixarene B (BI: n = 4; BII: n = 6; BIII: n = 8), c: resorcinarene (n = 4); and d: synergy polar-RP chromatographic.[42]

Three different mixtures of model analytes, consisting of alkyl-substituted benzene derivatives, 4-hydroxybenzoic acid esters, and polycyclic aromatic hydrocarbons, were used to verify the accuracy of DryLab prediction of retention times, as well as to compare the results of 20 different liquid chromatographic phases. The results showed that the prediction on the calixarene- and resorcinarene-bonded stationary phases as well as on other reversed-phase columns is highly accurate in both isocratic and gradient modes. As a result, DryLab could be applied with very accurate predictions in method development using calixarene- and resorcinarene-bonded stationary phases, which were used as an example for "new" stationary phase materials.

2.2 Gas Chromatography (GC) and Capillary Electrophoresis (CE)

The recent application of resorcinarene derivatives in GC systems has been reviewed in brief.[43–47] One of the earliest works goes back to Zhang et al. in 1997.[43] They synthesized a

resorcinarene derivative in which the lower rim was modified with pentane groups and the upper rim with phenyl groups (Figure 13). The ligand successfully coated onto a fused-silica capillary column. According to their TGA analysis, the newly designed stationary phase was thermostable to 240 °C and suitable for GC use.

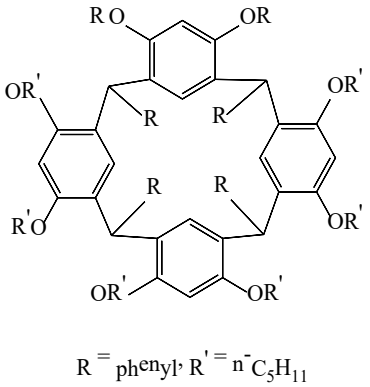

Figure 13 The structure of resorcinarene derivative stationary phase.[43]

Later, chiral resorcinarene derivatives were also introduced into GC stationary phases. Ruderisch et al. introduced an enantiomerically pure resorcinarene as a chiral stationary phase in an enantioselective capillary GC.[44] The upper rim of the resorcinarene molecule was derivatized with the chiral amino acid valine to impose chirality through a series of reactions. The presence of unsaturated functions in the long alkyl groups on the lower rim allowed the attachment of the chiral resorcinarene to a polysiloxane of the stationary phase through a catalytic reaction (Figure 14). This type of GC column successfully separated several proteinogenic D,L N(O,S)-TFA amino acid methyl esters, as shown in Figure 15.

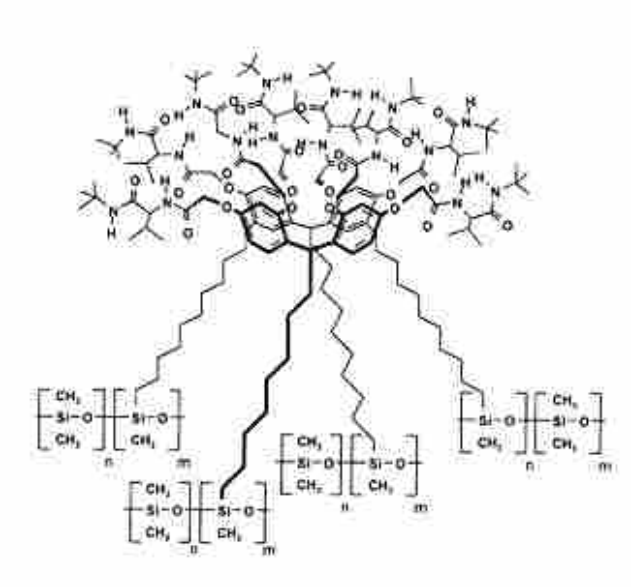

Figure 14 Structure of chiral resorcinarene derivative coated the silica-fused column in capillary GC.[44]

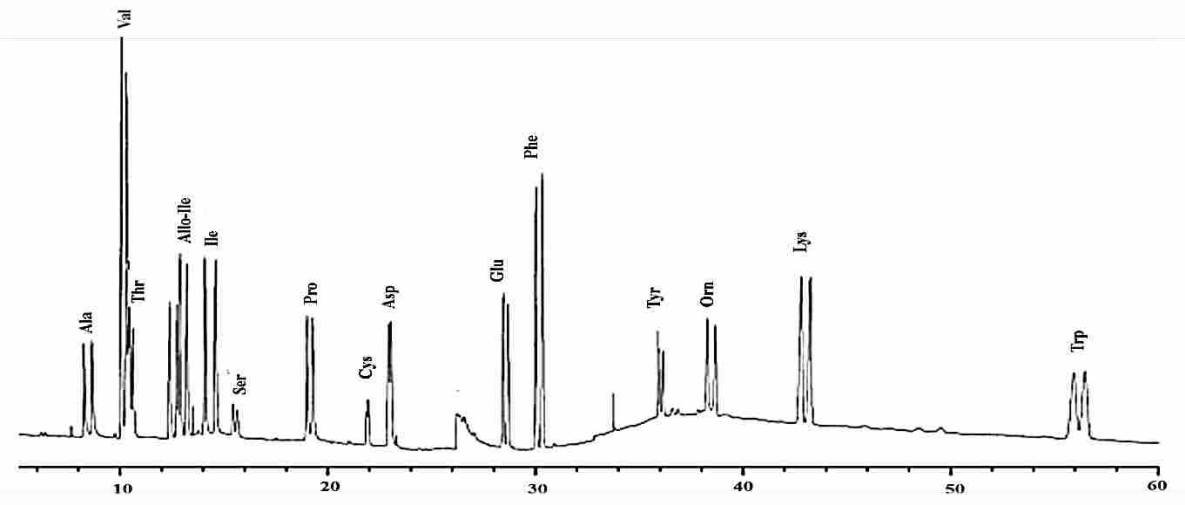

Figure 15 Gas chromatographic separation of enantiomers of 16 N(O)-trifluoroacetyl-DL-amino acid ethyl esters on a 20 m × 0.25 mm fused-silica column coated with Chirasil-Calixval-Dex (film thickness 0.25 µm). Temperature program: 70 °C (3 min); 3 °C/min; 170 °C; carrier gas: 0.5 bar hydrogen; split: 1:100.[44]

Due to the ability of resorcinarenes to form reversible complexes with charged and uncharged analytes, some applications of these molecules were investigated with electrophoretic methods.[48–53] Resorcinarene incorporation in capillary electrophoresis (CE) helps to improve the separation of neutral species. Resorcinarenes can develop a pseudo-stationary phase in CE to improve the interactions between neutral analytes and the stationary phase for better column efficiency.

Although the presence of resorcinarenes assists in achieving better separation of neutral analytes, their use is limited by the high UV-absorbance of the resorcinarene derivatives; a stronger baseline noise was observed in most investigations. Therefore, other detectors, such as electrochemical detectors, or noncovalent or covalent bonding of the resorcinarenes to the capillary wall were used to overcome these problems. Different varieties of resorcinarene derivatives have been used in CE methods, such as resorcinarene with sulfonic, carboxylic, or substituted ammonium groups. These media have been used to separate positional isomers, amines, polycyclic aromatic hydrocarbons, and organic anions.

2.3 Ion Chromatography (IC)

Our group has developed new stationary phases using resorcinarenes for IC techniques. One phase was based on a resorcinarene molecule that was modified with cyclen groups on the upper rim; and undecyl chains on its lower rim.[54,55] Stationary phases were made by adsorbing N-undecyl cyclen and cyclen–resorcinarene (cyclenbowl) onto resin (Figure 16). Research showed that the column loaded with cyclen-resorcinarene gave significantly better performance.

In addition to the investigation of this column's ability to separate common anions, this column was examined for pre-concentration of anions. The column was operated under basic

conditions. According to the pKa of cyclen (10.6), at a lower pH, the cyclen column will be protonated; at a higher pH, it will remain neutral. Therefore, the pH of the eluent adjusted the capacity of the cyclen column. Sodium bicarbonate and sodium hydroxide were used in a multistep gradient for pre-concentration of perrhenate and perchlorate ions. Figure 17 shows a separation and pre-concentration of perrhenate from six other anions.

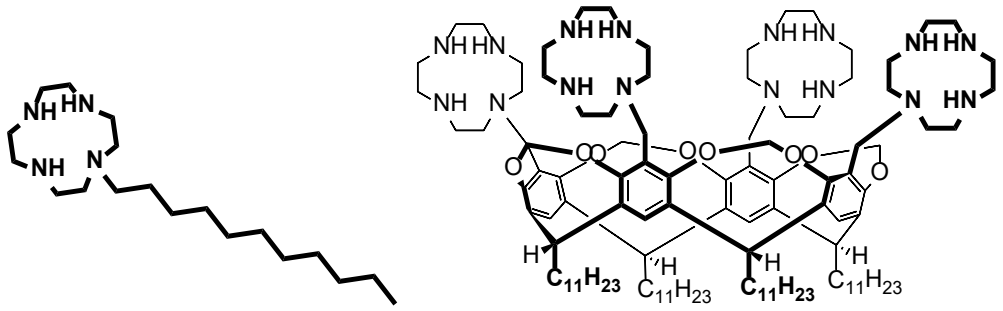

Figure 16 Structure of N-undecyl cyclen and cyclenbowl molecules.[56]

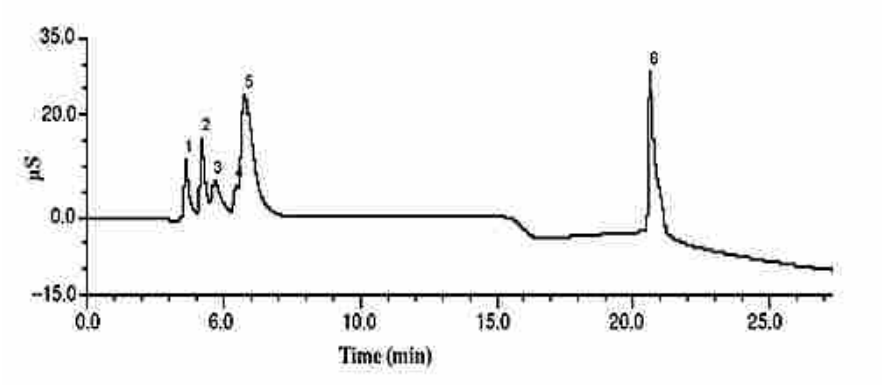

Figure 17 Pre-concentration of perrhenate on cyclen bowl column by step gradient. Peaks: 1 = F^-, 2 = Cl^-, 3 = NO_2^- , 4 = NO_3^-, 5 = SO_4^{2-} & PO_4^{3-}, 6 = ReO_4^-. A step gradient from 10 mM $NaHCO_3$ (pH 7.6–8.0) to 10 mM NaOH (pH 12) was used to accomplish the separation.[56]

A year later, in 2012, Li et al. used cyclen derivative stationary phases for the separation and pre-concentration of cations.[56] The binding strength was compared for different transition metal ions and a high binding constant of cyclen for Cu^{2+} was discovered. The separations were done under acidic conditions. Due to the pKa of the cyclen group and protonation of cyclen sites on the stationary phase, the column could be used as a cation exchange column. A multi-step gradient with nitric and oxalic acids was used for the separation of six cations, which is shown in Figure 18.

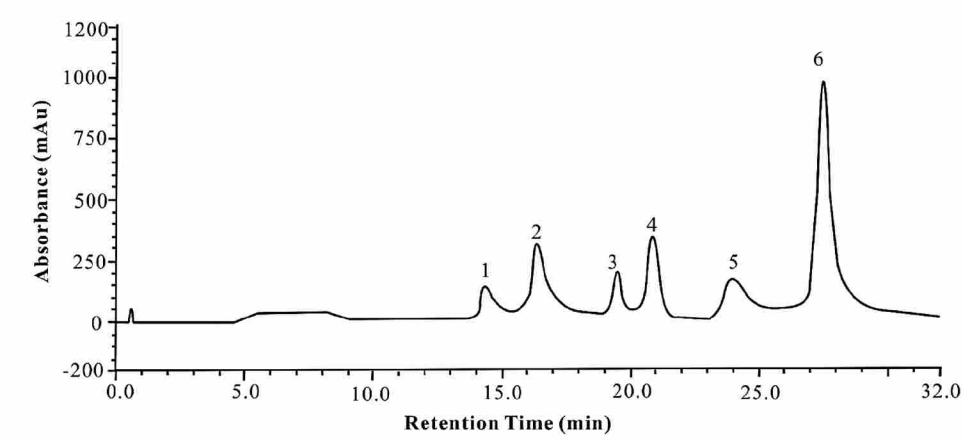

Figure 18 Separation of transition metal ions with gradient elution on the cyclenbowl column. Eluent: 2 mM oxalic acid for 10 minutes before injection; after injection, eluent step change: 0 - 10 min, 1 mM oxalic acid + 10 mM HNO_3; 10 – 32 min, 50 mM HNO_3. Peaks: 1 = Mn^{2+} (0.6 mg L^{-1}); 2 = Cd^{2+} (0.8 mg L^{-1}); 3 = Co^{2+} (0.2 mg L^{-1}); 4 = Zn^{2+} (0.2 mg L^{-1}); 5 = Ni^{2+} (0.6 mg L^{-1}); 6 = system peak. Flow rate: 0.35 mL/min.[56]

This column showed a significant selectivity for Cu^{2+} in the presence of high concentrations of matrix ions such as Mn^{2+}, Co^{2+}, Ni^{2+}, Cd^{2+}, and Zn^{2+}. The pre-concentration experiment successfully separated and pre-concentrated parts per billion levels of Cu^{2+} with a multi-step gradient using low and high concentrations of nitric acid. In order to pre-concentrate the Cu^{2+}, first a low concentration of HNO_3 (5 mM) was used to elute the mixture of Mn^{2+}, Co^{2+},

Ni^{2+}, Cd^{2+}, and Zn^{2+} while Cu^{2+} in the sample was bound more strongly to the stationary phase of the column. Several injections of 2 mL of analyte were made to the column consecutively. Second, higher concentrations of nitric acid (up to 50 mM) were used to elute the Cu^{2+} from the stationary phase (Figure 19).

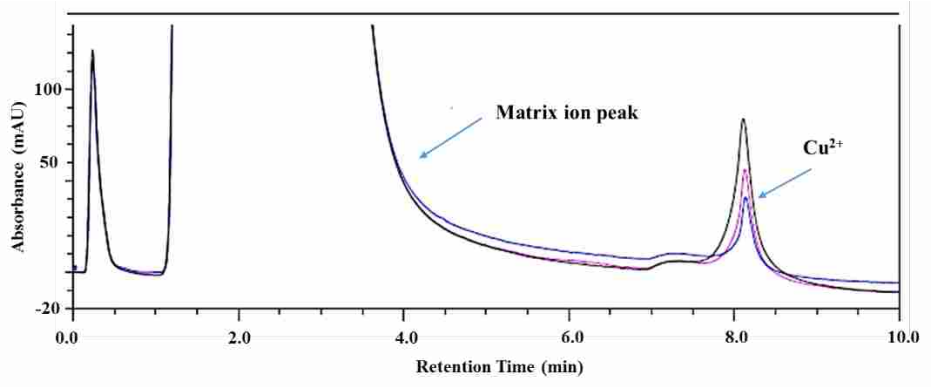

Figure 19 Preconcentration of Cu^{2+} using HNO_3 as eluent. Mixture of analytes: Mn^{2+}, Co^{2+}, Ni^{2+}, Cd^{2+}, Zn^{2+} (1 mg L^{-1} each), and 15 µg L^{-1} Cu^{2+}. Eluent flow rate: 1.0 mL/min.[56]

Li et al. also introduced a new type of resorcinarene derivative in our group.[23] They synthesized a new resorcinarene molecule in which the upper rim was elongated with four identical substituents of alanine and glycine groups (Figure 4). The newly designed deep cavitand was applied to ion chromatography. These molecules adsorbed onto a 55% cross-linked styrene-divinylbenzene resin in preparation of an IC column. The presence of carboxylic acids on the upper rim creates cation exchange sites for IC stationary phases. They successfully used this column for the separation of six metal ions (Mn^{2+}, Co^{2+}, Ni^{2+}, Cd^{2+}, Cu^{2+}, and Zn^{2+}). The pKa value of the AUA ligand was determined by pH titration and resulted in 5.19 ± 0.08 at the

95% confidence interval. Therefore, at a lower pH, the newly packed stationary state performed as cation exchange sites.[57]

To choose the appropriate acidic eluents, a group of acids were selected, including nitric acid (HNO_3), oxalic acid, dipicolinic acid (PDCA), succinic acid, and citric acid. The separation of six metals was studied using HNO_3. Lower concentrations of HNO_3 (up to 5mM) was eluted all of the metal ions except Cu^{2+}, which showed stronger retention to the stationary phase. Higher concentrations of HNO_3 (up to 10 mM) helped the elution of Cu^{2+} from the column. According to their studies, HNO_3 was selected as the most suitable eluent due to a shorter separation time and higher resolution. The separation of all six metal ions is shown in Figure 20.

The UV-vis absorbance method was used for the detection of metal ions by recording dual wavelengths at 520 nm and 620nm. Detection of transition metals was assisted by using a 4-(2-pyridylazo) resorcinol (PAR) solution. This solution was used as a post-column reagent with the ability to bind to the metal ion analytes. The method was very sensitive for all the ions, but particularly for Cu^{2+} and Mn^{2+}.

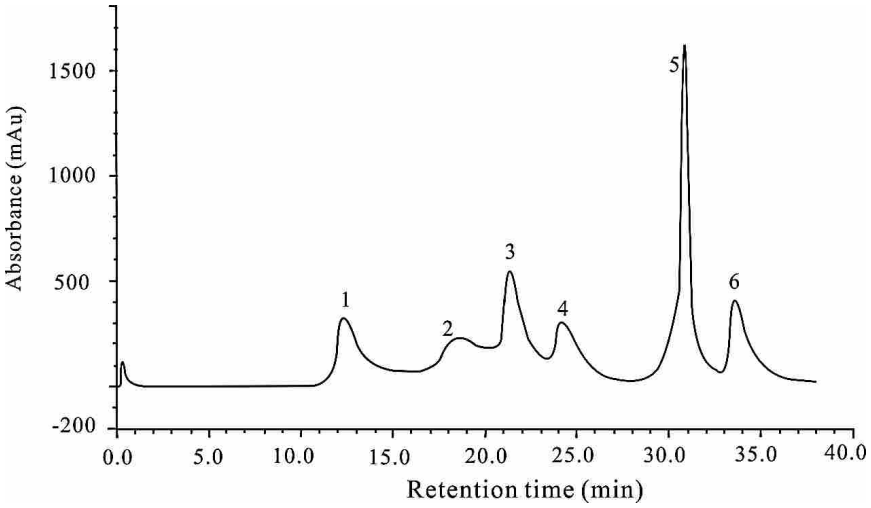

Figure 20 Separation of six transition metal ions with oxalic acid gradient on AUA column. Conditions: 10 mM HNO_3 for 10 minutes before injecting analyte, after injection, 0-24 min, 1.5 mM oxalic acid; 24-40 min, 15 mM oxalic acid. Peaks: 1 = Cu^{2+} (1.28 ppm); 2 = Ni^{2+} (1.28 ppm); 3 = Zn^{2+} (1.28 ppm); 4 = Co^{2+} (1.28 ppm); 5 = Mn^{2+} (0.32 ppm); 6 = Cd^{2+} (1.28 ppm).[57]

3. Ion Chromatography

3.1 Principles and applications

Ion chromatography (IC) has been growing in popularity since 1975 when it was introduced by Small et al.[58] This type of analysis is useful for the separation of ions, as the name suggests. IC separates compounds based on their ionic potential or electrostatic interactions with other molecules. Generally, the smaller compounds have a greater charge to size ratio and are less attracted to the column material; therefore, they interact with the column less and elute from the column more quickly. This trend might be different from traditional HPLC, which separates compounds based on their polarity. After Lee and his team in the late 1980s introduced high performance anion exchange chromatography (HPAEC) with pulsed amperometric detection

(PAD) for the analysis of mono and oligosaccharides, ion chromatography has been widely used in the biotechnology industry and academic research.[59]

Today, different kinds of IC are widely used in biological research.[60] The most predominant forms of IC are ion exchange chromatography, ion exclusion chromatography and ion paired chromatography. In ion exchange chromatography (IC), the analyte enters the mobile phase and is carried to the stationary phase, which has a charge opposite to the analyte. The analyte forms ionic bonds with the stationary phase and then is replaced or exchanged by the ions in the eluent. Two general trends are observed in ion exchange chromatography. The first trend is that the smaller the ion, the faster it elutes from the column. The second trend is that more polar compounds elute faster from the column than nonpolar compounds, due to their attraction to the mobile phase. The potential for the molecule to make ionic interaction with the stationary phase also plays a large role in the elution order of compounds. Nitrite will elute before nitrate because of the size of the molecule, but also because the nitrate has more oxygen atoms that can create ionic interaction with stationary phase.

Variations in the chemical nature of the ion-exchange functional group play an important role in the selectivity of ion exchange chromatography. Generally, two types of columns are involved in separating ionic species in ion exchange chromatography: anion exchange and cation exchange columns. A large number of excellent columns for anion and cation exchange chromatography are now available commercially. Dionex Ion Pac hydroxide-selective and carbonated-base columns are anion exchange columns that consist of a polymeric spherical material coated with an outside layer of functionalized latex.

Ion exclusion chromatography (IEC) is a form of chromatography that has been used to separate relatively small weak acids (carbonic acid, carboxylic acids, hydrocarboxylic acids,

etc.), weak bases (ammonia, amines), and hydrophilic molecular species such as carbohydrates, glycols, and alcohols. Ion exclusion chromatography has a stationary phase with the same charge as the analyte, which is the opposite of ion exchange chromatography. The separation in IEC is based more on molecular species than ionic charge. This is a relatively old technique, which was introduced by Wheaton and Bauman for the first time.[61] Substances that can be separated with IEC are weak organic and inorganic acids, as well as hydrophilic neutral compounds such as sugars. The mechanism for ion exclusion chromatography is still not clear; however, the trend observed is that less polar compounds elute from the column later than polar compounds, which is the same trend as ion exchange chromatography. The separator in IEC is similar to the exchangers used in ion exchange chromatography. Weak acid analytes are separated with sulfonated cation exchangers or polyacrylate resins with carboxylic acid functional groups; gel exchangers with quaternary ammonium are used to separate weak bases. The main difference with ion exchange chromatography is the column capacity, which is generally higher for ion exclusion chromatography.

Ion pair chromatography (IPC) can separate ions on the standard reverse-phase columns used for HPLC; this separation is accomplished by adding an ionic reagent to the mobile phase to pair with sample ions of opposite charge. In this chromatography, separation of different ions is based on differences in ion pair retention time on the stationary phase. The common ion pair for anionic samples is liphophilic cations, such as tetrapropylanions, and for cationic species are sulfonated alkyl groups (C_6-C_{10}), as well as certain inorganic anions such as perchlorate or hexafluorophosphate.

3.2 Mobile phase and column selection

The separation mechanism of IC is based on ionic interactions; therefore, the eluent type and pH can affect the separation efficiency of columns. For ionic species, changing the pH will have little effect on the ionic state as long as the species is fully ionized (cations or anions). However, for polar basic compounds such as amines, a decrease in the pH of the mobile phase will cause an increase in the analyte cationic species. This is due to the protonation of basic ionic species under low pH. On a cation exchange column, the retention times of such compounds under low pH are expected to increase. This phenomenon can occur when the mobile phase pH is close to the pKb (pKb = 14 – pKa) of the analyte; otherwise, when the mobile phase pH is significantly lower than the pKb of the analytes, the retention time will decrease. The decrease in retention time of the analytes comes from increasing the mobile phase concentration and increasing the protonation of anionic functional groups in the stationary phase. Anion exchange chromatography will follow the same scenario using alkaline pH instead of acidic pH. Therefore, to achieve the optimum separation, it is necessary to evaluate the effect of the mobile phase pH on the analyte characterization, peak resolution and column capacity. Due to the hydrophobicity of some drug molecules and their strong interaction with the polymeric stationary phase of IC columns, adding organic solvents and choosing a column with lower hydrophobic resin characteristics will result in shorter retention times and better peak shape (symmetrical and near symmetrical).

3.3 Detection Techniques in Ion Chromatography

A variety of detectors can be used for detection and quantification of analytes in IC. Detectors need to be selected according to the nature of the analyte molecules. The common detectors in IC include the universal refractive index (RI), UV detector (for analytes that absorb

UV), fluorescence detector (for analytes that contain fluorophores), or radio- chemical detectors. Traditionally, IC techniques were incorporated with electrochemical detection methods that included conductivity (suppressed and non-suppressed) and pulsed amperometry techniques.

In this chapter, the newer detection systems in IC are discussed. As was mentioned previously, the type of detector selected depends upon the nature of the analytes and therefore, based on our work, the electrochemical detection mechanism and techniques are under review. It is not intended to suggest that other detectors should not be used with IC.

3.3.1 Conductivity Detection

The principle of conductivity detection is based on the generation of current due to passing ionic species between electrodes. When voltage is applied to the electrodes, the ionic species in solution can produce current. The intensity of this current is proportional to the conductivity of the solution, which depends upon the concentration of ions and polar molecules. The presence of any ionic species between the electrodes can generate current, and includes eluent ionic species, which can provide the background (baseline) conductivity. A problem occurs, however, when the conductance of the eluent is significantly stronger than that of the analytes. The concentrations of ions in eluents are normally 10^4-10^5 times higher than analyte concentrations. This was one of the limitations of conductivity detection, which has led to the invention of suppressors.

3.3.1.1 Suppressed and Unsuppressed Conductivity Detectors

Today, suppressors are commonly associated with ion chromatography, and have become an integral part of the IC systems. The role of suppressor is to remove the eluent ionic species before they reach the detector. The suppression process decreases the intensity of the eluent conductivity by converting the ionic species to weakly dissociated species, while enhancing the

analyte signals by converting the analyte ions to fully dissociated species. Consequently, this leads to the overall enhancement of the signal to noise ratio for conductivity detection. Small et al. first introduced the concept of suppressed IC.[58] Their suppressor was a packed column that was termed a stripper column. The column material was in hydroxide form to change the eluents chemically before they reached the conductivity detector. His designed suppressor converted mineral acids to water, reducing background signal and noise significantly. Meanwhile, the analyte species was converted to its base form, which was fully dissociated and carried more charge. This enhanced the sensitivity of the detection. To obtain a better vision of suppression, the eluent containing HA (A^- being the anion) was passed through the suppressor, where the exchange of A^- for OH^- to produce water could occure. This eliminated the background noise signal, and consequently provided a more stable baseline and improved the analyte sensitivity. Some unsuppressed methods have also been offered by researchers; for instance, in 1979 Gjerde et al. used IC without any suppressor.[62] They used dilute solutions of acids and bases to avoid a large background signal.

The non-suppressed detection method has some significant limitations in practical application. In the suppressed method, the eluent passing through the detector is essentially pure water with approximately zero conductivity, but in the non-suppressed method, the acidic and basic eluents pass through the detector. The presence of strong acid or base at the conductivity detector can generate baseline noise of 1000-1500 μS. Therefore, it is necessary to use dilute weak acid and base eluents in the non-suppressed method because they are only slightly dissociated. Another limitation of the non-suppressed methods is having to use a low-capacity ion-exchange column; there is no limitation on column capacity for suppressed methods. This is due to the ability of suppressed methods to use fairly concentrated acid and base eluents.

In addition, the signal to noise ratio reported for the suppressed method is about an order of magnitude better than the non-suppressed systems. Due to this fact, the limit of detection and limit of quantification are more than an order of magnitude better than in non-suppressed methods. The present suppressor mechanism is based on electrical suppression. To explain the mechanism of operation of electrolytic suppressors, we present the operation of anion suppression techniques in Figure 21.

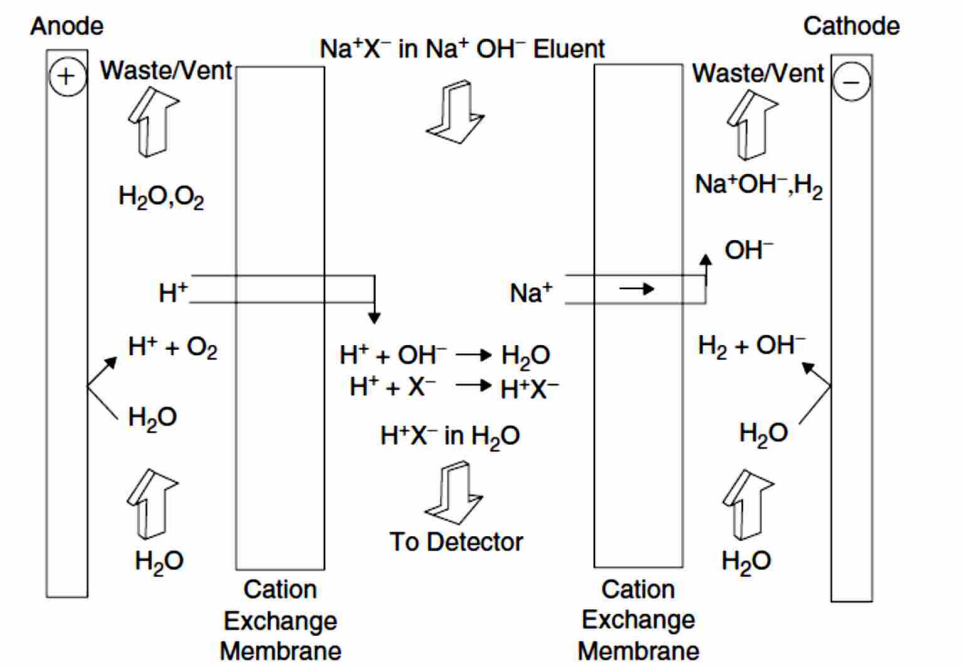

Figure 21 A Schematic diagram explaining the mechanism of ion suppression of an effluent from an anion-exchange column by an electrolytic suppressor. This image is from the book "Application of Ion Chromatography for Pharmaceutical and Biological Products" by Lokesh Bhattacharyya and Jeffrey S. Rohrer.[63]

3.3.2 Pulse Amperometric Detection

The first commercial electrochemical (EC) detector was introduced in 1974 for HPLC systems.[64] Since then, this type of detector has become popular with different types of chromatography systems. High sensitivity, high selectivity, and a wide linear range are the reasons for the successful widespread use of this type of detector. In addition, EC detectors are relatively inexpensive, simple to construct, and rugged. The ability to miniaturize easily is another advantage of this kind of detector.

When EC detectors and high efficiency separation techniques are combined, they can be applied to relatively complex samples.[65] Some early works with EC detectors dealt with biological compounds and drugs. These samples were able to undergo oxidation and, less commonly, reduction. Most of these samples were aromatic in nature (e.g., phenols, aminophenols, catecholamines, and other metabolic amines). The oxidation of such compounds happened readily at the surface of noble metals or inert electrodes (e.g., Au, Pt, and carbon) by applying a constant potential. This constant potential method is called DC amperometry. The presence of the aromatic ring with extended conjugation stabilizes the free radical intermediates formed during the anodic oxidation process. Therefore, the activation energy is lowered significantly. The electrode's role is to accept or donate electrons in the detection process, which is the reason for using inert metals for the electrode. Electrode deactivation is the result of electrochemical involvement (i.e., adsorption of reactant and/or products) in the detection process. One reason for the popularity of glassy carbons in EC methods is their resistance to fouling in dc amperometry. It is important to note that the electrode's exposure to analyte is much less than its exposure to the eluent. Therefore, the fouling and deactivation process often

occurs over a period of hours or days. In dc amperometry, mechanical polishing is required to reactivate the electrode surface.

Alternative methods include the application of alternate positive and negative potential pulses at the surface of the electrode; pulse potential waveforms have been used extensively to reactivate fouled noble metal electrodes. Because radical intermediates in polar aliphatic molecules (e.g., carbohydrates and biogenic amines) do not self-stabilize and have a slow oxidation process, stabilizing the reaction intermediates by adsorption at "clean" noble metal electrodes can increase the efficiency of oxidation. This means that the deactivation or fouling of the working electrode dramatically increases, and causes complete passivation within seconds. This phenomenon is the reason for the non-reactivity of polar aliphatic organic compounds observed in the past. Addressing this problem required continuous reactivation or cleaning the surface of the electrode on-line, which only electrochemical reactivation methods can accomplish effectively.

Today's electrochemical systems perform at high pH. Oxidation occurs by the application of pulses of positive potentials. The generated current is proportional to the analyte concentration, which can be detected and quantified. To prevent electrode fouling, a series of potential pulses at fixed times are applied that clean the electrode surface. The basis of pulsed amperometry detection (PAD) is a repeated series of potentials (E_1, E_2, E_3…) over defined time periods (t_1, t_2, t_3…). The series of potentials is called a waveform. The original waveform applied to Au and Pt electrodes was a three-step potential-time waveform. The initial part of the waveform is E_{det}; detection occurs at this potential during the time period t_{det}. At the same time, sampling of the faradaic signal takes place over the time period t_{int} after a delay of t_{del} to overcome capacitance currents. The average of the current (amperes or coulombs per second) is

the output signal. E_{oxd} (an oxidative cleaning potential) occurs at t_{oxd} and is followed by reductive reactivation at E_{red} during the period t_{red}. The total final waveform cycle ($t_{total} = t_{det} + t_{oxd} + t_{red}$) is ca. 1 s with a frequency of ca. 1 Hz, as shown in Figure 22.

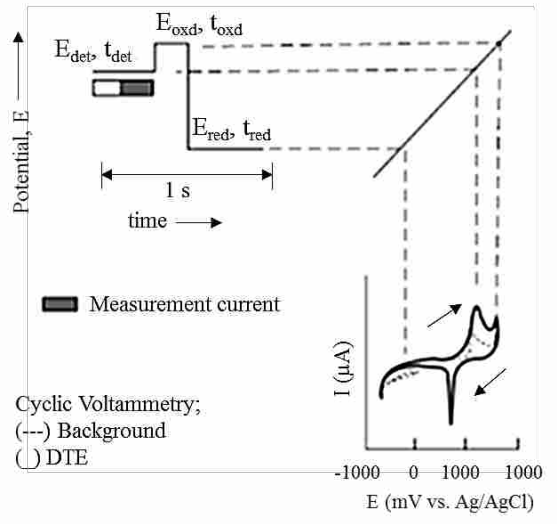

Figure 22 The waveforms known as PAD as translated to cyclic voltammetric response. This image is from the book "Application of Ion Chromatography for Pharmaceutical and Biological Products" by Lokesh Bhattacharyya and Jeffrey S. Rohrer.[63]

Integrated pulse amperometry detection (IPAD) is the latest advancement in electrochemical waveforms. IPAD differs from PAD in that the signal current integrates through a rapid cyclic scan during the detection potential step within a pulsed potential time waveform. IPAD can easily diminish the baseline offset and drift that occurs in PAD due to small variations in the mobile phase, changes in the total surface area of the noble-metal electrode, and analyte-induced effects. At high pH, analytes are oxidized at the surface of the gold electrode by applying pulses of potentials. Among detectable compounds, numerous amines can be oxidized and detected directly at gold electrodes in alkaline solutions. The presence of a non-bonded

electron pair on the nitrogen atom of the amines facilitates the adsorption process at the electrode surface. This helps in the detection of primary, secondary and tertiary amines, but not quaternary amines.

Based on previous research, the detection of amines is best performed using an IPAD waveform. For example, Draisic et al used cation-exchange chromatography with IPAD to detect biogenic amines (i.e., putrescine, histidine, cadaverine, histamine, and spermidine) in spoiled canned herring.[66] Using electrochemical detection greatly improved amino acid detection. Anion exchange columns were used for the separation of amino acids with a quaternary gradient that incorporated both a pH and organic modifier gradient. The IPAD detection method has been used for detection of amino acids, with recent studies showing typical detection limits of 1–50 pmol with electrochemical detection systems. (Figure 23)

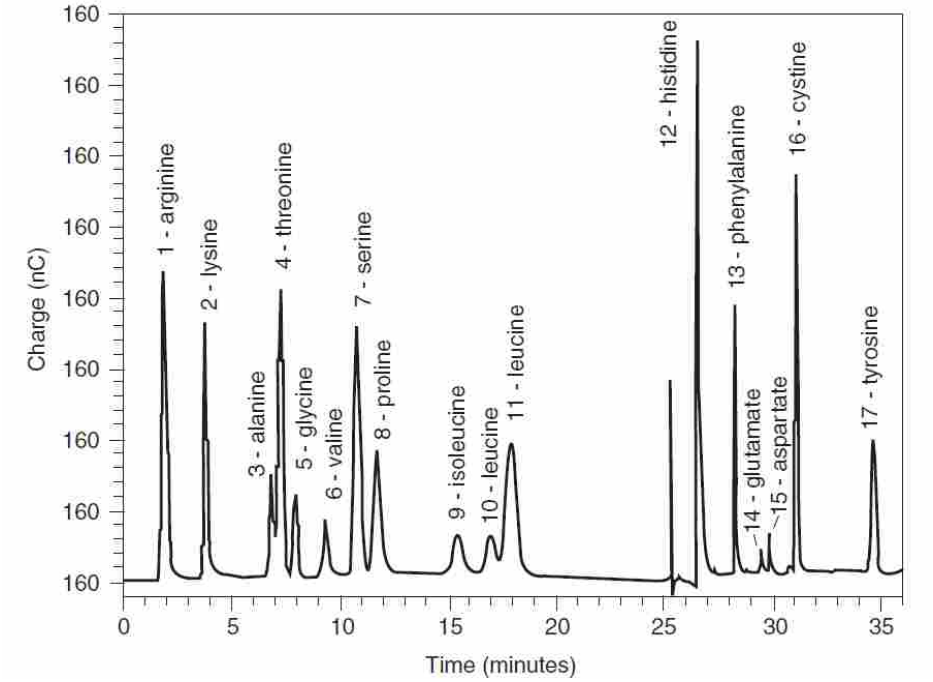

Figure 23 HPAEC-PED results for a mixture of seventeen amino acids (AA S-18 standard from Sigma) at 500 pmol each. Run conditions can be found in Technical Note 50 (2001) from Dionex (Sunnyvale, CA). [66]

4. Application of IC in Pharmaceutical and Biological Compounds

4.1 IC determination of pharmaceutical ingredients

Ion chromatography has been widely used in determination of active pharmaceutical ingredients (API). [67–69] API are the components of a pharmaceutical product that combat disease or bacteria, and are commonly termed the active ingredients. Quantification of API can be especially difficult because pharmaceutical products contain cations, anions, and neutral compounds, which cannot be simultaneously separated. The application of IC in analysis of API provided precision, accuracy, and reproducibility consistent with current industry practice, and led to the further application of IC for analysis in the pharmaceutical area.

However, the disadvantages of applying IC universally in the pharmaceutical field remained a serious matter for pharmaceutical scientists. Many drugs do not have enough stability to be assayed under the acidic and basic conditions normally used in IC. Another problem is that some drugs contain a hydrophobic motif in their structure, which can attach to the IC column material. The elution of such compounds requires using organic solvents, and the suppressor and electrochemical detection systems do not perform well in organic solvents.

In contrast, normal- and reversed-phase chromatographies showed greater utility in relatively high concentrations of organic solvents. This eliminated the problem of hydrophobic compounds sticking to the column materials. The ease with which mass spectrometers can be used with reversed-phase chromatography resulted in strong interest in applying these techniques in the pharmaceutical industry. Therefore, the application of IC has been limited to ionic or very polar molecules such as aminoglycoside antibiotics and bisphosphonates.

However, the popularity of IC applications in the pharmaceutical industry has been increasing due to the introduction of new types of pharmaceutical drugs (new molecular entities), the presence of counter ions in the structures of pharmaceutical molecules (to improve stabilities and solubility properties of pharmaceutically active drug molecules), the development of detection systems with a higher tolerance to organic solvents, and the availability of mixed mode columns. Another important reason for the growing popularity of IC is the use of dilute acidic and basic eluents modified with little to no organic solvent. Such eluents can be disposed of easily after neutralization or dilution. Organic solvents cost more, and their disposal is often more complex, expensive, and environmentally unfriendly. One example is acetonitrile, a common solvent in reversed-phase chromatography.

One of the ionic groups of pharmaceuticals is the guanidine class of compounds.[70–72] Recent research shows that the level of some guanidine derivatives in surface waters is elevated. There may be no immediate effect of small doses of these pharmaceuticals in humans, but there is concern that long-term, low-level exposure could be harmful. For example, a recent report describes the effect of long-term exposure to cimetidine on zebrafish and other freshwater fish. Cimetidine is a histamine H (2)-receptor antagonist that inhibits stomach acid production. Endocrine disruption resulted from long-term exposure to cimetidine levels as low as 30 mgL^{-1}. The ultimate excretion of drugs to urine is the apparent source of such contaminants in surface water. These contaminants are called "contaminants of emerging concern" by the EPA, and there is a growing need to be able to detect and remove them.

The most common analytical methods for detecting such drugs are chromatography techniques, which have several advantages over enzymatic and spectrochemical methods. Pharmaceutical compounds tend to lack suitable chromophores for detection by UV absorbance, and cannot be detected by this means unless the concentration is high. The use of derivatizing reagents in the form of post or pre- column reagents is a common way to detect these compounds, although derivatization has limitations. Our group was the first to report the combination method IC-ED as the most effective detector of these compounds in surface water. Three methods of detection, electrochemical (IPAD), conductivity detection (CD), and UV-vis, were tested; IPAD was found to work best for all of the guanidine derivative compounds, and UV-vis was very sensitive for cimetidine.[73]

One of the most important classes of antibiotics is the aminoglycosides such as amikacin, gentamicin, kanamycin, neomycin, and others. They lack suitable chromophores for detection by UV absorbance and cannot be detected by this means unless the concentration is high. One of the

earliest works in the detection of aminoglycosides occurred in 1994.[74] Kaine and Wolnik used anion exchange chromatography equipped with pulsed electrochemical detection and a NaOH eluent to separate gentamicin in formulations. Since then, scientists have introduced different methods using ion exchangers for the preliminary extraction of aminoglycoside antibiotic components.

Rohrer and Hanko applied a newly developed method in the determination of tobramycin (class of antibiotics) and its impurities.[75] They used CarboPac PA1 (4mm × 250 mm) and its guard (4mm × 50mm) columns with a weak potassium hydroxide eluent (2.00 mM) at a column temperature of 30 °C. Due to the lack of chromophoric groups in this family of antibiotics, detection by UV absorbance usually requires high concentrations, and studies show that refractive index detection suffers the same problem. Derivatization with different groups leads to decreased efficiency in detection and causes instability in some reagents. The introduction of pulsed amperometric detection (PAD) provided a nearly complete solution. Detection was performed with an AAA-Direct waveform using a disposable electrode replaced over 7 days. This method was later replaced by conventional EP using a waveform consisting of 3 potential pulsed amperometric waveforms: detection at 0.05 V, oxidative cleaning at +0.75 V, and ending with gold oxide reduction at -0.15 V. Carbohydrate determination had been attempted using the same waveform in earlier studies, but gold loss from the working electrode resulted in losing peak area response over a shorter time of use. The introduction of a 4-potential program that replaced reductive cleaning by oxidative cleaning was able to maintain the gold working electrode for a longer time of use.

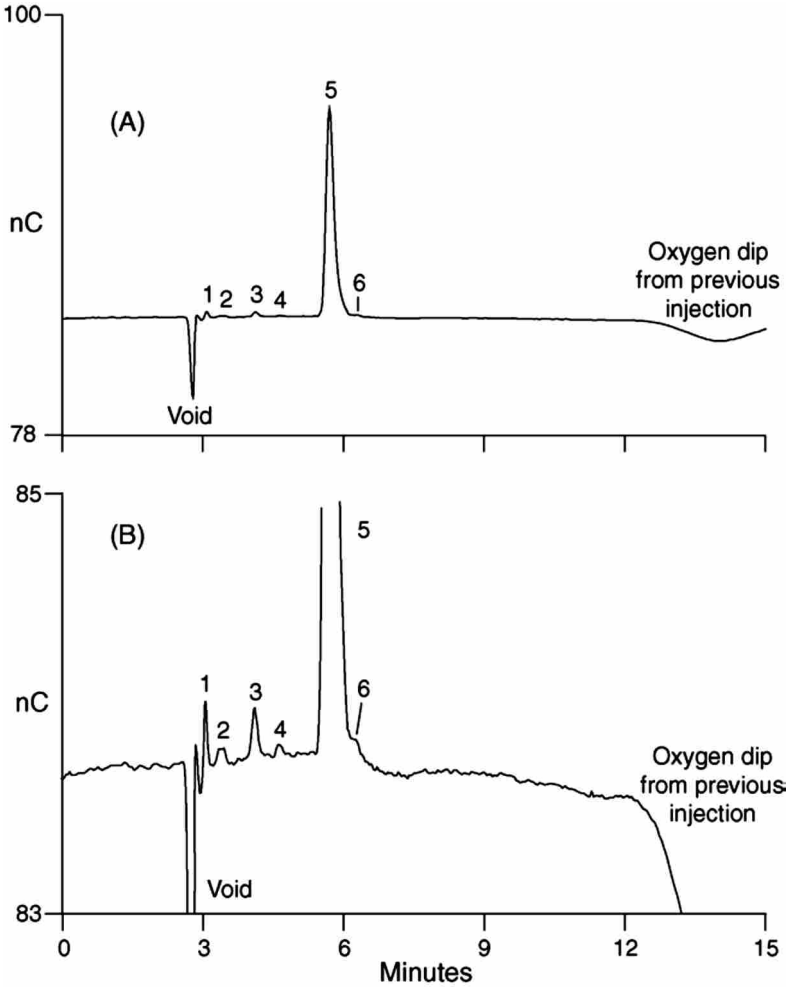

Fig 1.25 Determination of 21 pmol tobramycin (1.07 M, 20L injection) using a CarboPac PA1 column with a 2.00mM KOH eluent (produced by an eluent generator) at 0.5 mL/min, a 30 ◦C column temperature, and IPAD. Full view (A), and expanded view of baseline (B). Peaks 1, 2, and 6: unknown impurities; Peak 3: kanamycin B; Peak 4: neamine; Peak 5: tobramycin; Peak 7: oxygen dip from the previous injection.[75]

Furthermore, IC has been widely applied in analysis of phosphonates, a class of drugs used to treat diseases such as hypercalcemia and osteoporosis, and also to prevent the loss of bone mass. [76–79] The phosphonate drugs are water-soluble and ionic, with very low solubility in organic solvents, which makes them very well suited for IC analysis. Phosphonates suffer from the lack of strong chromophore groups in their structures and therefore a very high concentration of the compound is needed to be detected by UV-vis detectors. Additionally, their volatility is

not sufficient for gas chromatography. Another important limitation is the high tendency of phosphonates to chelate metal ions; therefore, a metal-free system is required for analysis. Commercial IC systems are metal-free and frequently use dilute acids, alkalis, or salt solutions as eluents. The eluent solution also contains nitric acid, which permits the indirect detection of phosphonates with UV detectors. Some methods have been reported that used derivatizing reagents in the form of a post column reactor to assist with UV detection. Both suppressed and non-suppressed conductivity detection of phosphonates have been reported as well.[76-79]

4.2 IC Determination of Biological Compounds

IC has been applied in biological product analysis to measure buffer ions, ionic impurities, monosaccharides, oligosaccharides, and small repeating saccharide units of polysaccharides in vaccines, hematologic products, and allergenic extracts.

One small group of biological products that has been analyzed with different LC techniques consists of the uremic toxins.[80] Uremic toxins resulting from chronic kidney disease (CKD) range from small water-soluble molecules to large proteins; abnormally high levels of these molecules are toxic. One study found that the levels of some guanidine compounds increased greatly in the serum and cerebrospinal fluid of uremic patients, while the levels of other uremic toxins were unchanged or even decreased. Chromatography is the most common technique for measuring uremic toxins. HPLC is used regularly for analysis of these molecules. Several detection methods have been developed for use with HPLC. The lack of strong chromophoric groups in some of the uremic toxins required either a high concentration of analyte for detection by UV-vis, or the use of derivatizing reagents combined with reverse-phase HPLC. In some cases, mass spectrometry can assist in enhancing the detection limit.[81,82]

One subgroup of uremic toxins consists of very polar molecules containing a guanidine unit. Although they are polar and water-soluble, there are only a few examples in which ion chromatography (IC) has been applied to their separation. One of the earliest works relates to the application of IC columns in conjunction with HPLC to pre-concentrate or separate polar compounds.[83,84] Different types of IC columns, such as a strong cation-exchanger (RSO_3^-), weak cation-exchanger ($RCOO^-$) and a reversed-phase column, were compared in the determination of uremic toxins.[85] The weak cation exchange method was preferable due to simplicity, less matrix interference, and higher success in determining the analyte. A recent study used a Dionex CS14 (4 × 250 mm) cation exchange column and a guard column (4 × 50 mm).[86] The authors analyzed guanidine in a high salt and protein matrix with UV-vis. Introducing ED alleviated the need for derivatization and improved the detection limit significantly.

In our group, we have reported a new IC packing material that effectively separates uremic toxins in aqueous media and urine by a straightforward method. The new IC column allowed separation of the five guanidine compounds. Gradient elution at ambient temperature with methanesulfonic acid (MSA) solution as the eluent resulted in detection levels in water from 10 to 47 ppb and in synthetic urine from 28 to 180 ppb. Limits of quantification for the analytes using pulsed amperometric detection were 30 to 160 ppb in water and 93 to 590 ppb in urine. Trace levels of creatinine (1 ppt) were detected in the urine of a healthy individual using the columns.[87]

Vaccines is another class of biological compounds which have been studied by IC-PAD. For example, IC-PAD has been widely adopted for the determination of saccharide content as a measure of product characterization and potency determination in bacterial capsular polysaccharide (PS) vaccines.[63] The measurement of PS content was originally performed using

the orcinol colorimetric assay to quantify the ribose moiety.[63] Tsai et al. were the first to report the combination of IC-PAD to quantify PS in Haemophilus influenzae type b PS and glycoconjugate vaccines using methodologies that had been previously reported for natural glycoconjugate proteins.[88]

Conclusion

Resorcinarene-based cavitands are synthesized from the condensation of resorcinol and various aldehydes. Resorcinarenes having structures easily functionalized with polar, cationic and anionic groups, have achieved excellent separations of some species. The attachment of one or more chiral groups introduce chirality to the resorcinarene derivatives and aid their application in chiral recognition and chiral NMR shift agents. Resorcinarene derivatives have been applied in both the mobile phase and the stationary phase of different chromatography techniques. Our group has developed new stationary phases using resorcinarene derivatives in IC techniques. The resorcinarene derivatives were applied as cation exchange and anion exchange sites in IC for separation of transition metals, pharmaceuticals and biological compounds. Different detection techniques including IPAD, CD and UV-vis were applied in our recent studies in IC. The recent application of IC in the analysis of pharmaceuticals and biological compounds exhibit the potential of such techniques for further innovations and studies.

Acknowledgments

We are grateful for financial support from Thermo Scientific and Brigham Young University.

References

(1) Hogberg, A. G. S. *J. Am. Chem. Soc* **1980**, *102*, 6046–6050.

(2) Petrov, G. S.; Grigor've, A. P. *Zhurnal Khimicheskoi Promyshlennosti* **1941**, *18*, 23–24.

(3) Niederl, B. J, Vogel, J. H. *Aldehyde-Resorcinol Condens.* **1940**, *62*, 2512–2514.

(4) Högberg, A. G. *J. Org. Chem.* **1980**, *45* (10), 4498–4500.

(5) J. R. Moran, S. Karbach, D. J. C. *J. Am. Chem. Soc* **1982**, *104* (7), 5826–5828.

(6) Biros, S. M.; Rebek, J. *Chem. Soc. Rev.* **2007**, *36* (1), 93–104.

(7) Hooley, R. J.; Rebek, J. *Chemistry and Biology*. 2009, pp 255–264.

(8) Helttunen, K.; Shahgaldian, P. *New J. Chem.* **2010**, *34* (12), 2704–2714.

(9) Muppalla, K. Functionalization of Resorcinarenes and Study of Antimicrobial Activity, University of South Florida, 2001.

(10) Arnott, G.; Hunter, R. *Tetrahedron* **2006**, *62* (5), 992–1000.

(11) Wenzel, T. J.; Wilcox, J. D. *Chirality* **2003**, *270* (15), 256–270.

(12) Cram, D. J. *Science* **1983**, *219* (4589), 1177–1183.

(13) Högberg, A. G. *J. Am. Chem. Soc* **1980**, *102*, 6046–6050.

(14) Timmerman, P.; Verboom, W.; Reinhoudt, D. N. *Tetrahedron* **1996**, *52* (8), 2663–2704.

(15) Kashapov, R. R.; Pashirova, T. N.; Zhiltsova, E. P.; Lukashenko, S. S.; Ziganshina, A. Y.; Zakharova, L. Y. *Russ. J. Phys. Chem. A* **2012**, *86* (2), 200–204.

(16) Shirakawa, S.; Shimizu, S. *Synlett* **2008**, *1* (10), 1539–1542.

(17) Hu, Y.-J.; Yang, J.; Liu, Y.-Y.; Song, S.; Ma, J.-F. *Cryst. Growth Des.* **2015**, *15* (8), 3822–3831.

(18) Wenzel, T. J.; Rollo, R. D.; Clark, R. L. *Magn. Reson. Chem.* **2012**, *50* (4), 261–265.

(19) Hagan, K. a.; O'Farrell, C. M.; Wenzel, T. J. *European J. Org. Chem.* **2009**, *2009* (28), 4825–4832.

(20) Moran, J. R.; Ericson, J. L.; Dalcanale, E.; Bryant, J. A.; Knobler, C. B.; Donald, C. J. *J. Am. Chem. Soc* **1991**, *113*, 5707–5714.

(21) Boger, L. B.; Panek, S. *J. Am. Chem. Soc* **1985**, *107* (20), 5745–5754.

(22) Warnmark, K.; Thomas, J. a; Heyke, O.; Lehn, J. *Chem. Comm.* **1996**, 701–702.

(23) Li, N.; Yang, F.; Stock, H. a; Dearden, D. V; Lamb, J. D.; Harrison, R. G. *Org. Biomol. Chem.* **2012**, *10* (36), 7392–7401.

(24) Dumele, O.; Trapp, N.; Diederich, F. *Angew. Chemie Int. Ed.* **2015**, *54*, 1–7.

(25) Schalleya, C. A.; Rebek, J. *Chemical Encapsulation in Self-Assembling Capsules, Stimulating Concepts in Chemistry*; Stoddart, J. F., F. Vogtle and M. Shibasaki, Eds.; Weinheim (Germany), 2000.

(26) Tiefenbacher, K.; Zhang, K.; Ajami, D.; Rebek, J. *J. Phys. Org. Chem.* **2015**, *28* (3), 187–190.

(27) Szumna, A. *Chem. Soc. Rev.* **2010**, *39* (11), 4274–4285.

(28) Wiegmann, S.; Mattay, J. *Org. Lett.* **2011**, *13* (12), 3226–3228.

(29) Klaes, M.; Neumann, B.; Stammler, H.; Mattay, J. *Eur. J. Org. Chem.* **2005**, 864–868.

(30) Botta, B.; D'Acquarica, I.; Nevola, L.; Sacco, F.; Lopez, Z. V.; Zappia, G.; Fraschetti, C.; Speranza, M.; Tafi, A.; Caporuscio, F.; Letzel, M. C.; Mattay, J. *European J. Org. Chem.* **2007**, *2007* (36), 5995–6002.

(31) Szumna, A. *Chem. Commun. (Camb).* **2009**, No. 28, 4191–4193.

(32) Mann, E.; Rebek, J. *Tetrahedron* **2008**, *64* (36), 8484–8487.

(33) Saito, S.; Nuckolls, C.; Rebek, J. *J. Am. Chem. Soc.* **2000**, *122* (40), 9628–9630.

(34) Pham, N. H.; Wenzel, T. J. *Chirality* **2012**, *24*, 193–200.

(35) Pietraszkiewicz, O.; Pietraszkiewicz, M. *Pol. J. Chem.* **1998**, *72* (11), 2418–2422.

(36) Pietraszkiewicz, O.; Pietraszkiewicz, M. *J. Incl. Phenom. Macrocycl. Chem.* **1999**, *35*, 261–270.

(37) Sokoliess, T.; Menyes, U.; Roth, U.; Jira, T. *J. Chromatogr. A* **2002**, *948* (1-2), 309–319.

(38) Ruderisch, A.; Iwanek, W.; Pfeiffer, J.; Fischer, G.; Albert, K.; Schurig, V. *J. Chromatogr. A* **2005**, *1095* (1–2), 40–49.

(39) Tan, H. M. I. N.; Soh, S. H. U. F.; Zhao, J. I. A.; Yong, E. L.; Gong, Y.; Al, T. A. N. E. T. *Chirality* **2011**, *97*, 91–97.

(40) Lipkowski, J.; Kalchenko, O. I.; Slowikowska, J.; Kalchenko, V. I.; Lukin, O. V.; Markovsky, L. N.; Nowakowski, R. *J. Phys. Org. Chem.* **1998**, *11* (6), 426–437.

(41) Lipkowski, J.; Kalchenko, O. I.; Slowikowska, J.; Kalchenko, V. I.; Lukin, O. V.; Markovsky, L. N.; Nowakowski, R. *J. Phys. Org. Chem.* **1998**, *11* (6), 426–437.

(42) Chamseddin, C.; Jira, T. *Chromatographia* **2014**, *77* (17-18), 1167–1183.

(43) Zhang, H.; Dai, R.; Ling, Y.; Wen, Y.; Zhang, S.; Fu, R.; Gu, J. *J. Chromatogr. A* **1997**, *787* (1), 161–169.

(44) Ruderisch, A.; Pfeiffer, J.; Schurig, V. *Tetrahedron: Asymmetry* **2001**, *12*, 2025–2030.

(45) Pfeiffer, J.; Schurig, V. *J. Chromatogr. A* **1999**, *840*, 145–150.

(46) Ruderisch, A.; Pfeiffer, J.; Schurig, V. *J. Chromatogr. A* **2003**, *994* (1-2), 127–135.

(47) Levkin, P. A.; Ruderisch, A.; Schurig, V. *Chirality* **2006**, *18* (1), 49–63.

(48) Terabe, S.; Otsuka, K.; Ando, T. *Anal. Chem.* **1989**, *61* (3), 251–260.

(49) Bazzanella, A.; Mörbel, H.; Bächmann, K.; Milbradt, R.; Böhmer, V.; Vogt, W. *J. Chromatogr. A* **1997**, *792* (1-2), 143–149.

(50) Bächmann, K.; Bazzanella, A.; Haag, I.; Han, K. Y.; Arnecke, R.; Böhmer, V.; Vogt, W. *Anal. Chem.* **1995**, *67* (10), 1722–1726.

(51) Sokoließ, T.; Gronau, M.; Menyes, U.; Roth, U.; Jira, T. *Electrophoresis* **2003**, *24* (10), 1648–1657.

(52) Britz-mckibbin, P.; Chen, D. D. Y. *Anal. Chem.* **1998**, *70* (5), 907–912.

(53) Bazzanella, A.; Bächmann, K.; Milbradt, R.; Böhmer, V.; Vogt, W. *Electrophoresis* **1999**, *20* (1), 92–99.

(54) Gardner, J.; Peterson, Q.; Walker, J.; Jensen, B.; Adhikary, B.; Harrison, R.; Lamb, J. *J. Memb. Sci.* **2006**, *277* (1-2), 165–176.

(55) Wang, J.; Harrison, R. G.; Lamb, J. D. *J. Chromatogr. Sci.* **2009**, *47* (7), 510–515.

(56) Li, N.; English, C.; Eaton, A.; Gillespie, A.; Ence, T. C.; Christensen, T. J.; Sego, A.;

Harrison, R. G.; Lamb, J. D. *J. Chromatogr. A* **2012**, *1245*, 83–89.

(57) Li, N.; Allen, L. J.; Harrison, R. G.; Lamb, J. D. *Analyst* **2013**, *138* (5), 1467–1474.

(58) Small, H.; Stevens, T. S.; Bauman, W. C. *Anal. Chem.* **1975**, *47* (11), 1801–1809.

(59) Lee, Y. C. *Anal. Biochem.* **1990**, *189* (2), 151–162.

(60) Weiss, J. *Ion Chromatography*, Second.; Dyllick, C., Bock, B., Eds.; VCH Publishers Inc: New York, 1995.

(61) Wheaton, R. M.; Bauman, W. C. *Ann. NY Acad. Sci* **1953**, *57*, 159–176.

(62) Gjerde, D. T.; Schmuckler, G.; Fritz, J. S. *J. Chromatogr. A* **1980**, *187* (1), 35–45.

(63) Bhattacharyya, L. *Application of Ion Chromatography for pharmaceutical and Biological Products*; Rockville, MD, 2012.

(64) Adams, N. R. *New York: Marcel Dekker*. 1969.

(65) Bhattacharyya, L.; Rohrer, J. S. *Application of Ion Chromatography for Phamaceutical and Biological Products*; John Wiley & Sons. Inc.: Hoboken, New Jersey, 2012.

(66) Draisci, R.; Cavalli, S.; Lucentini, L.; Stacchini, A. *Chromatographia* **1993**, *35* (9), 584–590.

(67) Huang, Z.; Richards, M. A.; Zha, Y.; Francis, R.; Lozano, R.; Ruan, J. *J. Pharm. Biomed. Anal.* **2009**, *50* (5), 809–814.

(68) Liu, D. Q.; Sun, M.; Kord, A. S. *J. Pharm. Biomed. Anal.* **2010**, *51* (5), 999–1014.

(69) Keast, R. S. J.; Breslin, P. A. S. *Pharm. Res.* **2002**, *19* (7), 1019–1026.

(70) Lee, S.; Jung, D.; Kho, Y.; Ji, K.; Kim, P.; Ahn, B.; Choi, K. *Chemosphere* **2015**, *135*, 208–216.

(71) Marescau, B.; Qureshi, I. a; De Deyn, P.; Letarte, J.; Ryba, R.; Lowenthal, a. *Clin. Chim. Acta.* **1985**, *146* (1), 21–27.

(72) Van den Berg, J. D.; Smets, L. a; Rutgers, M.; Grummels, a; Fokkens, R.; Jonkergouw, P.; van Rooij, H. *Cancer Chemother. Pharmacol.* **1997**, *40* (2), 131–137.

(73) Panahi, T.; Weaver, D. J.; Lamb, J. D.; Harrison, R. G. *Analyst* **2016**, *141*, 939–946.

(74) Kaine, L. A.; Wolnik, K. A. *J. Chromatogr. A* **1994**, *674* (1-2), 255–261.

(75) Cooper, G. A.; Rohrer, J. S. *Anal. Biochem.* **1995**, *226* (1), 182–184.

(76) Kosonen, J. P. *J. Pharm. Biomed. Anal.* **1992**, *10* (10-12), 881–887.

(77) Tsai, E. W.; Ip, D. P.; Brooks, M. A. *J. Chromatogr. A* **1992**, *596* (2), 217–224.

(78) Den Hartigh, J.; Langebroek, R.; Vermeij, P. *J. Pharm. Biomed. Anal.* **1993**, *11* (10), 977–983.

(79) Kovačevič, M.; Gartner, A.; Novič, M. *J. Chromatogr. A* **2004**, *1039* (1-2), 77–82.

(80) Eetjen, J. U. P. A.; Odriguez, M. A. R.; Tegmayr, B. E. S. *Kidney Int.* **2003**, *63*, 1934–1943.

(81) Boelaert, J.; Lynen, F.; Glorieux, G.; Eloot, S.; Van Landschoot, M.; Waterloos, M.-A.; Sandra, P.; Vanholder, R. *Anal. Bioanal. Chem.* **2013**, *405* (6), 1937–1947.

(82) Niwa, T. *Mass Spectrom. Rev.* **1998**, *16* (6), 307–332.

(83) Saigusa, D.; Suzuki, N.; Takahashi, M.; Shiba, K.; Tanaka, S.; Abe, T.; Hishinuma, T.;

Tomioka, Y. *Anal. Chim. Acta* **2010**, *677* (2), 169–175.

(84) Kandhro, A. J.; Mirza, M. A.; Khuhawar, M. Y. *Anal. Lett.* **2010**, *43* (13), 2049–2060.

(85) Kågedal, B.; Olsson, B. *J. Chromatogr. B Biomed. Sci. Appl.* **1990**, *527*, 21–30.

(86) Qiu, J.; Lee, H.; Zhou, C. *J. Chromatogr. A* **2005**, *1073* (1-2), 263–267.

(87) Panahi, T.; Weaver, D. J.; Lamb, J. D.; Harrison, R. G. *J. Chromatogr. A* **2015**, *1376*, 105–111.

(88) Tsai, C.-M.; Gu, X.-X.; Byrd, R. A. *Vaccine* **1994**, *12* (8), 700–706.

Chapter 2 Resorcinarene-Based Cavitands with Glutamic Acid Substituents and their Ability to Bind Amines

Abstract

Resorcinarene-based deep cavitands including glutamic acid methyl resorcinarene (**GMA**) and glutamic acid undecyl resorcinarene (**GUA**) have been synthesized. The upper rim of the cavitands is functionalized with glutamic acid groups and the lower rim is functionalized with either a methyl or undecyl alkyl group. The cavitands were characterized by nuclear magnetic resonance (NMR), mass spectrometry (MS), UV-vis spectroscopy, dynamic light scattering (DLS) and electron microscopy. The **GMA** and **GUA** cavitands form kite-like structures in dimethylsulfoxide, acetone, and water. The ester derivative (**GUE**) showed vase-like structure in benzene and kite-like structure in DMSO, acetone and chloroform. The binding of **GMA** with amine guests was studied in DMSO by UV-vis titration and compared to that of phthalyl glutamic acid. The obtained binding constants (K values) were in the range of 12,000-136000 M^{-1}. The binding constants for **GMA** to guanidine compounds were measured and found to be from 4300-153,000 M^{-1}. The ester and acid derivatives of the cavitands were shown to form aggregates in a variety of solvents. The aggregates were spherical as confirmed by DLS, SEM and TEM experiments. Dynamic light scattering (DLS) experiments revealed that the size of the aggregates could be controlled by cavitand concentration, pH, and temperature. For example, 1×10^{-4} M GMA gave 50 nm diameter particles and 0.1 M cavitand gave particles of 400 nm.

Keywords: resorcinarene; characterization; binding constant; UV-vis titration; aggregation.

1. Introduction

A one of the traditional families of molecules in supramolecular chemistry, resorcinarenes have a highly interesting multipurpose scaffold.[1–3] Applications of these molecules range from the formation of capsules, coordination cages, and molecular loops, to applications in supramolecular sensors and phase-transfer catalysts. Resorcinarenes and the similar calixarenes with their bowl-shaped structure are at the center of a number of significant host-guest studies.[4–11]

The ability of resorcinarene molecules to be decorated at both their upper and lower rims provides them with unique properties and advantages over other host molecules. These molecules are synthesized by condensation of resorcinol (1,3-dihydroxybenzene) and various aldehydes. Varying the nature of the substituent group on the aldehyde facilitates the preparation of resorcinarenes with different solubility properties.[1,3]

Chirality in resorcinarene derivatives is rare, yet has been achieved by two primary methods. First, inherent chirality, which refers to resorcinarene molecules with achiral substituents that create a chiral molecule due to their arrangement or twist.[12,13] Second, attachment of one or more enantiomerically chiral groups to the molecule.[4,14–18] The chiral cavitands bind to enantioactive guest molecules through non-covalent interactions. The chirality of the cavitand along with its size, shape and surface characteristics controls the selective binding between two enantiomeric guests.

The most common methods to evaluate binding of guests by resorcinarenes are ^{1}H NMR and UV-vis studies. One component (guest) is incrementally added to the system (host) while monitoring a physical property such as a specific chemical resonance (NMR) or absorption band

(UV) that is sensitive to the supramolecular interaction of interest. The resulting data are fitted to binding models to obtain association constants K_a. [19]

Recognition and selective binding by macrocyclic compounds has been achieved recently for the separation of pharmaceuticals and for enantioselective catalysis. One example of chiral resorcinarenes is their use as catalyst for the addition reaction of diethylzinc to benzaldehyde. The chiral resorcinarene was synthesized by the Mannich reaction between resorcinarene tetratosylate, diamine and excess paraformaldehyde, which resulted in a bridged dimethoxy ketal diamine ligand. This structure showed enantioselectivity for (R)-1-phenyl propyl alcohol (ee 51%).[18]

Chiral NMR solvating agents based on resorcinarene have been introduced for green chemistry applications and analysis of enantiomeric purity. Association of the enantiomers with the chiral resorcinarene solvating agent involved noncovalent interactions such as hydrogen bonding, other dipole-dipole interactions, and π-stacking between electron-rich and electron-deficient aromatic rings. This leads to different chemical shifts of enantiomers in the NMR spectrum and thus can be used to examine enantiomeric purity. For example, chiral resorcinarenes were synthesized by bonding enantiomerically chiral proline groups or pipecolinic acid derivatives to the upper rim of resorcinarenes.[14,20,21] Different types of guest molecules, including neutral and protonated primary amines, amino acids, and amino alcohols were shown to bind to the hosts. This cavitands demonstrated chiral discrimination for pyridyl, phenyl, and bicyclic aromatic substrates.

Introduction of chiral moieties through phthalimide units bridged to the hydroxyl groups of the resorcinol rings is a fruitful method to develop chiral resorcinarenes.[22,23] These hosts were shown to discriminate between enantiomeric guests. Guest molecules, including racemic trans-

1,2-cyclohexanediol were encapsulated in the resorcinarene cavities. The large shielding in the ^{1}H NMR spectra was used as evidence of binding and enatioselectivity of 33% ee for trans-1,2-cyclohexanediol was achieved.[24] Arm elongation was also achieved by using Fmoc-protected chiral alanine chlorides at the upper rim of the resorcinarene to provide a deep chiral pocket. A racemic mixture of (+)- and (−)-pinanediol underwent a slow exchange of bound and unbound forms in d_6-acetone and substantial shielding of the substrates. The complexation of (-)-pinanediol was favored.[25]

Our group has investigated resorcinarenes with chiral phthalimide units on their upper rim.[15] We have observed chiral recognition of benzyl amines which is important class of guests amenable to study. The ^{1}H NMR titration experiments with chiral primary, secondary, and tertiary amines showed that this cavitand causes different chemical shift changes for these three types of amines. Also. it shows chiral discrimination for secondary amines at greater than two equivalents. A vast majority of drugs are amines or contain functional groups derived from amines. Studies show that stereoisomers of racemic drugs often differ in pharmacological activity; thus assessment of their optical purity is critical.[26,27] Chiral resorcinarenes can bind to alkyl ammonium cations in solution or gas phase.[28,29] For example, we showed a chiral resorcinarene with alanine moieties on the phthalimide unit performed chiral recognition of amines such as 1-phenylethylamine, N-methyl-1- phenylethylamine and N,N-dimethyl-1-phenylethylamine.[15] Enantiomeric differentiation was achieved in d_6-DMSO. The protonation of the amines enhanced the interaction between the host anion and guest cation as a mimic of the molecular recognition features of naturally occurring proteins for small molecules.

In addition to chiral recognition by one host molecule, aggregates of deep cavitands have also been used for chiral recognition to selectively bind guest molecules.[30] Some resorcinarenes

form micelles and bilayer structures, mimicking biological membranes. The presence of both hydrophilic and hydrophobic parts within one cavitand structure makes this possible.[31–33] The acid chloride (2, 5, 8, 11, 14 pentaoxaheptadecan-17-oyl chloride) was used to modify the upper rim of an octaamino cavitand with long alkyl groups on the lower rim.[34] The cavitand formed vesicles and a bilayer structure in water, which was revealed by TEM measurements. Guest complexation was essentially driven by the hydrophobic effect in aqueous media. The complexation of guests depended on their size and hydrophilic properties.

In this chapter, we report the design and synthesis of deep chiral cavitands with glutamic acid groups on the upper rim and methyl or undecyl alkyls on the lower rim. The glutamic acids on the upper rim enrich the resorcinarene with eight carboxylic acids, which can enhance the interaction with guests through hydrogen binding. The binding of the resorcinarenes with amines and guanidine compounds is presented. Binding constant were calculated and chiral selectivity observed. The amphiphilic properties of these resorcinarenes caused the formation of spherical particles, as confirmed with DLS, TEM and SEM studies. The formation of these particles and their size were controlled by factors such as concentration, pH, and temperature.

2. Experimental

2.1 General Methods

All the chemicals were obtained from Sigma-Aldrich., unless otherwise noted. Deuterated NMR solvents were used as supplied from Cambridge Isotope Laboratories. The methyl and undecyl resorcinarenes were synthesized according to literature procedures.[1,15] Compounds quinoxaline-2,3-diol (**Q**) , 2,3-dichloroquinoxaline (**Cl-Q**), 5,6-dichloropyrazine-2,3-dicarboxylic acid (**Cl-Py-COOH**), 2,3-dichlorofuro[3,4-b]pyrazine-5,7-dione (**Cl-Py-CO**),

and phthalyl glutamic acid (**PGA**) were synthesized according to published methods.[15,35] Acronyms: **Q** = quinoxaline, **Py** = pyrazine, **G** = glutamic acid, **M** = methyl, **U** = undecyl, **E** = ester and **A** = acid of the glutamic acid.

VXR 500-MHz multinuclear FT-NMR was used to record ^{1}H and ^{13}C NMR spectra. The proton chemical shifts (^{1}H) were reported in parts per million (δ) with respect to tetramethylsilane (TMS, δ = 0 ppm) or solvent peaks. Mass spectrometry was equipped with a micro-electrospray ionization (ESI) source with a heated metal capillary drying tube and was modified based on the design of Eyler. The typical operating flow rate of the ESI source was 10 $\mu L \cdot h^{-1}$. The matrix-assisted laser desorption/ionization (MALDI) instrument used to measure the mass of GEM and GEU was an API QSTAR pulsar I from AB Applied Biosystems MDS SCIEX. The applied matrix was alpha-cyano-4-hydroxycinnamic acid (alpha-CHC matrix) obtained from Agilent Technology. The Zetasizer nano ZS dynamic light scattering instrument (Malvern instrument, Malvern, Worcestershire, UK) was used to analyze the particle size distribution of the compounds. The transmission electron microscopy (TEM) instrument was a FEI Tecnai F30. Scanning electron microscopy (SEM) was performed with a FEI Helios NanoLab 600 DualBeam FIB/SEM. Sputter coating was used to apply an ultra-thin coating of gold metal on the SEM samples. Melting points were determined using a SRS DigiMelt MPA 160 apparatus from Stanford Research Systems, Inc. Optical rotations were measured using a Perkin-Elmer 241 polarimeter (sodium D-line, 529 nm) and D values are given in 10^{-1} deg cm^2 g^{-1}. Elemental analyses were performed by M-H-W Laboratories, Phoenix, AZ. Simultaneous thermogravimetry – differential scanning calorimetry (STA/TG-DSC) was performed with Netzsch STA 409 PC.

2.2 Synthesis

Dimethyl 2-(2,3-dichloro-5,7-dioxo-5,7-dihydro-6H-pyrrolo[3,4-b]pyrazin-6-yl)pentanedioate (**GPy**). 5,6-Dichloropyrazine-2,3-dicarboxylic acid anhydride (0.4360 g, 2.00 mmol) and L-glutamic dimethyl ester (0.761 g, 4.34 mmol) were put in a closed heavy walled glass container. 2.0 mL of acetic anhydride was added to the mixture and the reaction was stirred at 120 ℃ for 6 h. The reaction mixture was cooled to room temperature and poured into 20 mL of distilled water and extracted with 20 mL dichloromethane (CH_2Cl_2). The extraction was repeated 3 times with CH_2Cl_2 and the collected solution was reduced to 5 mL by rotary evaporator. The yellow oil was purified by column chromatography (SiO_2) with eluent ethyl acetate and hexane (v:v 1:1). The solvent was evaporated to produce a slightly yellow oil. The oil was washed with 10 ml of 10 % HCl solution and then extracted with 30 ml of CH_2Cl_2. After removing the solvent under vacuum, 0.74 g (92 %) of pale yellow oil was obtained. ^{1}H NMR ($CDCl_3$, 500 MHz δ = 5.03 (dd, ^{1}H), δ = 3.76 (s, 3H, OCH_3), δ = 3.62 (s, 3H, OCH_3), 2.67 (m, 1H, CH), 2.43 (m, 3H, CH & CH_2CO). ^{13}C NMR (500 MHz, $CDCl_3$) δ (ppm): 172.4, 168.1, 161.5, 153.9, 143.2, 53.2, 52.2, 51.9, 30.6, 24.0. $[\alpha]_D^{23}$ = -34.0 (c 1.00, acetone). HRMS (ESI) calculated for $[M + H]^+$ 376.1460, found 376.0104.

Glutamic methyl resorcinarene ester (GME). Methyl-resorcinarene (0.04040 g, 0.0742 mmol) and **GPy** (0.1240 g, 0.329 mmol) were put in a 10 mL two-neck dry flask connected to a condenser and nitrogen gas inlet. 3 mL of dry DMF was added to the flask. Triethylamine (TEA) (0.1140 g, 1.13 mmol) dissolved in 1 ml of dry DMF was added dropwise to the flask under an atmosphere of N_2. The stirring was continued for 8 hours at room temperature, followed by 12 h at 60 ℃. The solvent was removed under reduced pressure, and the solid was purified by column chromatography (SiO_2, ethyl acetate/hexane, 1:1) to yield as a yellow solid (0.0511 g, 38.8 %).

Mp: 220-230 °C ^{1}H NMR (500 MHz, $CDCl_3$) δ (ppm): 7.39 (s, 2H), 7.27 (s, 2H), 7.18 (s, 2H), 6.90 (s, 2H), 5.017 (q, 4H), 3.98 (q, 4H), 3.64 (s, 12H), 3.51 (s, 12H), 2.40 (m, 8H), 2.18 (m, 8H), 1.69 (d, 12H). ^{13}C NMR (500 MHz, d6-DMSO) δ (ppm): 172.9, 169.3, 163.6, 163.2, 155.3, 151.7, 150.7, 149.0, 142.3, 138.8, 135.2, 133.6, 125.8, 117.9, 53.2, 51.7, 51.0, 29.8, and 24.2. $[\alpha]_D^{23}$ = -24.8 (c 1.00, acetone). HRMS (ESI) calculated for $[M + H_2O + H]^+$ 1775.5350, found 1775.4465 , HRMS (MALDI) calculated for $[M + Na]^+$ 1779.3935, found 1779.2547.

Glutamic methyl resorcinarene acid (GMA). Compound **GME** (0.1000 g, 0.0569 mmol) was dissolved in 3 mL tetrahydrofuran (THF) by stirring for 15 min at room temperature. 0.100 g of NaOH in 10 mL of H_2O was added to the solution and the mixture was refluxed for 12 h until both layers turned to one clear layer. The solvent was neutralized to pH 7 and evaporated. The solid was washed with CH_2Cl_2 and extracted with H_2O. The H_2O layer was collected and acidified with 2 M HCl. The yellow precipitate was filtered. The filtrate was dried under vacuum to dryness 0.0842 g (85.4 %). Mp: 240-250 °C. ^{1}H NMR (500 MHz, d_6-DMSO) δ (ppm): 12.451 (br, 8 H), 8.60 (m, br, 2H), 7.45 (m, br, 2H), 7.01 (m, br, 2H), 6.21 (m, br, 2H), 4.61 (s, br, 4H), 4.251 (s, br, 4H), 1.8 (m, br, 16H), 1.21 (s, br, 12H). ^{13}C NMR (500 MHz, DMSO) δ (ppm): 173.4, 155.7, 148.5, 48.6, 42.0, 17.5. $[\alpha]_D^{23}$ = + 9.57 (c 1.00, methanol). Anal. calcd. for **GMA** + $4H_2O$ + 7HCl: C 46.28, H 3.74, N 7.74 %; found: C 46.28, H 3.42, N 8.52%. HRMS (ESI) calculated for $[M + 9H_2O + H]^+$ 1806.3877, found 1806.3761.

Glutamic undecyl resorcinarene ester (GUE). Undecyl-resorcinarene (0.124 g, 0.113 mmol) and **5** (0.1860 g, 0.495 mmol) were put in a 10 mL two-neck dry flask connected to a condenser and nitrogen gas inlet. 2.5 mL of dry dimethyl formamide (DMF) were added to the flask. Triethylamine (TEA) (0.1140 g, 1.13 mmol) was dissolved in 1 ml of dry DMF and added dropwise under an atmosphere of N_2. The stirring was continued for 8 hours at room

temperature, followed by 12 hours at 60 °C. The solvent was removed under reduced pressure, and the solid was purified by column chromatography (SiO_2, ethyl acetate/hexane, 1:1) to yield as a yellow solid (0.226 g, 82.8 %). Mp: 190-200 °C ^{1}H NMR (500 MHz, d_6-DMSO) δ (ppm): 7.59 (s, 4H), 7.29 (s, 4H), 4.98 (q, 4H), 4.79 (t, 4H), 3.26 (s, 24H), 2.59 (m, 4H), 2.44 (m, 4H), 2.15 (m, 16H), 1.28 (m, 72H), 0.926 (t, 12H), ^{13}C NMR (500 MHz, d_6-benzene) δ (ppm): 172.0, 168.2, 161.9, 154.2, 152.2, 141.6, 141.5, 134.2, 134.1, 123.7, 117.8, 51.0, 51.8, 52.2, 36.0, 32.0, 30.2, 29.9, 27.5, 24.3, 22.7, 14.0. $[\alpha]_D^{23}$ = - 6.12 (c 1.00, acetone). HRMS (ESI) calculated for $[M + H_2O + H]^+$ 2335.0428, found 2335.0873, HRMS (MALDI) calculated for $[M + Na]^+$ 2340.0215, found 2340.8124 .

Glutamic undecyl resorcinarene acid (GUA). Compound **GUE** (0.1000 g, 0.431 mmol) was dissolved in 3.00 mL tetrahydrofuran (THF) by stirring for 15 min at room temperature. 0.100 g of NaOH in 10.0 mL of H_2O was added to the solution and the mixture was refluxed for 12 h until both layers turned to one clear layer. The solvent was neutralized to pH 7 and evaporated. The solid was washed with CH_2Cl_2 and extracted with H_2O. The H_2O layer was collected and acidified with diluted HCl (2 M). The yellow precipitate was filtered. The filtrate was dried under vacuum to dryness 0.0812 g (81.2 %). Mp: 220-230 °C, ^{1}H NMR (500 MHz, d_6-DMSO) δ (ppm): 12.99 (br, 8H), 9.21 (m, br, 2H), 8.65 (m, br, 2H), 7.41 (m, br, 2H), 6.39 (m, br, 1H), 6.05 (m, br, 1H), 4.45 (s, br, 4 H), 4.21 (s, br, 4 H), 2.19 (s, br, 4H), 2.10 (s, br, 4H), 2.81 (m, br, 16H), 1.28 (s, br, 72H), 0.926 (t, 12H). ^{13}C NMR (500 MHz, d6-acetone) δ (ppm): 42.5, 33.0, 23.6, 14.7. $[\alpha]_D^{23}$ = + 3.48 (c 1.00, methanol)Anal. calcd. for GUA + $6H_2O$ + 4HCl: C 55.94, H 6.62, N 6.00%; found: C 55.81, H 6.14, N 6.73%. HRMS (ESI) calculated for $[M + 9H_2O + H]^+$ 2368.0055, found 2368.0144.

2.3 Sample Preparation for Binding and Job Plot Studies

A 3.6 mM **GMA** stock solution was prepared by adding 0.0295 g of **GMA** to 5.00 mL of DMSO at room temperature. Dilute solution of 0.0360 mM **GMA** was prepared in DMSO by adding 30 µL of stock solution and diluting it to 3.00 mL. Amine guests, 8.20 mM were prepared in DMSO. Guanidine compounds were purchased in HCl salts and therefore neutralized before titration. They were neutralized in MeOH with KOH before the titration (1:1 molar ratio for compounds guanidine (**G)**, methylguanidine (**MG)**, dimethylbiguanidine (**DMG)** and 1:2 for Agmatine (**AGM)**). The methanol was to obtain neutral guests, which were dissolved in DMSO for titration. To perform the binding constant titrations, 2.00 µL aliquots of each guest were added to 3.00 mL of 0.0360 mM **GMA** solution and UV-vis spectra were taken after each addition until the end point. The **GMA** solution was stirred between measurements. The binding constant of guanidine compounds was calculated with a similar method using 0.0360 mM of **GMA** and 6.60 mM of guests.

The binding constant was calculated using the following equation,

$$1/(I-I_0) = 1/K(Ic-I_0)[guest] + 1/(Ic-I_0)$$

where K is the binding constant, I_0 is the absorbance intensity of the free host, I is the observed absorbance intensity of the [guest-host] complex, and Ic is absorbance intensity at saturation. In order to find K, $1/Ic-I_0$ was plotted against 1/[guest].[19]

The 3.6 mM **GMA** stock solution was prepared by adding 0.0295 g of **GMA** to 5.00 mL of DMSO at room temperature. Dilute solution of 0.018 mM **GMA** was prepared in DMSO by adding 100 µL of stock solution and diluting it to 20.00 mL. 2.7, 2.4, 2.1, 1.8, 1.5, 1.2, 0.9, 0.6 and 0.3 mL of the 0.018 mM **GMA** solution were taken and transferred to vials. The 1.2 mM

guest **3** stock solution was prepared by adding 0.0121 g of guest **3** to 5.00 mL of DMSO at room temperature. Dilute solution of 0.018 mM guest **3** was prepared in DMSO by adding 18 µL of stock solution and reaching it to 20.00 mL. 0.3, 0.6, 0.9, 1.2, 1.5, 1.8, 2.1, 2.4 and 2.7 mL of the 0.018 mM guest **3** solution were taken and transferred to the each **GMA** solution. Each vial had a total volume of 3 mL. After mixing them for a few seconds, UV-vis spectra were taken at room temperature.

2.4 Sample Preparation for Mass Spectrometry and Electron Microscopy Imaging

Two different types of mass spectrometry were used, including electrospray ionization (ESI) and matrix assisted laser desorption/ionization (MALDI). ESI mass spectra were obtained by dissolving 5.00 mg of sample in 1.00 mL acetone and operating in positive mode. To obtain mass spectra with MALDI, matrix preparation was required. The matrix was prepared by adding 10.00 mg of 3,5-dimethoxy-4-hydroxycinnamic acid (sinapinic acid) to 500 µL water: acetonitrile (1% TFA). The obtained mixture was vortexed thoroughly for approximately 1 minute. The matrix solution was centrifuged for 30 seconds at 2,000 to 5,000 rpm. The supernatant was collected and used as the matrix. Equal amounts of matrix and sample solution (1.00 mg in 1.00 mL acetone) were mixed and 1.0 µL of the sample containing matrix mixture was applied onto a stainless steel MALDI target.

Samples for SEM images were prepared by placing 0.00150 mM of samples in acetone and water on silicon wafer chips with carbon-coated copper grids and sputtering 2-3 nm gold nanoparticles on it. Samples for TEM were prepared by placing 0.0350 mM of samples in acetone on the carbon grids.

2.5 TGA

Water loss was studied through simple mass difference and Thermogravimetric analysis (TGA). Mass loss of the sample was investigated by heating up to 200 °C. The mass loss occurred at 100-140 ˚C with a corresponding DSC peak showing a chemical change at that temperature. Gas chromatography was run during the TGA experiment and water vapor was the only gas detected.

3. Results and Discussion

We have chosen to attach quinoxaline panels to resorcinarene molecules in preparing large host molecules with deep cavities. The resorcinarenes were synthesized by condensation of methyl or undecyl aldehyde with resorcinol. The synthesis of the panel quinoxaline was more complex and required several steps to attach the amino acids to the upper rim. The first synthetic steps entailed converting 1,2-phenylenediamine through four steps to dichloropyrazine anhydride (**Cl-Py-CO**, Scheme 1). To form the panel with the amino acid ester (**GPy**), the anhydride was reacted with glutamic amino acid ester. The anhydride provides a gateway into many chiral panels simply by changing the amino acid.

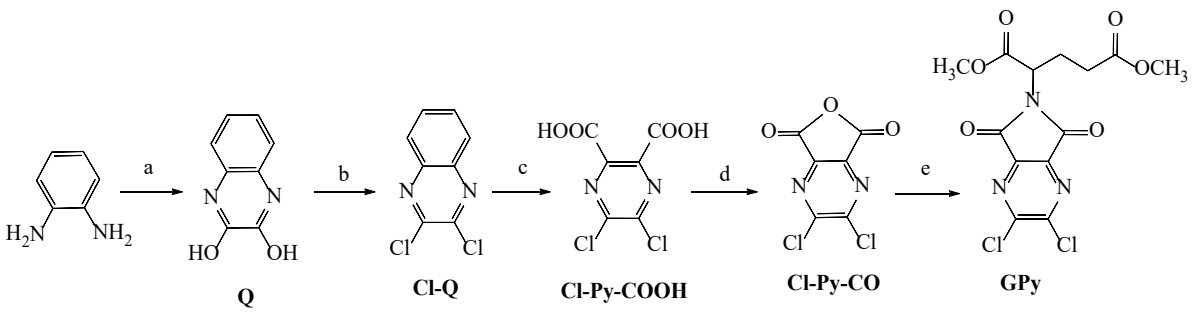

Scheme 1 Synthetic procedure for pyrazine molecules with glutamic ester. Conditions: (a) oxalic acid, 2 M HCl, 2 h; (b) N, N-diethylanaline, phosphoryl chloride ($POCl_3$), 120 °C 6 h; (c) $KMnO_4$, reflux 4 h, HCl; (d) oxalyl chloride $(COCl)_2$, pyridine, dry THF, 0 °C 2 h, 50 °C 1 h; (e) L-glutamic methyl ester hydrochloride in acetic anhydride, 120 °C 4 h.

After the quinoxaline panel containing glutamic acid was added to the resorcinarene, the new cavitand was formed (**GME** or **GUE**, Scheme 2). Methyl groups are incorporated into the cavitand structure at the lower rim to facilitate greater solubility in polar solvents versus substances with undecyl groups. The presence of undecyl chains at the lower rim provides enough hydrophobicity to enhance solubility in non-polar solvents and adherence to hydrophobic IC resins. The four pyrazine panels are bonded to the upper rim of the resorcinarene on the same face of the molecule while each one has attached a glutamic acid residue. The ester derivatives were hydrolyzed by sodium hydroxide and acidified with hydrochloric acid to form acid derivatives of glutamic resorcinarenes (**GMA** or **GUA**, Scheme 2). The amino acids are bonded to rings that contain heteroatoms. Therefore, these molecules are capable of forming both hydrogen bonds and dipole-dipole interactions with other molecules. The presence of eight carboxylic acid groups held in proximity to each other, are designed to facilitate binding to amine compounds through hydrogen bonding and dipole–dipole interactions.

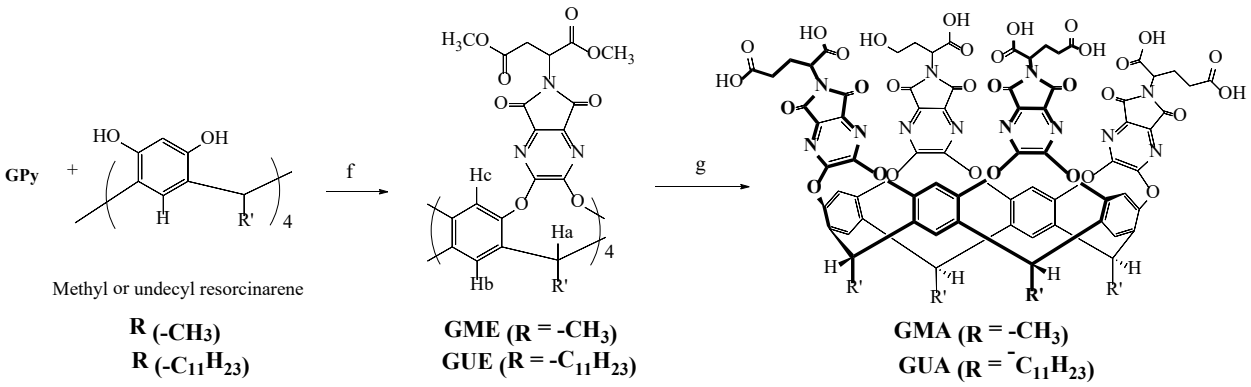

Scheme 2 Synthetic steps to form the glutamic acid resorcinarene cavitands. Conditions: (f) dry DMF, Et_3N, rt 12 h; (g) THF, NaOH, 12 h, and HCl, H_2O.

3.1 Characterization

3.1.1 Characterization by NMR

Resorcinarene cavitands have two spatial conformations: an expanded kite and a contracted vase (Figure 1). The kite form has C_{2v} symmetry and the vase form has C_{4v} symmetry. If the four panels are positioned vertically, the cavitand is the vase conformer and if the panels are flat and extend outward, it is the kite conformer.[2] One indication of the conformer is the chemical shift of the lower rim methine proton. Others have shown that in less polar solvents such as chloroform, benzene, and THF, the methine proton of the vase conformer appears at $\delta \approx$ 5.5 ppm or further downfield, while the methine in the kite conformer appears at $\delta \approx 3.7$ ppm.[36] Along with solvent, temperature and pH can influence conformer concentration.

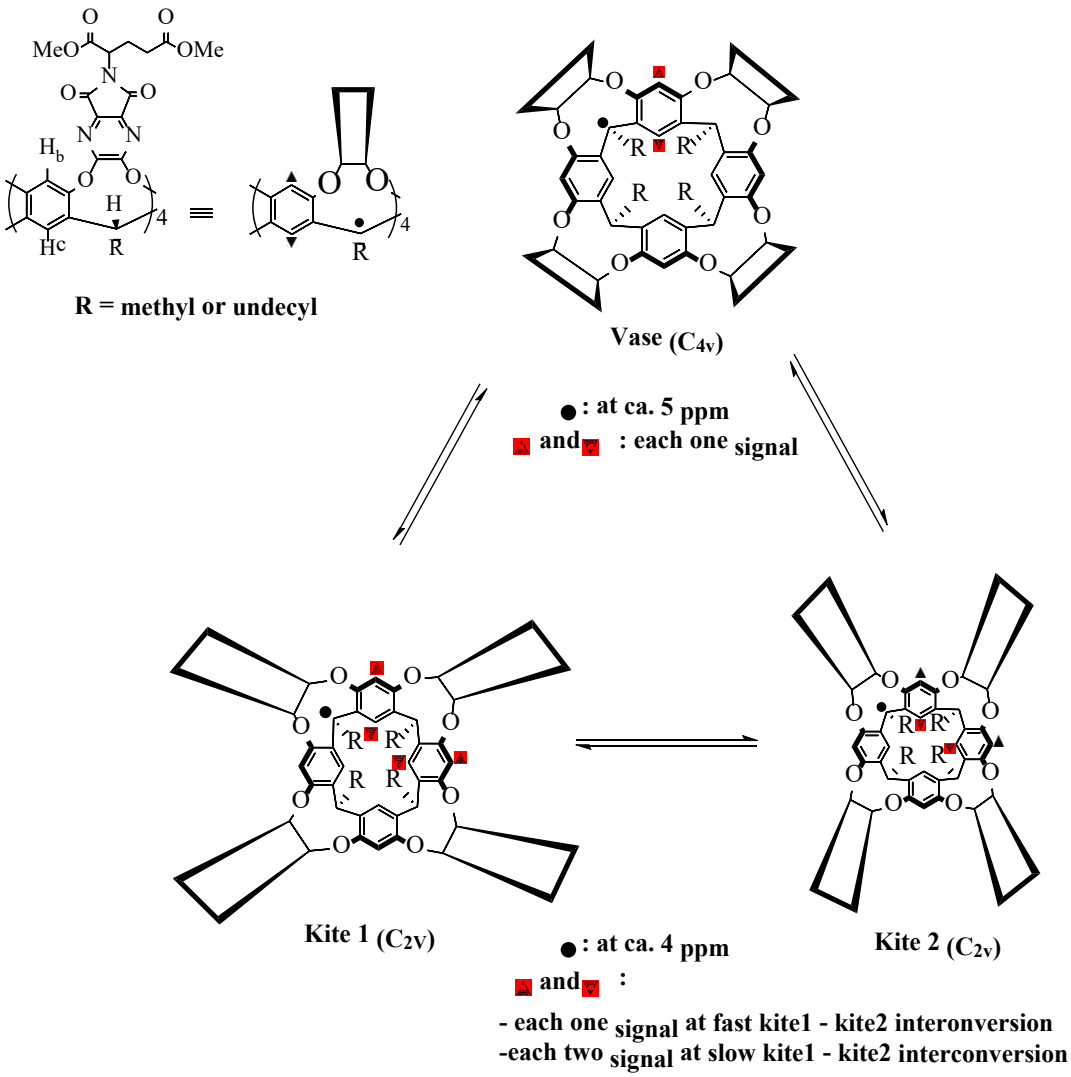

Figure 1 Conformational interconversion of kite and vase. ^{1}H NMR of methine proton in vase, kite with slow kite1−kite2 interconversion, and kite with fast kite1−kite2 interconversion has indicated. Four aromatic signals of kite with slow kite1−kite2 interconversion, and two aromatic signals for kite with fast kite1−kite2 interconversion has shown.

The chemical shift of the methine protons (Ha in Scheme 2) in **GME** in $CDCl_3$, d_6-acetone and d_6-DMSO appeared at 3.87, 4.14 and 4.01 ppm, respectively. These values are intermediate in chemical shift between reported vase and kite structures, but closer to the kite conformation. The methine protons of **GUE** in $CDCl_3$, d_6-acetone and d_6-DMSO appeared at 4.12, 3.92 and 3.77 ppm, respectively, and are also closer to the kite conformation. However, in d_6-benzene the methine was downfield and appeared at 4.79 ppm, which indicates the structure is closer to the vase conformation. In accordance with a recent report on vase-kite conformational interconversion by Diederich and Pochorovski,[37] the repulsive interactions between the protonated nitrogens and carbonyl groups on the resorcinarene cavitand promote the kite conformer and hinder the formation of the vase conformer.

The presence of two signals for the aromatic protons (H_b and H_c) of **GME** in $CDCl_3$ and d_6-acetone, shows the slow interconversion between the two kite conformations (Figure 1). However, **GME** showed four aromatic signals in d_6-DMSO at room temperature; at 6.91, 7.19, 7.28 and 7.40 ppm, which indicates some distortion and lack of perfect C_{2V} symmetry of the kite conformation.

According to previous studies, the vase conformation is favored at higher temperatures.[36] **GME** didn't show any specific changes of methine signals at higher temperature up to 80 ºC in d_6-acetone, d_6-DMSO, and $CDCl_3$, which indicates the stability of the kite conformer (Figure 2). Although, as temperature was increased to 80 °C in d_6-DMSO, the four signals of aromatic protons started to coalesce into one sharp peak at 7.23 ppm. This trend indicates the fast interconversion between kite1-kite2 conformations at higher temperatures with preference for C_{2v} symmetry structure.

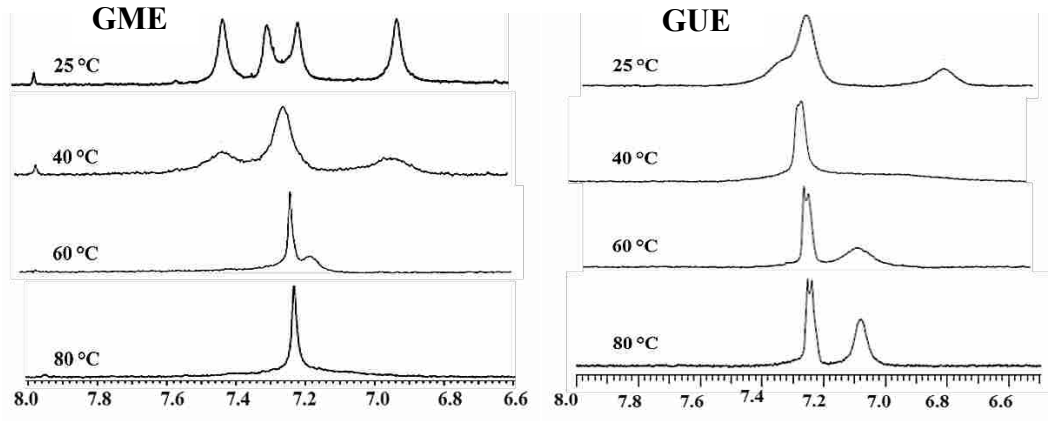

Figure 2 ^{1}H NMR spectra of aromatic signals GME (left) and GUE (right) in d_6-DMSO at different temperatures.

Although **GUE** appears to be in the vase form in benzene, the presence of two aromatic peaks at 7.24 and 7.60 ppm shows that **GUE** is not in a perfect vase conformation. Benzene is better at stabilizing the vase conformation than the other solvents. Two important factors contribute to destabilize the vase conformation of such cavitands: cavity solvation and solvent hydrogen-bonding acidity.[38] Benzene can stabilize the vase conformation because benzene is nearly complementary to the cavity size and consequently can fit into the inner cavity of the vase structure. The lack of hydrogen-bonding interactions between benzene and nitrogens of the quinoxaline arms promotes the vase conformation.[37]

As mentioned earlier, based on the chemical shift of the methine protons, **GUE** prefers the kite structure. **GUE** showed two signals for aromatic peaks in d_6-acetone, $CDCl_3$, and d_6-benzene which indicates slow interconversion between kite1-kite2 conformations. Two relatively broad aromatic signals at 7.24 and 6.78 ppm were observed for **GUE** in d_6-DMSO. Based on this observation and signal integration, **GUE** prefers one conformer of kite with very slow interconversion to the other conformer. Further investigation was performed with ^{1}H NMR

studies at various temperature (VT-NMR) and is shown in Figure 2. As temperature was increased to 80 °C, two aromatic signals appeared at 7.24 and 7.08 ppm. They were resolved equally and sharpened compared to 25 °C. Thus, **GUE** at elevated temperatures in DMSO undergoes slow interconversion between kite1-kite2 conformations.

According to published studies, the kite structure is the predominant conformation at lower temperatures.[38] At low temperature, solvation energies stabilize the kite structure with its solvent-exposed surface. The methine signals appeared at 4.01 (**GME**) and 4.10 (**GUE**) ppm in $CDCl_3$ at 25 °C. As the temperature was lowered to -5 °C in $CDCl_3$, the ^1H NMR signals of **GME** and **GUE** started to broaden and lose splitting. The aromatic signals broadened and underwent coalescence as the temperature reached -5 °C (Figure 3). Apparently, at lower temperatures, the chemical exchange is slower than the NMR timescale, and therefore signals are broader.

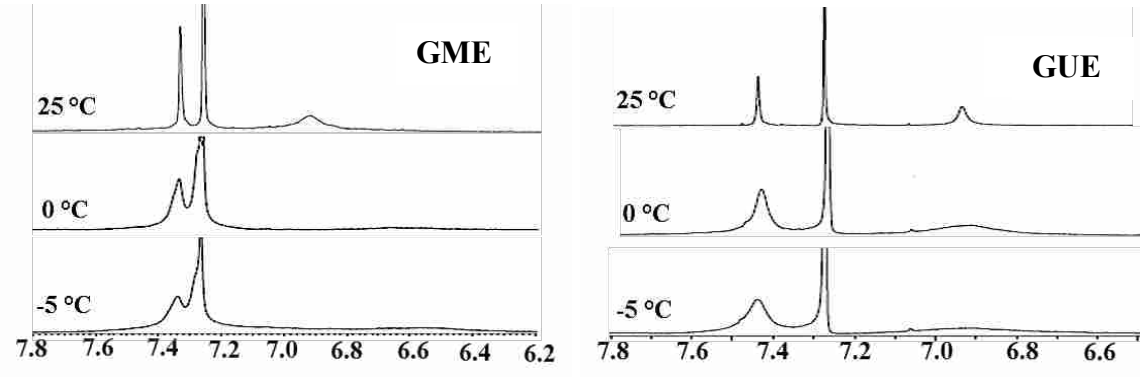

Figure 3 ^1H NMR spectra of aromatic signals GME (left) and GUE (right) in d_6-DMSO at different temperatures.

GMA and **GUA** showed the kite structures in d_4-methanol, d_6-acetone and d_6-DMSO. VT-NMR experiments on the **GMA** showed that the chemical shift of the methine proton didn't change in acetone from 25 to -5 °C. Likewise, the methine peak did not show any obvious movement from 25 to 80 °C in d_6-DMSO. These observations indicate that the kite structure is stable for **GMA**. The ^{1}H NMR signals **of GMA** and **GUA** were broad. These cavitands have polar and non-polar ends, which facilitate aggregation. The presence of eight carboxylic acids for each molecule can form inter- and intra-molecular hydrogen bonds in the aggregation which lock the movement of the molecule. This results in protons not being able to freely rotate, and thus chemically equivalent protons are in different environments, leading to broad NMR signals.

3.1.2 Characterization by MS

Mass spectrometry was used for further characterization of the resorcinarenes. By MALDI the **GME** mass was observed at 1779.25 m/z which is consistent with the calculated mass of **GME** + Na^+ of 1779.39 amu. The molecular ion peak was also observed at 1757.52 m/z with a smaller intensity. The **GME** mass was analyzed with ESI-MS as well. The **GME** mass was obtained with a +1 molecular ion peak at 1757.52 m/z. The mass difference between the calculated value and the experimental value (1775.53) was an ammonium ion.

The mass spectrum of **GUE** was obtained with similar methods. The molecular weight of the compound is 2317.03 g/mol. The **GUE** mass was observed at 2340.81 m/z, which is consistent with the mass of **GUE** + Na^+. The molecular ion peak was also observed at 2318.84 m/z, but with less intensity. The **GUE** mass was analyzed with ESI-MS as well and its mass was observed at 2335.08 amu. The mass difference between the calculate value (2317.03) and this experimental value (2335.08) was NH_4^+.

The acid derivatives of resorcinarene cavitands (**GMA** and **GUA**) were also analyzed with MALDI and ESI techniques. The molecular ion peaks were not able to be observed using MALDI. Using ESI, the molecular ion peak for **GMA** was found to be 1806.37 amu. The mass difference between this value and the calculated value for the parent ion was 162.09 amu. A mass of 162 equals eight water molecules and one ammonium, which waters and ammonium could have been picked up from the eluent. With eight carboxylic acids, **GMA** would have one water associated with each carboxylic acid. The **GUA** was analyzed by the similar method and a +1 molecular ion peak at 2368.01 m/z was observed. The mass difference between this mass and the calculated value is 163.10 amu. Apparently, **GUA** also flies with 8 water molecules, as well as a hydronium. Water was also observed in ^{1}H NMR spectra of **GMA** and **GUA,** but varied from 3-5 molecules per cavitand. Previously in our group, the presence of 8 water molecules associated with a similar resorcinarene was observed by SORI-CID FTICR MS technique.[15]

To further characterize the acid derivatives, they were analyzed with thermogravimetric analysis (TGA). An oven dried sample of **GMA** was used to measure the amount of water in the sample. As temperature was increased to 140° C, **GMA** lost water which was calculated to be 5.3 H_2O per **GMA** molecule on average. Further increase in temperature didn't change the amount of water given off, but caused sample burning.

3.2 Binding ability of GMA to amine and guanine compounds

3.2.1 Binding ability to amine compounds

The **GMA** molecule, with its carboxylic acids, was designed to bind amines through hydrogen bonding. A series of amine guests that varied in structure were chosen to test the factors important to binding (Figure 4). We first investigated primary, secondary and tertiary benzyl amines and then compared them to aliphatic and naphthyl amines. We then investigated

the affect of chirality on binding. The host and guest molecules were soluble in DMSO and so this was chosen as solvent for the binding studies. We also examined binding in water, but observed no significant changes in the UV-vis spectra. We attribute the weak binding in water to the highly solvated ammonium species that the guests form in water.

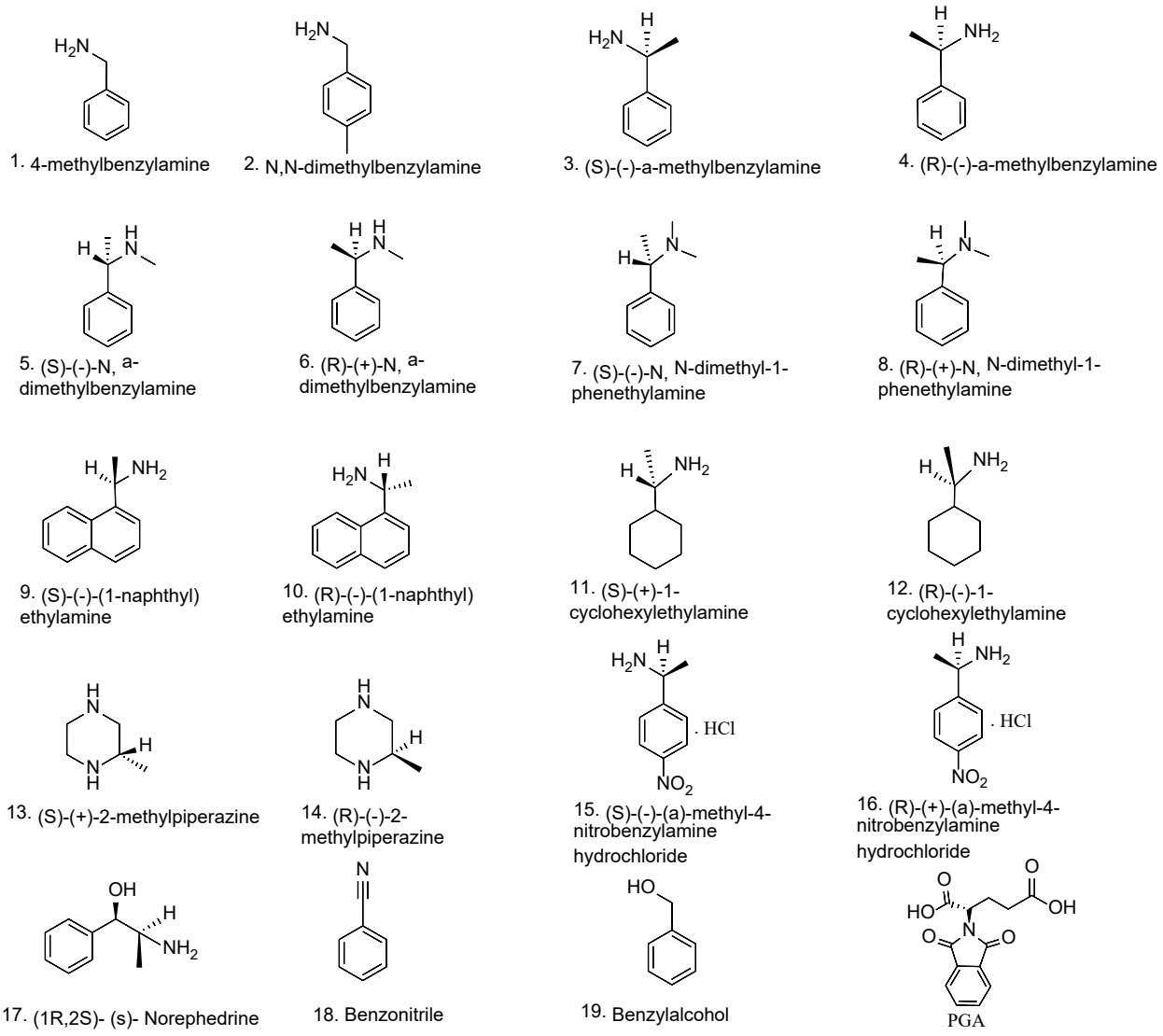

Figure 4 Structure of the guests and PGA.

As a solution of amine guest was incrementally added to a solution of **GMA**, the **GMA** peak at 280 nm decreased and the peak at 340 nm increased (Figure 5). Compound **3** is shown as an example, but a similar increase and decrease in the UV-vis spectra was observed for each of the amine guests in Figure 4. Plotting the absorbance at 340 nm versus [guest]/[host], showed an increase in absorbance to around four equivalents of guest (Figure 6), after which the absorbance did not change. This indicates that four guest molecules are associating with one **GMA** host.

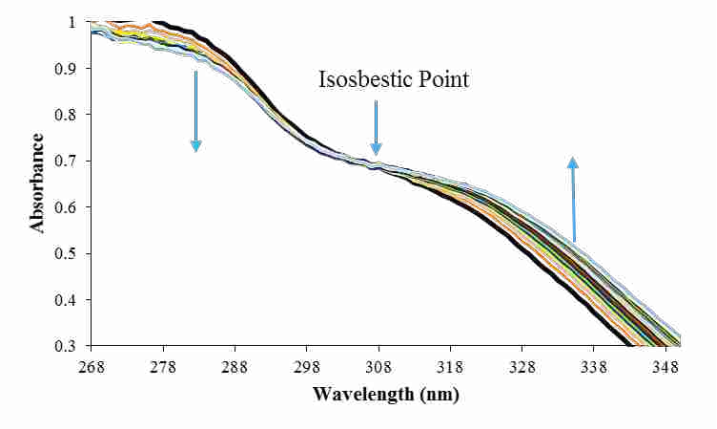

Figure 5 UV-vis absorption of GMA with amine guest (3). Conditions: 3 (0.0082 M) was added in 2 µL increments to GMA (0.0360 mM) at 22 °C in DMSO.

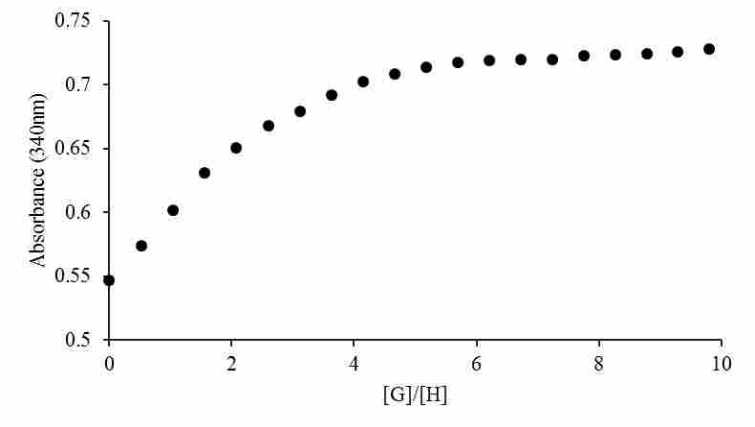

Figure 6 UV-vis absorbance change with added 3 (G) to GMA [H]. Conditions: 3 (0.0082 M) was added in 2 µL increments to GMA (0.0360 mM) at 22 °C in DMSO.

To determine the stoichiometry of the binding, job plot analysis was performed.[39] The mole fraction of guest was plotted against absorbance (Figure 7). The maximum point of the plot occurs at X = 0.8 and correlates to a 4:1 guest to host binding. (Figure 7 a) To confirm the stoichiometry of the binding, absorbance for another Job plot was obtained using one fourth the concentration of **GMA** corresponding to binding to just one of the resorcinarene arm per guest (Figure 7 b). The maximum at $X_{HG} = 0.5$ for this plot and shows 1:1 guest to arm of host binding. These job plots indicate that four guest molecules bind to each host or one guest molecule binds to each arm.

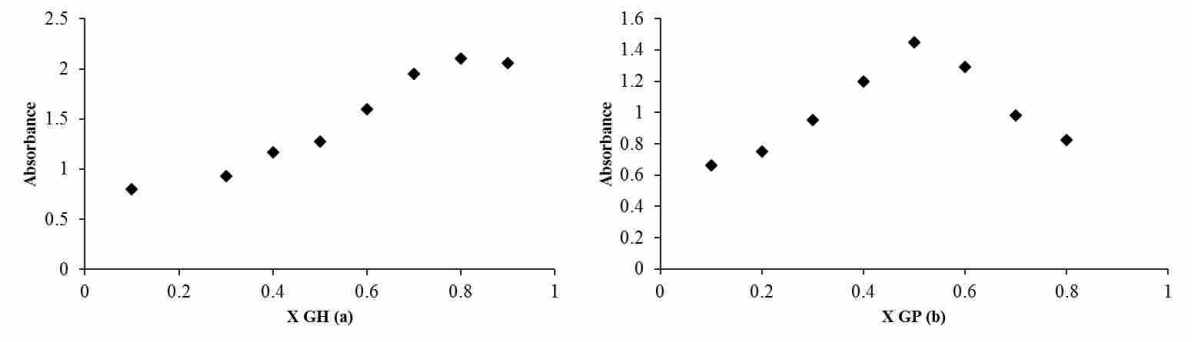

Figure 7 Job plots of guest 3 with GMA. [H] = [G] (a, left) and [Panel] = [G] (b, right). Conditions: [H] = [G] = 0.018 mM, [Panel] = [G] = 0.018 mM.

With the knowledge of the binding stoichiometry, host-guest titrations were performed so that binding constants could be calculated (Table 1). The binding constants were calculated using one guest per one arm of host so 1:1 binding isotherms could be used. The percent error for three binding constant measurements for one guest was 12 %. Different guest substituent factors such as size, type, number, and position were investigated.

Table 1 Binding constants of amines to GMA in DMSO. [H]: 0.0360 mM, [G]: 8.20 mM.

Guest	*K* (M^{-1})	Guest	*K* (M^{-1})
1	40,000	**2**	55,000
3	96,000	**4**	98,000
5	126,000	**6**	89,000
7	73,000	**8**	70,000
9	13,000	**10**	12,000
11	40,000	**12**	36,000
13	85,000	**14**	73,000
15.HCl	NC[a]	**16**.HCl	-----[a]
3.HCl	NC[a]	**17**	74000
18	-----[a]	**19**	-----[a]

a: Not calculated, too small to measure, < 1000.

3.2.1.1 The effect of substituent group

Benzylamine (**1**) and 4-methylbenzylamine (**2**) show binding to **GMA** and gave binding constants of 40,000 and 55,000 M^{-1}, respectively (Table 1). Although these binding constants are fairly similar to each other, they are very different from benzyl alcohol and benzonitrile, which showed no appreciable binding to **GMA**. We attribute the strong binding of organic amines to **GMA** to the formation of cation-anion complexes. The carboxylic acids of **GMA** will protonate the amine of the guest and form a carboxylate-ammonium ion pair ($R\text{-}NH_2 + R'\text{-}COOH \rightarrow R\text{-}NH_3^+ + R'\text{-}COO^-$). These ions form stronger attractions to each other than they do to the polar DMSO. This anion-cation interaction is critical as shown by the weak binding of the alcohol and nitrile guests.

The effect of electron donating group on the basicity of the amine functional group was studied. Guests **3** and **4** with binding constant of 96,000 and 98,000 M^{-1} respectively, carry an electron donating $-CH_3$ group on the α-carbon which increases the electron donating ability of the neighboring $-NH_3^+$ group by an inductive effect, thereby enhancing the binding between amine and **GMA** in comparison to **1** and **2**. Guest **5,** with a binding constant of 126,000 M^{-1}, showed a larger binding constant than **3** and **4**, which can be explained by the same hypothesis. The presence of methyl groups on the geminal carbon of **5** enriches the electron density on the amine group more than the methyl group on **4**.

The basicity of amine functional groups may be modified by steric hindrance. The binding constant of **7** and **8** are 73,000 and 70,000 M^{-1} respectively, significantly less than those for primary and secondary amines **3** and **5**. The presence of two methyl sterically inhibits the interactions between amine and acid groups. The effect of hindrance also was observed for **9** and **10**, which have naphthyl groups in their structures and gave binding constants of 13,000 and

12,000 M^{-1-}, respectively. Noticeably, their binding strength was smaller than those of the amines with one phenyl ring, such as **3** and **4**. Also, in the case of **9** and **10**, the presence of naphthyl groups increases the hydrophobicity of the compound resulting in more solvation by DMSO and less binding to **GMA**.

Whether the amine groups in the guest are bonded to aliphatic or aromatic groups plays a role in binding strength to the host molecule. The cyclic aliphatic guests **11** and **12** showed weaker binding (40,000 and 36,000 M^{-1} respectively) than the benzylic amines **3** and **4**. The aliphatic diamines **13** and **14**, with two amines per molecule, gave binding constant equal to 85,000 and 73,000 M^{-1} respectively, and showed stronger interaction with **GMA** than aliphatic amines **11** and **12**. The number of nitrogens enhances the binding. Secondary aliphatic amines **13** and **14** with binding constant of 73,000 and 70,000 M^{-1}, showed smaller binding strength than secondary aromatic amines **7** and **8**. This result also can be explained by lack of conjugate system in their structures.

Protonated amines proved not to bind to **GMA**. The amine guests **15** and **16**, which have their amines already protonated, showed no binding to **GMA**. To confirm this result, **3** was protonated with hydrochloric acid before the titration. Unlike **3,** the protonated species of **3** exhibited no measurable binding to **GMA**.

Phthalyl glutamic acid (**PGA**, Figure 4), an analogs of a cavitand side panel, here also titrated with primary and secondary amines **3** and **4**, and **5** and **6**. Their binding constants were found to be 5800 and 3400, and 10400 and 6400 M^{-1} respectively. Compared to **GMA** which contains eight carboxylic acid groups on the upper rim, the monoacid **PGA** showed much weaker interactions with amines. We propose the carboxylic acids on **GMA** are binding in a cooperative manner resulting in a larger binding constant.

3.2.1.2 Chiral recognition

Previously in our group, alanine-containing cavitands (**AUA** and **AMA**) were synthesized and studied for chiral recognition with chiral amines by ^{1}H NMR titrations. Since the glutamic acid-containing cavitands **GMA** and **GUA** carry chiral groups on the upper rim, experiments were conducted to examine the ability of these hosts to discriminate between enantiomeric guest molecules. The UV-vis titration studies showed that secondary amines **5** and **6** (enantiomeric pair) with binding constant of 126,000 and 89,000 M^{-1} respectively, showed distinct chiral discrimination. *S* enantiomers showed larger binding constants for most of the chiral amines (Table 1).

3.2.2 Binding ability to guanidine compounds

Guanidine compounds are water contaminants of emerging concern and their detection and quantification is essential to their removal from water. Noting the ability of **GMA** to bind amines, we tested its ability to bind guanidines. The binding of **GMA** to guanidines would potentially lead to its use as an ion exchange material in ion chromatography stationary phases. Indeed, the undecyl derivative, **GUA**, was successfully used as an ion exchange material for ion chromatography (IC) columns.[40]

A family of guanidine known pharmaceuticals compounds, were chosen that had different substituents (Figure 8). As a solution of guanidine guest was incrementally added to a solution of **GMA**, the **GMA** peak at 280 nm decreased and the peak at 340 nm increased as was observed for the amine guests. Plotting the absorbance at 340 nm versus [guest]/[host], showed an increase in absorbance to around four equivalents of guest **23**, after which the absorbance did not change (Figure 9). As with the other amines, four guests are associating strongly with **GMA**, corresponding to the 4 arm.

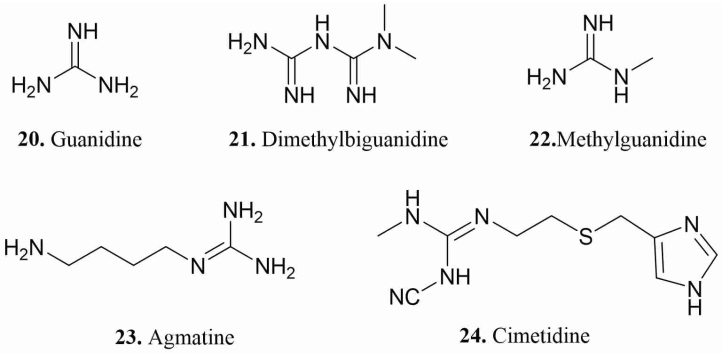

Figure 8 Guanidine compounds.

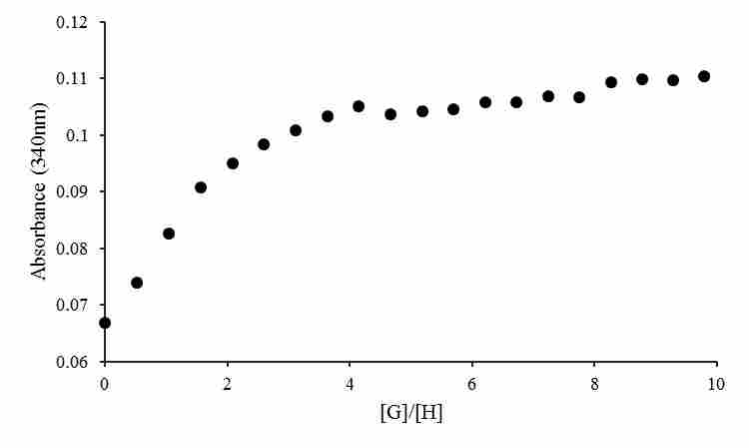

Figure 9 UV-vis absorbance change with added 23 to GMA. Adding guest 23 to the 0.0360 mM of GMA and monitoring the peak shift at 340 nm. The absorbance at 340 nm is plotted vs the [guest 23]/[host] concentration.

Table 2 Binding constants of GMA and guanidine molecules. [GMA] = 0.0360 mM, [G] = 6.6 mM.

Guest	K (M^{-1})
20	153,000
21	128,000
22	102,000
23	43,000
24	4300

Guanidine (**20**) showed the strongest binding, K = 153,000 M^{-1} while the guanidine derivatives showed smaller binding constants (Table 2). Guanidine derivatives can be protonated and form cations and di-cations in solution. The high polarity and charge density of **20** leads to strong interactions with carboxylic acids of **GMA**. The presence of alkyl groups in their structure increases the hydrophobic properties of the molecule and, interestingly, guest **24** (the most hydrophobic molecule in the list) showed the smallest binding constant of 4300 M^{-1}. The highly solvated guests interact more weakly than the non-solvated ones. We also examined binding in water, but observed no significant changes in the UV-vis spectra. We attribute the weak binding in water to the highly solvated guanidine species that the guests form in water.

3.3 Particle size Analysis

As mentioned, the presence of polar and non-polar ends in resorcinarene molecules can result in the formation of aggregates. DLS was used to confirm the presence of agglomerated glutamic acid resorcinarene cavitands in different solvents. For the esters, 0.854 mM **GME** and 0.647 mM **GUE** were analyzed in acetone, chloroform and DMSO and the results are shown in Figure 10 a and b. The observed average diameter of **GME** aggregates was ~200 nm. As the peak broadness shows, there is larger particle size distribution in DMSO than acetone and chloroform. The average diameter of **GUE** was ~400 nm and, again, the greatest size distribution was in DMSO.

Acid derivatives **GMA** and **GUA**, showed one or two major particle distributions, one at a small diameter particle size and another at a larger diameter (Figure 10, c and d). Average particle diameter for **GMA** showed larger size distribution in water (~100 nm) and DMSO (~200 nm), while a sharper peak appeared in acetone and methanol (~140 nm). The **GUA** average diameter was observed at ~ 300 nm in DMSO and ~ 400 nm in acetone and MeOH.

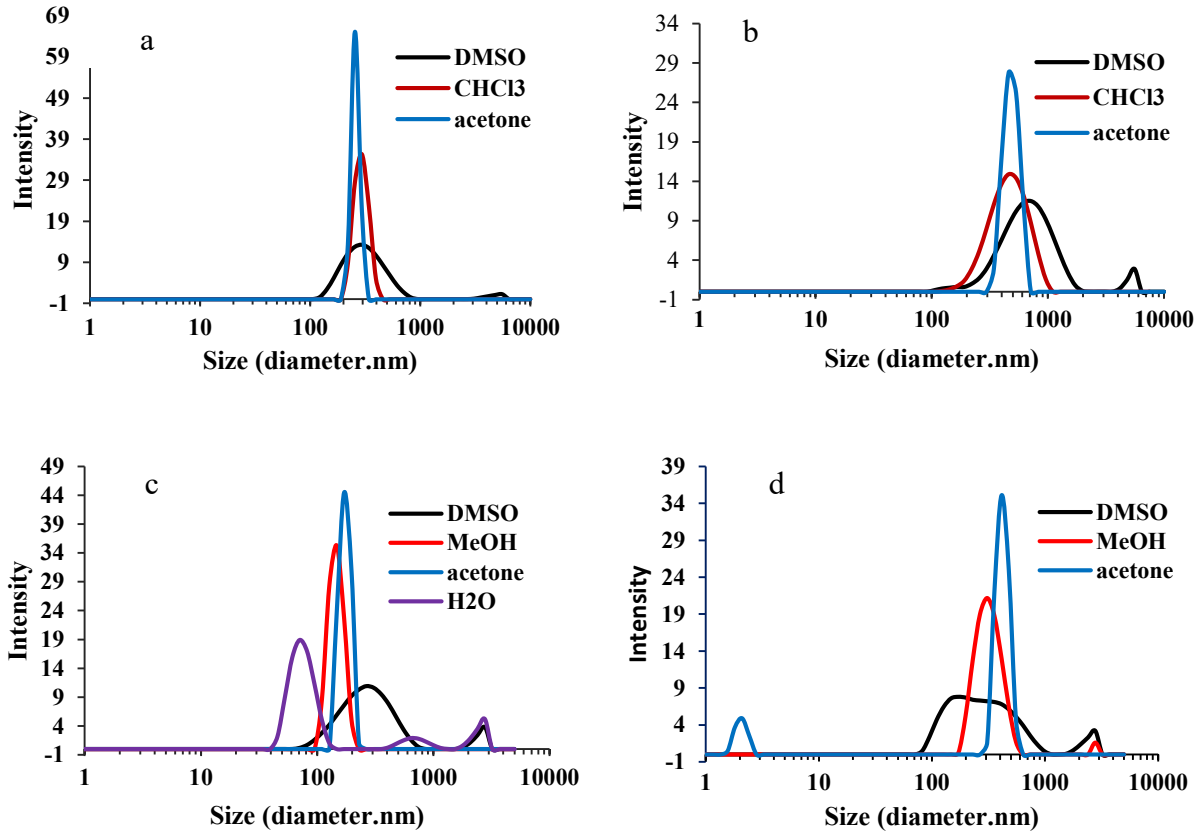

Figure 10 Particle size comparisons of GME (a) and GUE (b) in acetone, $CHCl_3$ and DMSO, GMA (c) and GUA (d) in DMSO, MeOH, acetone and H_2O. Conditions: GME (0.854 mM), GUE (0.647 mM), GMA (0.608 mM) and GUA (0.453 mM), room temperature measurements.

Several factors affect agglomeration formation including concentration, pH, and temperature.[41–43] According to previous studies, dilution may assist in reducing agglomeration.[44] The size distribution range for **GMA** (1.940 – 0.0061 mM) in DMSO showed the presence of a large numbers of smaller particles (≤ 5 nm) at lower concentrations. (Figure 11). This analysis represents the number of particles versus their sizes. The majority of particles at 0.015 mM have sizes of ≤10 nm. However, DLS analysis indicated that larger particles (~ 100 nm) with less numbers are also present at 0.015 mM **GMA** solution.

The effect of pH on the aggregation behavior of **GUA** was investigated by DLS measurements. Results were obtained for range of pH (10.1 – 3.80), as shown in Figure 12. Both acidic and basic environments helped to reduce the size of particles. More importantly, larger particles were transformed to micellar structures at acidic pH (3.80). A significant decrease in the agglomeration diameter from 200 nm at pH 7 to 10 nm at pH 3 were obtained. The decrease in pH results in protonation of amine groups which can enhance the electrophilic repulsion among the particles. The effect of acidic pH on **GUA** provides potential for applications in selective drug delivery to a certain tissues with lower pH, such as tumor tissues.[43]

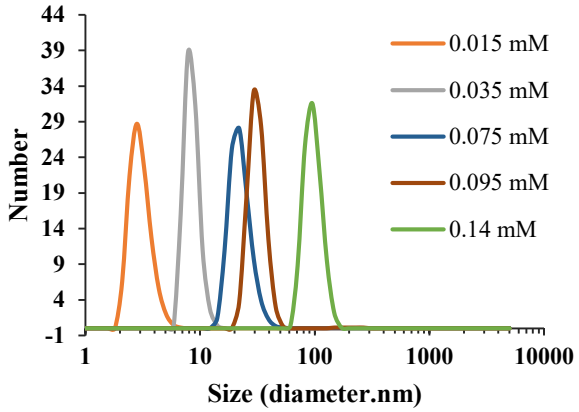

Figure 11 Particle size distribution of GMA in DMSO at different concentrations. Conditions: Room temperature measurements.

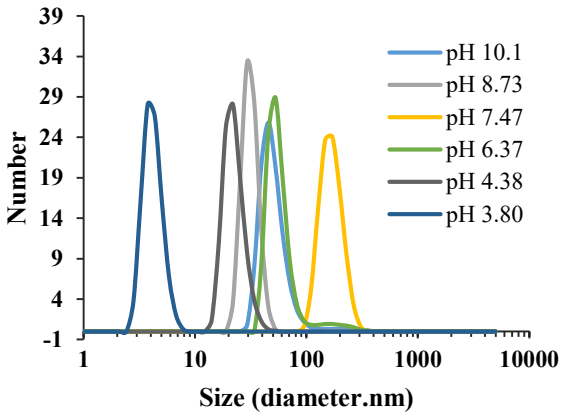

Figure 12 Particle size distribution of GUA at different pHs Condition: GUA in H_2O (0.253 mM), room temperature measurements.

The effect of temperature on particle size was also studied. Higher temperatures tended to reduce the particle size distribution and sharpen the signals (Figure 13, a). As temperature increased to 80 °C, 0.854 mM **GUA** showed significantly sharper peaks. The VT-NMR of **GUA** also showed sharpened proton signals at higher temperatures. In the other hand, as the temperature was lowered in acetone, peak sharpness decreases and particle size distribution noticeably increased. This can explain the VT-NMR studies of **GME** at lower temperatures where peak broadness and loss of splitting occurred (Figure 13, b).

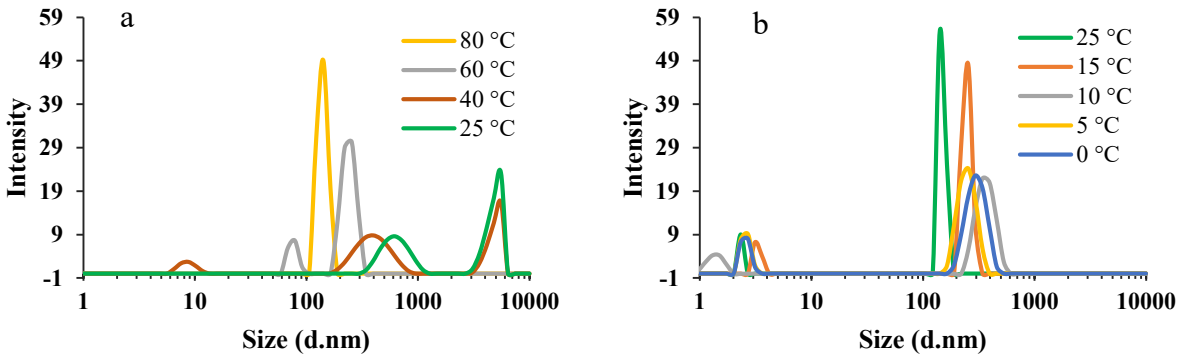

Figure 13 Particle size distribution of GUA in DMSO and GME in acetone at different temperatures. Condition: GUA (0.854 mM) and GME in acetone (0.253 mM).

3.4 Electron Microscopic Analysis

The aggregation behavior of ester and acid derivatives of glutamic acid resorcinarene cavitand was investigated by TEM and SEM. The **GME** and **GUE** showed spherical agglomerations with average dimension of 200 - 500 nm, respectively (Figure 14, a and b). The observed dimensions were consistent with the DLS measurements. Furthermore, **GME** and **GUE** showed a narrow distribution of spherical agglomeration by SEM (Figure 14, c and d).

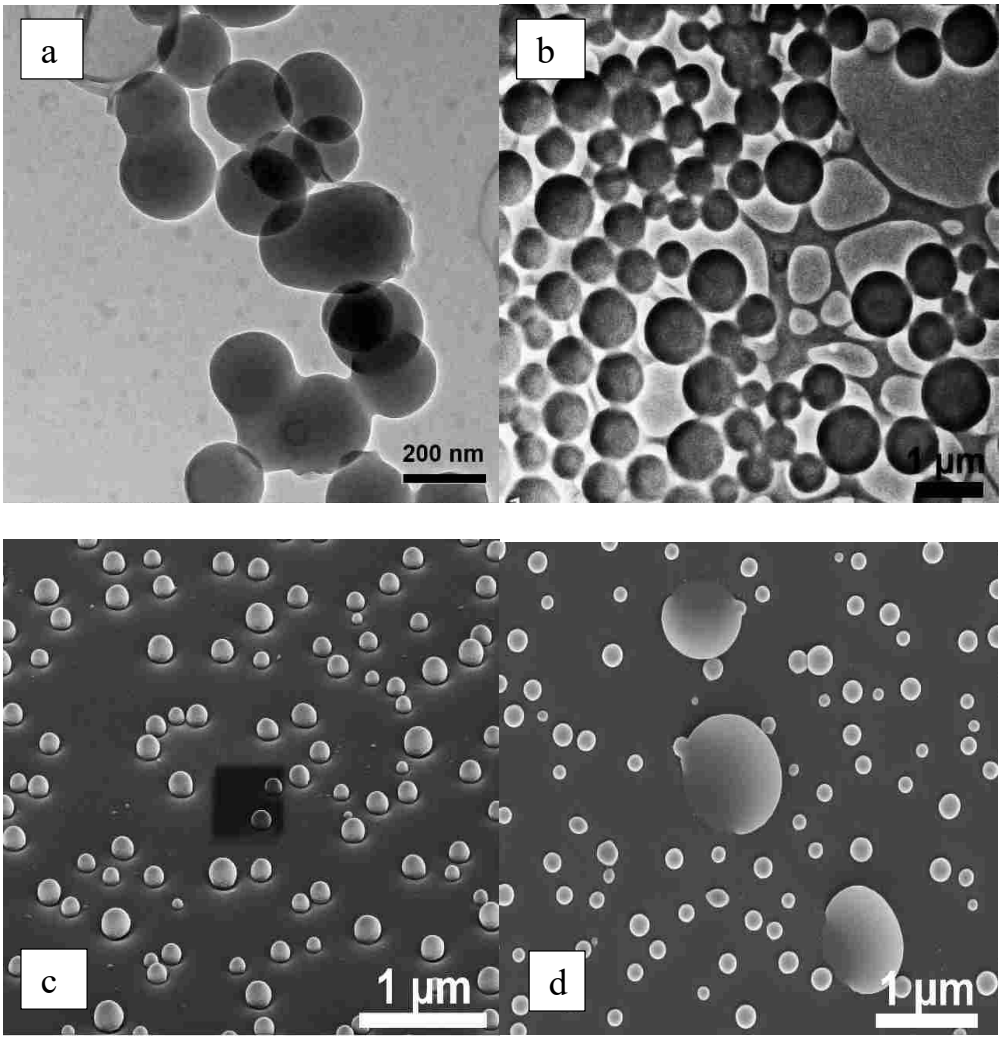

Figure 14 TEM and SEM images of GME (a and c) and GUE (b and d). Conditions: 0.0066 mM ester derivatives were prepared in acetone for TEM and SEM analysis. SEM samples were sputtered with gold before imaging.

SEM images of the **GMA** and **GUA** were obtained and showed spheres with wider size distributions than ester derivatives (Figure 15, a and b). Additionally, floccule structures were observed in a water solution of **GUA** after 1 week. Previous studies by Huang et al. showed that these type of structures became consistently larger the incubation time increased.[45] The morphology of these aggregates was examined by SEM are shown in Figure 15, c and d.

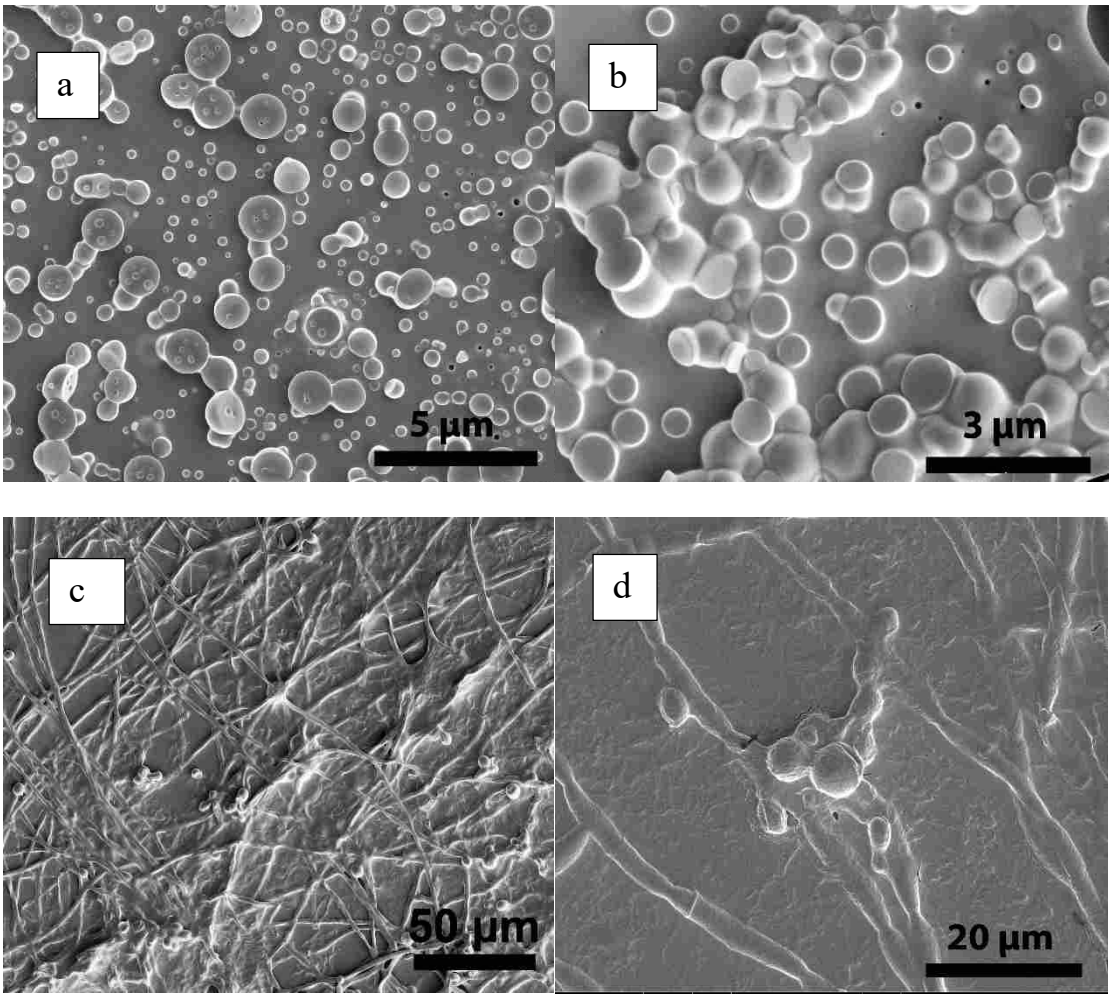

Figure 15 TEM images of GMA (a), GUA (b), and GUA (c and d). Conditions: 0.0066 mM of GMA (a) and GUA (b) were prepared in acetone. 0.0066 mM of GUA incubated for 1 week in water.

As mentioned, increasing temperature leads to smaller particle size with significantly narrower size distribution. SEM images of **GME** (a) and **GUE** (b) were obtained from 0.0066 mM acetone solution on the surface of a hot silicon wafer (Figure 16, a and b). The obtained SEM images show the formation of smaller sized particles than the particles at room temperature (Figure 14) for the ester derivatives.

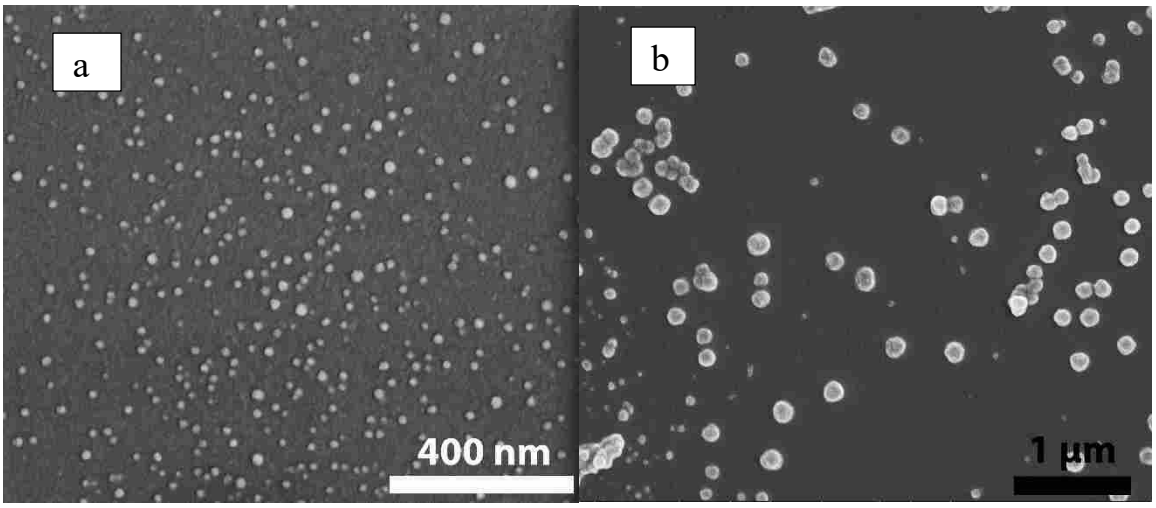

Figure 16 SEM images of GME (left) and GUE (right) cavitands, dissolved in acetone and dried on a silicon grid at 60 ˚C.

Conclusion

Deep chiral cavitands **GMA** and **GUA** were synthesized and characterized by different techniques. They have a tetramer structure. Ester and acid derivatives were fully characterized with NMR, mass spectroscopy, DLS, SEM, and TEM techniques. A series of amine guests with different substituent groups were used to analyze the binding strength and chiral recognition of **GMA** in DMSO. A comparison of binding constants between **GMA** and **PGA** showed the importance of tetramer structure in enhancing the binding strength between amines and host molecules. The greatest chiral discrimination was observed for secondary amines. DLS analysis showed the presence of agglomeration for ester and acid derivatives. The stimuli for reducing agglomerations were found to be concentration, pH, and temperature.

Acknowledgments

We are grateful for financial support from Thermo Scientific and Brigham Young University.

References

(1) Hogberg, A. G. S. *J. Am. Chem. Soc* **1980**, *102*, 6046–6050.

(2) Moran, J. R.; Ericson, J. L.; Dalcanale, E.; Bryant, J. A.; Knobler, C. B.; Donald, C. J. *J. Am. Chem. Soc* **1991**, *113*, 5707–5714.

(3) J. R. Moran, S. Karbach, D. J. C. *J. Am. Chem. SOC* **1982**, *104* (7), 5826–5828.

(4) Purse, B. W.; Rebek, J. *Proc. Natl. Acad. Sci. U. S. A.* **2005**, *102* (31), 10777–10782.

(5) Wieser, C.; Dieleman, C. B.; Matt, D. *Coord. Chem. Rev.* **1997**, *165*, 93–161.

(6) Szumna, A. *Chemistry* **2009**, *15* (45), 12381–12388.

(7) Restorp, P.; Rebek, J. *J. Am. Chem. Soc.* **2008**, *130* (36), 11850–11851.

(8) Evans, N. H.; Rahman, H.; Davis, J. J.; Beer, P. D. *Anal. Bioanal. Chem.* **2012**, *402* (5), 1739–1748.

(9) Qureshi, I.; Qazi, M. A.; Memon, S. *Sensors Actuators B Chem.* **2009**, *141* (1), 45–49.

(10) Cevasco, G.; Thea, S.; Vigo, D.; Williams, A.; Zaman, F. *J. Phys. Org. Chem.* **2006**, *19* (10), 630–636.

(11) El Moll, H.; Sémeril, D.; Matt, D.; Youinou, M.-T.; Toupet, L. *Org. Biomol. Chem.* **2009**, *7* (637858), 495–501.

(12) McIldowie, M. J.; Mocerino, M.; Ogden, M. I. *Supramol. Chem.* **2010**, *22* (1), 13–39.

(13) Szumna, A. *Chem. Soc. Rev.* **2010**, *39* (11), 4274–4285.

(14) Pham, N. H.; Wenzel, T. J. *Tetrahedron: Asymmetry* **2011**, *22* (6), 641–647.

(15) Li, N.; Yang, F.; Stock, H. a; Dearden, D. V; Lamb, J. D.; Harrison, R. G. *Org. Biomol. Chem.* **2012**, *10* (36), 7392–7401.

(16) Kodiah Beyeh, N.; Cetina, M.; Rissanen, K. *Chem. Commun. (Camb).* **2014**, *1* (0), 12–14.

(17) Ruderisch, A.; Pfeiffer, J.; Schurig, V. *Tetrahedron: Asymmetry* **2001**, *12*, 2025–2030.

(18) Arnott, G.; Hunter, R. *Tetrahedron* **2006**, *62* (5), 992–1000.

(19) Thordarson, P. *Chem. Soc. Rev.* **2011**, *40* (3), 1305–1323.

(20) O'Farrell, C. M.; Wenzel, T. J. *Tetrahedron: Asymmetry* **2008**, *19* (15), 1790–1796.

(21) Wenzel, T. J. *J. Incl. Phenom. Macrocycl. Chem.* **2013**, *78* (1-4), 1–14.

(22) Dumele, O.; Trapp, N.; Diederich, F. *Angew. Chemie Int. Ed.* **2015**, *54*, 1–7.

(23) Persch, E.; Dumele, O.; Diederich, F. *Angew. Chemie - Int. Ed.* **2015**, No. 150, 3290–3327.

(24) Saito, S.; Nuckolls, C.; Rebek, J.; Torrey, N.; Road, P.; Jolla, L. *J. Am. Chem. Soc* **2000**, *122* (40), 9628–9630.

(25) Mann, E.; Rebek, J. *Tetrahedron* **2008**, *64* (36), 8484–8487.

(26) Tufvesson, P.; Lima-Ramos, J.; Jensen, J. S.; Al-Haque, N.; Neto, W.; Woodley, J. M. *Biotechnol. Bioeng.* **2011**, *108* (7), 1479–1493.

(27) Blacker, J.; Headley, C. E. *Green Chem. Pharm. Ind.* **2010**, 269–288.

(28) Mansikkama, H. *New J. Chem* **2005**, *29*, 116–127.

(29) Beyeh, N. K.; Pan, F.; Valkonen, a; Rissanen, K. *CrystEngComm* **2015**, *17*, 1182–1188.

(30) Dionisio, M.; Maffei, F.; Rampazzo, E.; Prodi, L.; Pucci, A.; Ruggeri, G.; Dalcanale, E. *Chem. Commun. (Camb).* **2011**, *47* (23), 6596–6598.

(31) Jie, K.; Zhou, Y.; Yao, Y.; Huang, F. *Chem. Soc. Rev.* **2015**, *44*, 3568–3587.

(32) Slovak, S.; Evan-Salem, T.; Cohen, Y. *Org. Lett.* **2010**, *12* (21), 4864–4867.

(33) Pashirova, T. N.; Lukashenko, S. S.; Kosacheva, E. M.; Leonova, M. V.; Vagapova, L. I.; Burilov, a. R.; Pudovik, M. a.; Kudryavtseva, L. a.; Konovalov, a. I. *Russ. J. Gen. Chem.* **2008**, *78* (3), 402–409.

(34) Kubitschke, J.; Javor, S.; Rebek, J. *Chem. Commun. (Camb).* **2012**, *48* (74), 9251–9253.

(35) Billman, J. H.; Harting, W. F. *Amin. Acids Phthalyl Deriv.* **1948**, 1473–1474.

(36) Azov, B. V. A.; Beeby, A.; Cacciarini, M.; Cheetham, A. G.; Diederich, F.; Frei, M.; Gimzewski, J. K.; Gramlich, V.; Hecht, B.; Jaun, B.; Latychevskaia, T.; Lieb, A.; Lill, Y.; Marotti, F.; Schlegel, A.; Schlittler, R. R.; Skinner, P. J.; Seiler, P.; Yamakoshi, Y. *Adv. Funct. Mater.* **2006**, *16*, 147–156.

(37) Pochorovski, I.; Diederich, F. *Acc. Chem. Res.* **2014**, *47* (7), 2096–2105.

(38) Dalcanale, E.; Azov, V. A.; Diederich, F. *Chem. Eur. J.* **2006**, *12*, 4775–4784.

(39) Ulatowski, F.; Kajetan, D.; Ba, T.; Jurczak, J. *J. Org. Chem* **2016**, *81* (6), 1746–1756.

(40) Panahi, T.; Weaver, D. J.; Lamb, J. D.; Harrison, R. G. *Analyst* **2016**, *141*, 939–946.

(41) Yao, Y.; Xue, M.; Chen, J.; Zhang, M.; Huang, F. *J. Am. Chem. Soc.* **2012**, *134* (38), 15712–15715.

(42) Duan, Q.; Cao, Y.; Li, Y.; Hu, X.; Xiao, T.; Lin, C.; Pan, Y.; Wang, L. *J. Am. Chem. Soc.*

2013, *135* (28), 10542–10549.

(43) Cao, Y.; Hu, X. Y.; Li, Y.; Zou, X.; Xiong, S.; Lin, C.; Shen, Y. Z.; Wang, L. *J. Am. Chem. Soc.* **2014**, *136* (30), 10762–10769.

(44) Ajami, D.; Rebek, J. *Supramol. Chem.* **2013**, *25* (9-11), 574–580.

Chapter 3 Separation of Uremic Toxins from Urine with Resorcinarene-based Ion Chromatography Columns

Abstract[1]

People with chronic kidney disease suffer from uremic toxins which accumulate in their bodies. Detection and quantification of uremic toxins help diagnose kidney problems and start patient care. The aim of this research was to seek a new method to assist this diagnosis by trace level detection and separation of guanidine containing uremic toxins in water and urine. To detect and quantify the uremic toxins, new stationary phases for ion chromatography (IC) columns based on glutamic acid functionalized resorcinarenes bound to divinylbenzene macroporous resin were prepared. The new column packing material afforded separation of the five compounds: guanidinoacetic acid, guanidine, methylguanidine, creatinine, and guanidinobenzoic acid in 30 minutes. Peak resolutions ranged from 7.6 to 1.3. Gradient elutions at ambient temperature with methanesulfonic acid (MSA) solution as eluent resulted in detection levels in water from 10 to 47 ppb and in synthetic urine from 28 to 180 ppb. Limits of quantification for the analytes using pulsed amperometric detection were 30 to 160 ppb in water and 93 to 590 ppb in urine. Trace levels of creatinine (1 ppt) were detected in the urine of a healthy individual using the columns.

Keywords: uremic toxins; resorcinarene; separations; ion chromatography

[1] This research has been published.
Panahi, T.; Weaver, D. J.; Lamb, J. D.; Harrison, R. G. *J. Chromatogr. A* **2015**, *1376*, 105–111.

1. Introduction

Chronic kidney disease (CKD) affects more than twenty million Americans. When the kidneys do not function correctly, molecules are not excreted from the body, resulting in adverse effects such as impaired cognitive functions and epileptic seizures [1,2]. These harmful compounds are called uremic toxins and range from small water-soluble molecules to large proteins. Detection of abnormal concentrations of uremic toxins in blood or urine indicates a person has CKD and needs treatment. New methods to quantify uremic toxins are being developed and one is the subject of this research [3-7].

One subgroup of uremic toxins contains the guanidine unit and includes: guanidine (G), methylguanidine (MG), guanidinoacetic acid (GAA), guanidinobenzoic acid (GBA), and creatinine (CRN) (Figure 1). It has been shown that the levels of these guanidine molecules increase in biological fluids and tissues in patients with CKD and that abnormal levels of these compounds are toxic [8-10]. In another study, it was found that the levels of some guanidine compounds increased greatly in serum and cerebrospinal fluid of uremic patients, while the levels of other compounds in this group were not changed or even decreased [11-13].

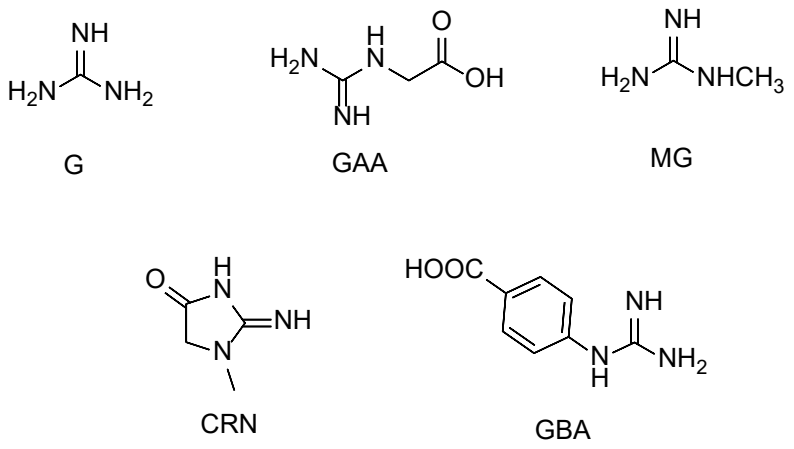

Figure 1 Uremic toxins guanidine (G), guanidine acetic acid (GAA), methylguanidine (MG), creatinine (CRN) and guanidine benzoic acid (GBA).

There is significant clinical importance for sensitive and selective methods to determine trace amounts of these compounds in biofluids. Chromatography is a common analysis method and has advantage over enzymatic and spectrochemical methods in that it has the ability to separate and detect multiple components while eliminating interfering species [11.12]. Among the different chromatography methods, reversed-phase high performance liquid chromatography (HPLC) has been applied to quantify uremic toxins [14]. Several detection methods have been used with HPLC. Lack of strong chromophoric groups for UV-vis detection in some of the uremic toxins led to the use of derivatizing reagents with reverse-phase HPLC [9,10,15,16]. Also, mass spectrometry has been coupled to HPLC to detect uremic toxins [17-20].

Although guanidino uremic toxins are protonated in aqueous solution and are thus ionic, there are only a few examples of ion chromatography (IC) applied to their separation [16,21-23]. As previously mentioned [14], IC columns were used in conjunction with HPLC to pre-concentrate or separate polar compounds [24,25]. Also, three ion exchange chromatography methods, a strong cation-exchanger (RSO_3^-), weak cation-exchanger ($RCOO^-$) and a reversed-

phase column, were compared for the determination of creatinine in serum [26]. The weak cation exchange method was preferred due to less interference of matrix, higher success in determination of the favored analyte, and the simplicity of the method.

IC has shown promise in the quantification of many pharmaceuticals such as antibiotics, drugs, drug impurities and excipients [27]. Two recent studies separated uremic toxins from biological fluids using IC. One study analyzed creatinine in mouse and rat serum by an ion exchange chromatography system [8]. Another study showed the determination of guanidine in a high salt and protein matrix and applied the cation exchange column Dionex CS14 (4 × 250 mm) and a guard column (4 × 50 mm) [16]. As with HPLC, several IC systems rely on pre- or post-column derivatization for detection of guanidino compounds and uremic toxins [11, 28, 29].

To alleviate the need of derivatization, we considered electrochemical detection (ED) to be a good option. The combination of ED and IC for the detection of guanidine compounds has not been explored; however ED has been successfully employed to detect some pharmaceuticals [27]. For example, one study reported using a Ni_2O_3 electrode with anion-exchange chromatography to determine the effect of eluent concentration on uremic dialysate and serum samples [30].

In this paper we demonstrate that a new IC packing material effectively separates uremic toxins in aqueous media and urine by a straightforward method. The new column packing material contains resorcinarene-based molecules functionalized with glutamic acids (GUA). Resorcinarenes have proven to be excellent separation materials for IC [31-33]. The separation and quantification in this work was accomplished with a cation-exchange stationary phase and the direct detection with ED; as a result, pre- or post-column derivatization reagents were not needed. The robustness of the column at room and elevated temperatures were examined and

found to be excellent. This direct detection of nanomolar amounts of uremic toxins in urine with easy sample preparation provides a simple method for determination of these toxins.

2. Materials and methods

2.1. Reagents

Analytical grade reagents including 50% NaOH solution, methanesulfonic acid (MSA), and guanidine compounds were obtained from commercial suppliers. Milli-Q water, 18 Megohm/cm resistivity, was utilized in the preparation of all eluents and standards. A solution of 1 M sodium hydroxide was used as the post column additive for pulsed amperometric detection. The glutamic acid resorcinarene was synthesized in a manner similar to previous compounds [34]. Thermo Scientific (Sunnyvale, CA) provided the 4.6 μm particle size styrene-divinylbenzene polymeric macroporous resin.

2.2. GUA column preparation

To prepare the column material, a slurry was made of 0.050 g of the glutamic acid resorcinarene, 1.5 g of polystyrene resin and 25 mL of methanol. After mixing thoroughly the slurry was dried at room temperature. Then the resin material was ground with a mortar and pestle for 4 hours while 30 mL of deionized water was added slowly. After this, the resin was packed into a 3 x 150 mm black PEEK column at 60 °C and 4000 psi for 15 minutes using a Haskel high pressure pump.

The GUA column was packed with 55% cross-linked divinylbenzene macroporous resin with the average diameter of 4.6 μm. The resin surface area was 350 m^2/g and the applied amount for each column was 1.5 g. With the length of GUA at 3 nm, the resin could accommodate 6.0 x 10^{-5} mol, (0.117 g) of GUA lying down lengthwise on the resin. Adding 0.050 g of GUA and

realizing all of it will not by lying flat on the surface, means that less than half of the resin is occupied by GUA.

2.3. Analyte preparation for separations and calibration curves

Dilute solutions (50 and 100 ppm) of each analyte were prepared in deionized water from 300 ppm stock solutions and stored in plastic bottles in the refrigerator at 4 °C. The synthetic urine was prepared according to the method published [35]. The urine was centrifuged at 4000 rpm for 5 min and filtered through a 0.25 μm mesh Thermo Scientific Nalgene syringe filter, which is a surfactant-free cellulose acetate filter. The filtered solution was kept in a plastic bottle in the refrigerator at 4 °C. The real urine sample from a healthy individual was filtered through cellulose filter paper and centrifuged at 1000 rpm for 10 min. It was then passed through a 2 μm Nalgene syringe filter, a 3k Millipore Amicon ultra centrifugal filter, and Strata C18-E (55 μm, 70A). Before analysis, 1 mL of synthetic urine was diluted to 5 mL and 0.5 mL of real urine was diluted to 5 mL with Milli-Q water.

For the calibration curves, each analyte was analyzed separately three times and the solution concentrations for integrated pulsed amperometric detection (IPAD) ranged from 1 - 10 ppm in water and 2 - 60 ppm in the synthetic urine. To calculate the limit of detection (LOD), the equation LOD = 3.3(SD/S) was used where SD is the standard deviation and S is the slope of the line of the calibration equation. Limit of quantification (LOQ) was obtained by the equation LOQ = 10(SD/S). To calculate the linearity of the procedure, 5 different concentrations of analytes were added to the urine solution.

2.4 Column capacity

Dynamic binding capacity was measured by breakthrough curves using guanidinebenzoic acid (GBA) as electroactive sample. The packed column was flushed with a 20 mM NaCl solution for 30 min and water for 30 min at 0.3 mL/min. Then, 1 mM GBA was passed through the column at 0.3 mL/min. The dynamic binding capacity was calculated using the equation: $Q = CF(t_b-t_v)$, where Q is the dynamic binding capacity (mM/column), C is the concentration of GBA, F is the flow rate (mL/min), t_b is the breakthrough time (min), and t_v is the void time (min) [36]. Column porosity was calculated by dividing the column void volume by the total empty column volume. The void volume, 0.66 mL, was found by multiplying the void time (2.2 min) by the flow rate, (0.30 mL/min). The total volume for the column (3 x 150 mm) was 1.06 cm^3.

2.5 SEM sample preparation

Resin for SEM images was prepared by placing resin on carbon-coated copper grids and sputtering 2-3 nm gold nanoparticles on it.

2.6 Pulse amperometric detector

The electrochemical waveform was +0.13V from 0.00 to 0.05 s, +0.33V from 0.05 s to 0.21 s, +0.55V from 0.22 s to 0.46 s, +0.33V from 0.47 s to 0.56 s, −1.67V from 0.57 s to 0.58 s, +0.93V at 0.59 s, and +0.13V at 0.60 s. The pH reference electrode mode with current integrated was set up between 0.21 and 0.56 s for detection. This waveform is an AAA-Direct waveform, which is composed of a 4-potential program and uses reductive cleaning rather than oxidative cleaning [37]. This pattern preserves the gold working electrode surface. In this study, an integrated pulsed amperometric detection (IPAD) waveform was used to determine uremic

toxins which is an enhanced 4-potential program. The basic advantage of the IPAD waveform is the detection of analytes using one more potential than the PAD waveform.

2.7. Instrumentation

A Dionex ICS-3000 chromatography system (Thermo Scientific, Sunnyvale, CA, USA) with an AS40 autosampler and integrated pulsed amperometric detector (IPAD) were used. A gold working electrode (conventional) and Ag/AgCl reference electrode were equipped on the IPAD. The injection volume for the IPAD was 5 μL. The Dionex Chromeleon workstation ran the collection and subsequent data analysis. Basic pH conditions were needed at the surface of the gold electrode and were provided by a post column reactor (pneumatic pump) containing 1 M NaOH by means of a mixing-T at a flow rate of 0.5 mL/min. The pH at the reference electrode was 12.5-13.0. The delivery rate of sodium hydroxide solution was adjusted to keep the pH constant at different concentrations of acidic eluent. Dionex IonPac CG17 was used a guard column for the real urine samples. Columns were operated at room temperature. SEM images were taken on a FEI Helios Nano lab 600.

3. Results and discussion

3.1. Separators

Macrocyclic compounds such as crown ethers, cryptands, and cyclodexterins have for years been incorporated into the stationary phases of chromatography systems to improve the separation selectivity and efficiency of the columns [38-40]. Calixarenes and resorcinarenes, another family of macrocycles, having surfaces easily functionalized with polar, cationic and anionic groups, have achieved excellent separations of some species [41-45]. As a way to create new stationary phases, our group has designed IC columns based on resorcinarenes that

selectively separate cations and anions [46,47]. In the present research, the resorcinarenes were synthesized by adding glutamic acid groups to quinoxalines, which quinoxalines were in turn bonded to a resorcinarene scaffold (Figure 2). These resorcinarenes contain eight carboxylic acid groups clustered on one face of the molecule. Depending on pH, the acid groups will be neutral or anionic and provide cation exchange sites. Furthermore, the phenyl groups at the midsection of the resorcinarene can interact through hydrophobic interactions with nonpolar groups on the analyte. The long alkyl chains on the lower rim of the resorcinarene are designed to act as adhering groups to the polystyrene packing material, a method that has repeatedly been shown to provide long-term column stability [31,34].

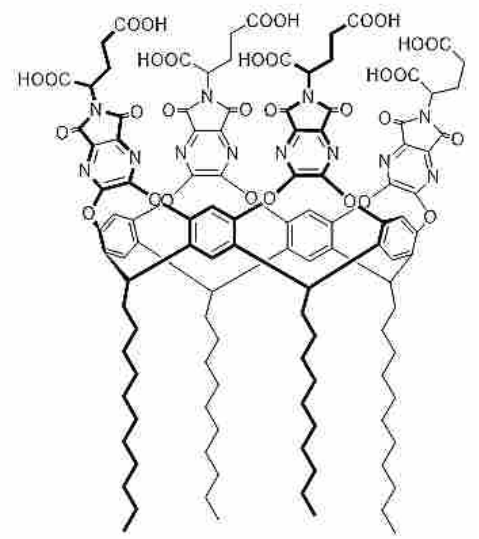

Figure 2 Glutamic acid resorcinarene with undecyl groups (GUA).

3.2 Separation of guanidine compounds in water and urine on the GUA column

3.2.1. Isocratic elution in water

The effect of different concentrations of MSA on the retention times of standards was examined and the results are shown in Figure 3. Rinsing the column with the concentration of MSA used as eluent for 10 min before each injecting allowed the column to equilibrate and was important to obtain a reproducible analyte separation. Concentrations of 1, 2, 3, and 4 mM MSA resulted in the elution of all of the compounds, except the GBA. With 1 mM MSA, retention times were 6.31 (GAA), 7.21 (G), 8.81 (MG), 9.66 (CRN) min. Increasing the eluent to 4 mM resulted in retention time decreases to 6.01 (GAA), 6.50 (G), 6.98 (MG), 8.13 (CRN); concurrently, resolution was reduced. Increasing the MSA concentration to 5 mM helped elute GBA in less than 40 min. When the concentration of MSA was increased to more than 5 mM, the first four compounds eluted with very close retention times and poor resolution. As is shown in Figure 3, with 8 mM MSA, retention times were 4.3 (GAA), 4.96 (G), 5.73 (MG), and 6.56 (CRN) min. In general, analyte retention order is dictated by analyte charge, solvated volume, and polarizability. In the case of these analytes, since they will all have the same charge at the acidic pH of the eluent, the solvated volume is predicted to be the most dominant factor in retention order.

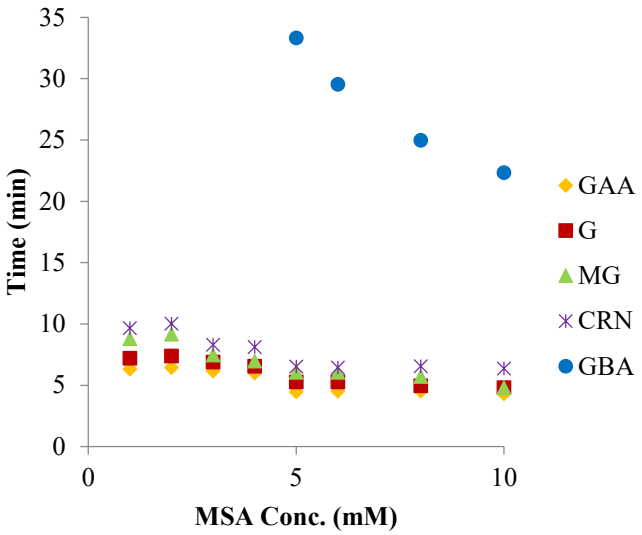

Figure 3 Effect of MSA concentration on the retention time of the guanidine compounds with the GUA column. Conditions: flow rate 0.3 mL/min; MSA eluent, ambient temperature, Au working electrode.

3.2.2. Two-step gradient elution in water

Separation of the five analytes (GAA, G, MG, CRN, GBA) was performed by a two-step gradient on the GUA column at a flow rate of 0.3 mL/min. The best separation with the two-step elution was achieved with 2 mM MSA for 20 min and 8 mM MSA for 20 min (Figure 4). This approach has the potential for baseline separation of five analytes in water, with the order of elution being GAA (6.88), G (7.88), MG (9.53), CRN (10.50) and GBA (24.88) min. Column efficiencies calculated using peak widths and retention times for the two-step gradient elution are good for IC separations as shown by the number of theoretical plates per meter in the 20,000 N/m range (Table 1) [48].

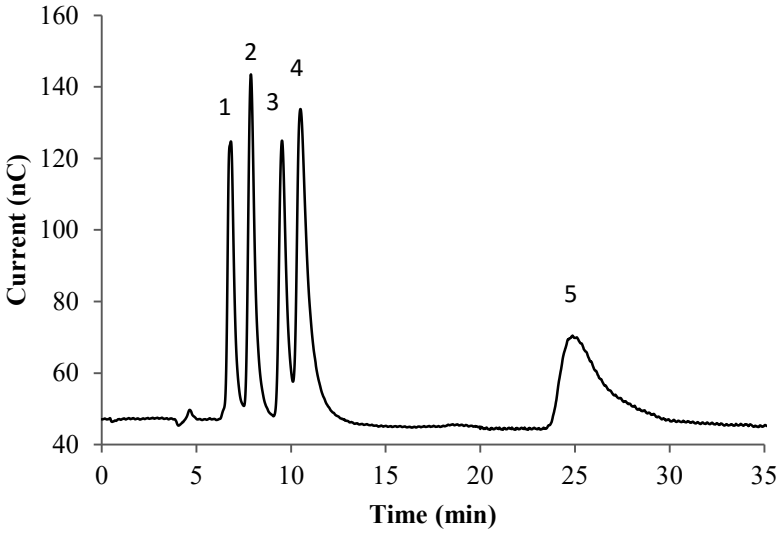

Figure 4 Two-step gradient separation of uremic toxins with GUA column and PAD with conventional working Au electrode. Peak assignment: 1-GAA, 2-G, 3-MG, 4-CRN, and 5-GBA. Condition: flow rate 0.3 mL/min; eluents: 2 mM MSA for 20 min, 8 mM MSA for 20 min. Concentration for each analyte was 10 ppm. Peak resolutions (Rs): Rs1 = 1.66, Rs2 = 2.59, Rs3 = 1.29, Rs4 = 9.84.

3.2.3. Three-step gradient elution in water

A 3-step gradient was performed to improve the baseline separation between analytes. The obtained order of elution was similar that with the 2-step gradient but with different retention times and resolutions. The best separation was achieved with the following program: 1 mM MSA for 10 min, 2 mM MSA for 5 min, 15 mM MSA for 15 min. The resolution factors were 5.6 (GAA-G), 3.7 (G-MG), 1.28 (MG-CRN) and 2.95 (CRN-GBA). Rinsing the column with 2 mM MSA for 10 min before injecting the analytes was important to obtain a good separation and reproducible retention times due to the rinsing protonating the ionic exchange sites.

The comparison of resolution factors between the 2- and 3-step gradients confirmed that a 3-step gradient leads to a better separation (Table 1). The number of theoretical plates per meter using the 3-step gradient was in the range of 20,000 to 100,000 N/m, which is more than the separation with the 2-step gradient with concomitant improvement in resolutions between peaks. The resolution between the first two peaks was much improved over the 2-step gradient. Preference for one gradient over the other depends on the application and matrix composition.

3.2.4. Three-step gradient elution in urine

Synthetic urine contains several compounds such as urea, lactic acid, citric acid and ammonium chloride, which could interfere with the detection of analytes. Indeed, several strong peaks in a chromatogram arise due to these compounds. This difficulty was overcome using the three-step gradient, which separated the five analytes effectively (Figure 5). The gradient was composed of 3 mM MSA for 10 min, 5 mM MSA for 7 min, and 15 mM MSA for 13 min. The order of elution (GAA, G, MG, CRN, and GBA) was the same as it was in water. Baseline separation of the analytes was achieved even though the urine peaks were strong. With this gradient program, the peak resolutions in most cases were even better than the gradient elution of analytes in water. The number of theoretical plates per meter for the analytes ranged from 20,000 to 90,000 N/m, which lies within respectable values for IC (Table 1). The efficiency of the column was confirmed by the separation of low concentrations of analytes. Concentrations of 500 and 250 ppb of analyte were detected in synthetic urine (Figure 6).

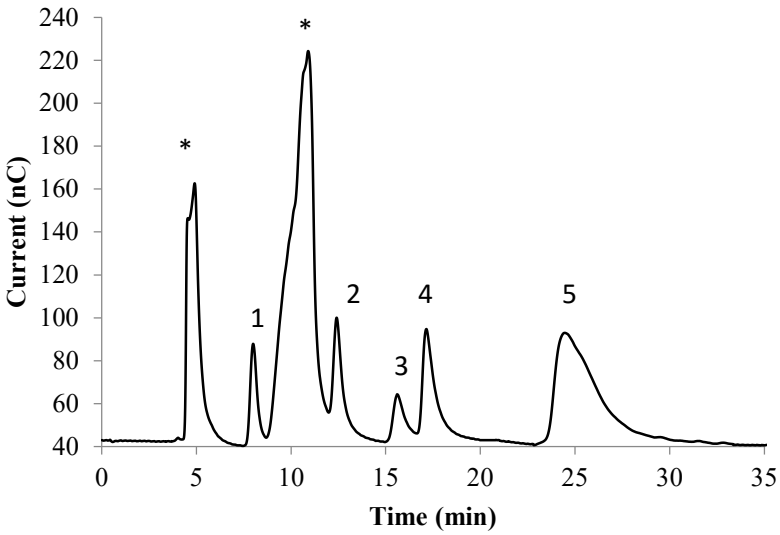

Figure 5 Separation of uremic toxins in urine. Peak assignments: 1-GAA, 2-G, 3-MG, 4-CRN, and 5-GBA (*urine peaks). Condition: flow rate 0.3 mL/min; gradient: 3 mM MSA for 10 min, 5 mM MSA for 7 min, and 15 mM MSA for 13 min. Concentration for each analyte was 4 ppm, except GBA which was 24 ppm. Peak resolutions (Rs): Rs1 = 3.70, Rs2 = 4.79, Rs3 = 4.28, Rs4 = 2.34.

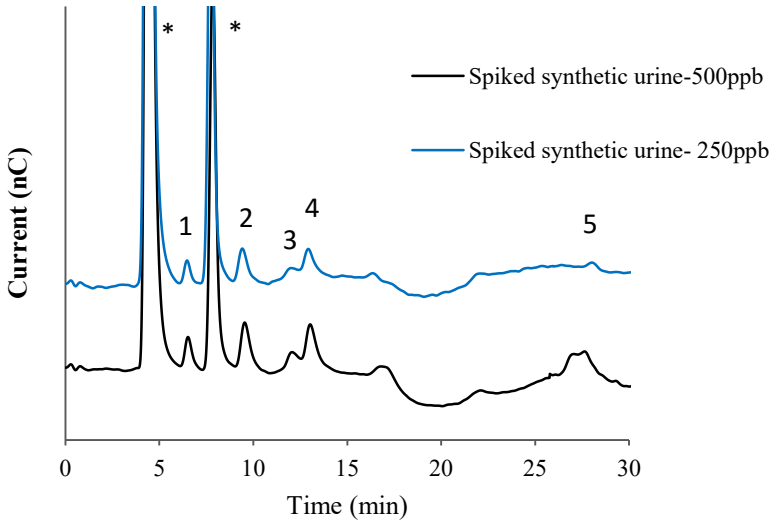

Figure 6 Separation of low concentrations of uremic toxins in urine. Peak assignments: 1-GAA, 2-G, 3-MG, 4-CRN, and 5-GBA (*urine peaks). Condition: flow rate 0.3 mL/min; gradient: 3 mM MSA for 10 min, 5 mM MSA for 7 min, and 15 mM MSA for 13 min. Concentration for each analyte was 500 ppb for lower line and 250 ppb for upper line. Peak resolutions for 500 ppb chromatogram (Rs): Rs1 = 3.86, Rs2 = 3.06, Rs3 = 1.20, Rs4 = 9.79.

Table 1 Chromatographic results for the determination of uremic toxins by gradient elutions with GUA column prepared by grinding.[a]

Solutes	2-step gradient			3-step gradient			3-step gradient in urine		
	t_R (min)[b]	Peak width (min)	Number of plates (N/m)	t_R (min)[b]	Peak width (min)	Number of plates (N/m)	t_R (min)[b]	Peak width (min)	Number of plates (N/m)
GAA	6.72	0.54	26000	8.43	0.71	23000	8.38	0.66	27000
G	7.65	0.58	29000	15.22	1.07	34000	14.12	0.72	64000
MG	9.17	0.59	40000	17.93	0.69	110000	17.13	0.72	94000
CRN	10.07	0.80	26000	19.02	0.94	68000	18.28	0.97	59000
GBA	24.88	2.27	20000	23.6	2.16	20000	26.38	2.26	23000

a. Conditions: 3 × 150 mm GUA column prepared by grinding, flow rate 0.3 mL/min, gradient programs with MSA eluent, ambient temperature. b. retention time.

3.2.5 Real urine analysis

A real urine sample was filtered, diluted and passed through a guard column before analysis. Due to the more complicated matrix, a 5-step gradient was necessary to achieve a successful separation. Unspiked and spiked urine samples were compared and the unspiked samples were found to contain creatinine (CRN), but not any of the other uremic toxins at levels high enough to be detected (Figure 7). The creatinine concentration was 1.6 ppm in the urine. Urine creatinine (24-hour sample) values can range from 500 to 2000 mg/day [2, 49]. The levels of GAA, G, MG, and GBA in a healthy person are normally below 50 ppb [2] and thus were not detected by our technique. The gradient was composed of 1 mM MSA for 10 min, 2 mM MSA for 5 min, and 3 mM MSA for 5 min, 4 mM MSA for 5 min, 15 mM MSA for 5 min. Spiked

urine samples (950 ppb of analyte) resulted in sharp and well resolved peaks in the presence of the complicated matrix.

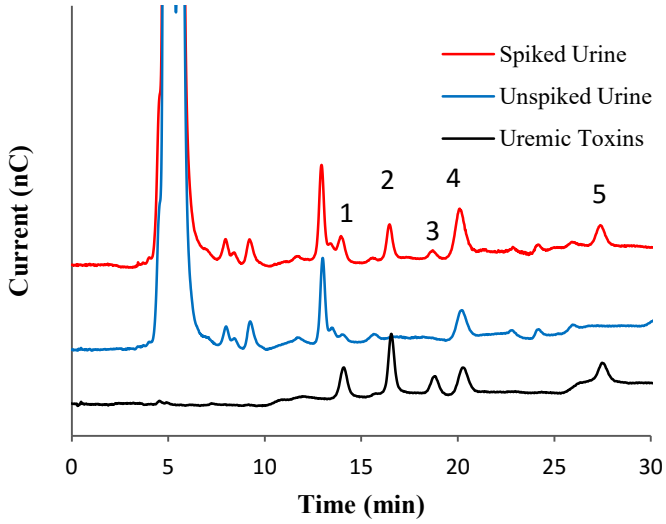

Figure 7 Identification of uremic toxins in real urine. Chromatograms: lower, analytes in water; middle, urine; upper, spiked urine. Peak assignments: 1-GAA, 2-G, 3-MG, 4-CRN, and 5-GBA; the urine components gave rise to the other peaks. Conditions: flow rate 0.3 mL/min; gradient: 1 mM MSA for 10 min, 2 mM MSA for 5 min, and 3 mM MSA for 5 min, 4 mM MSA for 5 min, 15 mM MSA for 5 min. Concentration of each analyte was 950 ppb in lower and upper chromatograms. Peak resolutions of uremic toxins in the spiked urine chromatogram (Rs): Rs1 = 4.58, Rs2 = 3.91, Rs3 = 1.75, Rs4 = 8.22.

3.2.6. Integrated pulsed amperometric detection

IPAD provided a method to detect all of the analytes whether they did or did not have a chromophoric group. This detection method in water and urine achieved good signal-to-noise and measured detection limits in water were (ppb) 10 (GAA), 9 (G), 12 (MG), 40 (CRN), and 12 (GBA) (Table 2). These detection limits were achieved at room temperature with a 0.3 mL/min flow rate. To confirm the reproducibility and sensitivity of the gold working electrode in the

presence of high matrix concentrations, calibration curves were obtained for the analytes in urine. The detection limits in urine turned out to be larger than those in water (Table 3); however, all of the analyte detection limits were in the ppb range. The decrease in the sensitivity of the detector to the analytes in urine is attributed to the interference at the electrode by the urine components: citric acid, ammonia, and lactic acid. The disturbance caused by the urine components was confirmed by injecting just urine. The detection limits for the column are within the concentrations observed in uremic patients' urine and serum, which lie in the range of 100 to 1800 ppb [2,4]. The low detection limits support the feasibility of using PAD for clinical analysis of guanidine compounds.

Table 2 Calibration equations and LODs for analytes at ambient temperature.[a]

Analytes	Linear equation	Correlation coefficient	Concentration range (ppm)	LOD (ppb)[b]	LOQ (ppb)[c]
GAA	y = 4.473x + 9.434	0.916	0.1-10	10	33
G	y = 8.716x + 17.45	0.953	0.1-10	10	30
MG	y = 6.761x + 11.19	0.919	0.1-10	12	41
CRN	y = 7.042x + 22.39	0.921	0.1-10	47	160
GBA	y = 5.166x + 0.949	0.999	0.1-10	12	41

a. Conditions: 3 x 150 mm GUA column prepared by grinding, Au conventional working electrode, flow rate 0.3 mL/min, MSA eluent, and ambient temperature.
b. limit of detection (LOD) which was calculated according to the formula LOD = 3.3(SD/S).
c. limit of quantification (LOQ) which was calculated according to the formula LOQ = 10(SD/S).

Table 3 Calibration equations and LODs for analytes in urine at ambient temperature.[a]

Analytes	Linear equation	Correlation coefficient	Concentration range (ppm)	LOD (ppb)[b]	LOQ (ppb)[c]
GAA	y = 1.016x + 25.87	0.9373	2-60	92	307
G	y = 1.528x + 32.67	0.9631	2-60	28	93
MG	y = 1.110x + 4.405	0.985	2-60	95	319
CRN	y = 1.401x + 15.77	0.9881	2-60	175	591
GBA	y = 4.34x + 28.01	0.9256	2-60	146	487

a. Conditions: 3 x 150 mm GUA column prepared by grinding, Au conventional working electrode, flow rate 0.3 mL/min, MSA eluent, and ambient temperature.
b. limit of detection (LOD) which was calculated according to the formula LOD = 3.3(SD/S).
c. limit of quantification (LOQ) which was calculated according to the formula LOQ = 10(SD/S).

3.2.7. Column robustness

The efficiency and performance of a column often decreases with use, and therefore the columns were tested for stability. The robustness of the packed GUA column was verified by eluting guanidine for 50 runs under isocratic conditions at 25 °C and an additional 50 runs at elevated temperatures. These runs were performed under a flow rate of 0.3 mL/min with 4 mM MSA. The peak areas were ± 1.73 nC and the retention times appeared between 5.57-5.60 min. Retention times, peak areas, and peak shapes did not change significantly from the first to the last run. Furthermore, continual use of the column over time resulted in consistent separations of analytes.

4. Column characterization

The SEM images from the GUA coated resin before and after grinding show that a significant amount of resin has been broken into smaller material (Figure 8). Grinding the resin is important to break up the resin aggregates. This preparation method results in higher

backpressures and slower separations. The slower separations were necessary to separate the analytes from the urine matrix peaks.

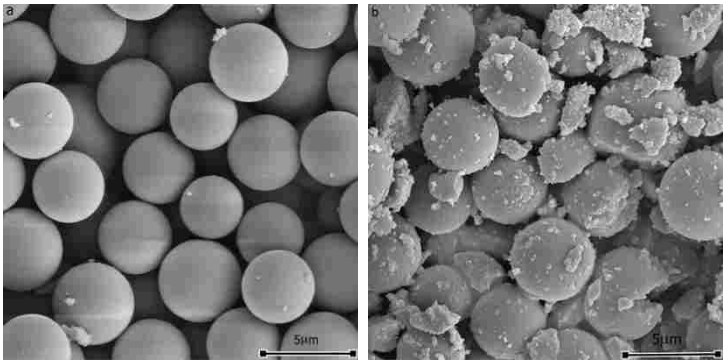

Figure 8 SEM images of resin. Pictures: left, divinylbenzene macroporous resin coated with GUA; right, resin coated with GUA and ground for 4 hours.

Column porosity and dynamic binding capacity affect column resolution and how concentrated the eluent needs to be. The total porosity of the packed column was calculated based on the void volume of the column and total volume of the empty column. The calculated total porosity of the column was found to be 63%. The dynamic binding capacity was found by using 25 mM GBA as eluent and noting a sharp increase in the baseline at 3.8 min. The total measured dynamic binding capacity for the column was 12 mM/column base on the breakthrough calculation. This high binding capacity of the column related to high surface area available for coating with GUA, which apparently arises from small pieces of particles during grinding.

5. Conclusions

This research shows the potential for packing materials based on resorcinarenes for the separation of uremic toxins in water and urine. Three and four step gradient elutions are necessary to obtain good separation of the analytes from each other and matric components. Even in the presence of urine matrix, uremic toxin concentrations were detected in the biological relevant range (ppb) with the new columns using PAD. The 4.5 micron resin was found to be crushed during preparation by grinding. The columns capacity for the 3 x 1500 mm column was 12 mM/column and the columns were stable over many runs. Ion chromatography, although used less often, is well suited to separate guanidino compounds in urine.

Acknowledgments

We are grateful for financial support from Thermo Scientific and Brigham Young University. We thank Chris Pohl (Thermo Scientific) and Andy Woodruff for helpful technical assistance.

References

[1] P. Evenepoel, B.K.I. Meijers, B.R.M. Bammens, K. Verbeke, Kidney Int. Suppl. 14 (2009) S12.

[2] J.U.P.A. Eetjen, M.A.R. Odriguez, B.E.S. Tegmayr, Kidney Int. 63 (2003) 1934.

[3] M. Dobre, T.W. Meyer, T.H. Hostetter, Clin. J. Am. Soc. Nephrol. 8 (2013) 322.

[4] F. Duranton, G. Cohen, R. De Smet, M. Rodriguez, J. Jankowski, R. Vanholder, A. Argiles, J. Am. Soc. Nephrol. 23 (2012) 1258.

[5] M. Idziak, P. Pędzisz, A. Burdzińska, K. Gala, L. Pączek, Exp. Toxicol. Pathol. 66 (2014) 187.

[6] M. Rossi, K. Campbell, D. Johnson, T. Stanton, E. Pascoe, C. Hawley, G. Dimeski, B. McWhinney, J. Ungerer, N. Isbel, Nutr. Metab. Cardiovasc. Dis. (2014) 1.

[7] R. Vanholder, U. Baurmeister, P. Brunet, G. Cohen, G. Glorieux, J. Jankowski, J. Am. Soc. Nephrol. 19 (2008) 863.

[8] A.L. B. Marescau, P. De Deyn, P. Wiechert, L. Van Gorp, J. Neurochem. 46 (1986) 717.

[9] R. Gatti, M.G. Gioia, J. Pharm. Biomed. Anal. 42 (2006) 11.

[10] R. Gatti, M.G. Gioia, J. Pharm. Biomed. Anal. 48 (2008) 754.

[11] T. Hanai, Y. Inamaoto, S. Inamoto, J. Chromatogr. B. Biomed. Sci. Appl. 747 (2000) 123.

[12] C.J. Kochansky, T.G. Strein, J. Chromatogr. B. Biomed. Sci. Appl. 747 (2000) 217.

[13] T. Niwa, Mass Spectrom. Rev. 16 (1998) 307.

[14] D. Saigusa, N. Suzuki, M. Takahashi, K. Shiba, S. Tanaka, T. Abe, T. Hishinuma, Y. Tomioka, Anal. Chim. Acta 677 (2010) 169.

[15] A.J. Kandhro, M.A. Mirza, M.Y. Khuhawar, Anal. Lett. 43 (2010) 2049.

[16] J. Qiu, H. Lee, C. Zhou, J. Chromatogr. A 1073 (2005) 263.

[17] J. Boelaert, F. Lynen, G. Glorieux, S. Eloot, P. Sandra, R. Vanholder, Anal Bioanal Chem 405 (2013) 1937.

[18] T. Niwa, Mass Spectrom. Rev. 30 (2011) 510.

[19] T. Niwa, J. Chromatogr. B. Analyt. Technol. Biomed. Life Sci. 877 (2009) 2600.

[20] M. Yasuda, K. Sugahara, J. Zhang, T. Ageta, K. Nakayama, T. Shuin, H. Kodama, Anal. Biochem. 253 (1997) 231.

[21] K.J. Fountain, A. Kloss, I. Garibyan, B. Blitshteyn, A. Brezzani, S. Kyostio-Moore, A. Zuk, R. Sacchiero, A.S. Cohen, J. Chromatogr. B. Analyt. Technol. Biomed. Life Sci. 846 (2007) 245.

[22] K. Guo, J. Peng, R. Zhou, L. Li, J. Chromatogr. A 1218 (2011) 3689.

[23] J.A. Resines, M.J. Arin, M.T. Díez, P.G. del Moral, J. Liq. Chromatogr. Relat. Technol. 22 (1999) 2503.

[24] Y. Yokoyama, M. Tsuchiya, H. Sato, H. Kakinuma, J. Chromatogr. B Biomed. Sci. Appl. 583 (1992) 1.

[25] Y. Yokoyama, A. Saito, T. Manji, K. Maeda, K. Ohta, J. Chromatogr. 162 (1979) 23.

[26] B. Kågedal, B. Olsson, J. Chromatogr. 527 (1990) 21.

[27] L. Bhattacharyya, J.S. Rohrer, Application of Ion Chromatography for Phamaceutical and Biological Products, John Wiley & Sons. Inc., Hoboken, New Jersey, 2012.

[28] Y. Kobayashi, H. Kubo, T. Kinoshita, J. Chromatogr. A 400 (1987) 113.

[29] B. Marescau, D. Devendra R, M. Kockx, L. Posserniers, I.A. Qureshi, and A.L. B. Marescau, P. De Deyn, P. Wiechert, L. Van Gorp, P.P. De Deyn, Metabolism 41 (1992) 526.

[30] H. Veening, R.M. Van Eften, J. Chromatogr. 526 (1990) 355.

[31] N. Li, L.J. Allen, R.G. Harrison, J.D. Lamb, Analyst 138 (2013) 1467.

[32] J. Wang, R.G. Harrison, J.D. Lamb, J. Chromatogr. Sci. 47 (2009) 510.

[33] J. Wang, J.D. Lamb, L.D. Hansen, R.G. Harrison, J. Incl. Phenom. Macrocycl. Chem. 67 (2010) 55.

[34] N. Li, F. Yang, H.A. Stock, D.V. Dearden, J.D. Lamb, R.G. Harrison, Org. Biomol. Chem. 10 (2012) 7392.

[35] Z. Nie, C.A. Nijhuis, J. Gong, X. Chen, A. Kumachev, A.W. Martinez, M. Narovlyansky, G.M. Whitesides, Lab Chip 10 (2010) 477.

[36] M.F. Wahab, C.A. Pohl, C.A. Lucy, Analyst 136 (2011) 3113.

[37] Dionex Corporation, Optimal settings for pulsed amperometric detection of carbohydrates using the Dionex ED40 electrochemical detector, Technical Note 21, Sunnyvale, CA, Literature product no. 034889-03, August, 1998.

[38] M.F. Wahab, C.A. Pohl, C.A. Lucy, J. Chromatogr. A 1270 (2012) 139.

[39] J. Chong, P. Hatsis, C.A. Lucy, J. Chromatogr. A 997 (2003) 161.

[40] M.C. Bruzzoniti, R.M. De Carlo, K. Horvath, D. Perrachon, A. Prelle, R. Tófalvi, C. Sarzanini, P. Hajós, J. Chromatogr. A 1187 (2008) 188.

[41] B.R. Edwards, A.P. Giauque, J.D. Lamb, J. Chromatogr. A 706 (1995) 69.

[42] K. Kimura, H. Harino, E. Hayata, T. Shono, Anal. Chem. 58 (1988) 2233.

[43] Y. Kitamaki, T. Takeuchi, Anal. Sci. 20 (2004) 1399.

[44] R.H. Pullen, J.J. Brennan, G. Patonay, J. Chromatogr. A 691 (1995) 187.

[45] M. Wössner, K. Ballschmiter, Fresenius. J. Anal. Chem. 366 (2000) 346.

[46] J. Gardner, Q. Peterson, J. Walker, B. Jensen, B. Adhikary, R. Harrison, J. Lamb, J. Memb. Sci. 277 (2006) 165.

[47] J. Wang, R.G. Harrison, J.D. Lamb, J. Chromatogr. Sci. 47 (2009) 510.

[48] S.D. Chambers, M.T. McDermott, C.A. Lucy, Analyst 134 (2009) 2273.

[49] N. Meert, E. Schepers, R.D. Smet, A. Argiles, G. Cohen, R. Deppisch, T. Drueke, Z. Massy, G. Spasovski, B. Stegmayr, W. Zidek, J. Jankowski, R. Vanholder, Artif. Organs. 31 (2007) 600.

Chapter 4 A New Approach for Trace Analysis of Guanidine Compounds in Surface Water with Resorcinarene-based Ion Chromatography Columns

Abstract[2]

Trace levels of pharmaceuticals have been detected in surface water and may pose a health risk to humans and other organisms. New chromatographic materials will help identify and quantify these contaminants. We introduce a new ion chromatographic (IC) material designed to separate cationic pharmaceuticals and report its ability to separate a group of guanidine compounds. Guanidine moieties are strongly basic and protonated under acid conditions, and therefore can potentially be separated on the newly designed stationary phase and detected by ion exchange chromatography. The new column packing material is based on glutamic acids bonded to resorcinarene moieties that in turn are bound to divinylbenzene macroporous resin. Detection limits in the range of 5 - 32 μg L^{-1} were achieved using integrated pulsed amperometric detection (IPAD) for guanidine (G), methylguanidine (MG), 1,1-dimethylbiguanide (DMG), agmatine (AGM), guanidinobenzoic acid (GBA) and cimetidine (CIM). Suppressed conductivity (CD) and UV-vis detection resulted in limits of detection similar to IPAD, in the range of 1.7 - 66 μg L^{-1}, but were not able to detect all of the analytes. Three water sources, river, lake, and marsh, were analyzed and despite matrix effects, sensitivity for

[2] This research has been published.
Panahi, T.; Weaver, D. J.; Lamb, J. D.; Harrison, R. G. *Analyst* **2016**, *141*, 939–946.

guanidine compounds was in the 100 μg L^{-1} range and apparent recoveries were 80-96 %. The peak area precision was 0.01 - 2.89% for IPAD, CD and UV-vis detection.

Keywords: Pharmaceutical contaminants; Ion chromatography; Cavitands; Guanidine compounds

1. Introduction

Trace amounts of pharmaceuticals, such as hormones, antibiotics, painkillers, psychiatric and cardiac medications have been detected in surface waters and even in drinking water.[1-3] There might be no immediate effect of small amounts of these pharmaceuticals on humans, but there is concern that long-term, low-level exposure could be harmful. Human exposure to these contaminants is not the only problem; environmental aquatic species have been affected.[2,4] For example, although short-term cimetidine exposure levels of below 30 mg L^{-1} did not affect freshwater fleas or zebrafish, long term exposure had a high potential for endocrine disruption.[5] In a related study, it was found that small cimetidine concentrations (70 μg L^{-1}) affected growth, reproduction, and survivorship of invertebrates.[6] These contaminants have been present in water for a long time, but their concentration has only recently been quantified and considered potentially hazardous to ecosystems. There is a need to achieve methods for detection and quantification of these contaminants from different water sources.[3,7-11]

With its ability to detect small quantities of ions in aqueous solutions, ion chromatography (IC), is well suited to quantify some pharmaceutical contaminants.[12-15] One of the most needed developments for applying IC to this problem is the production of new stationary phases.[16-21] These stationary phases must have functional groups that will selectively bind and separate the contaminants. Macrocyclic compounds such as crown ethers, cryptands, cyclodextrins and resorcinarenes have been introduced as effective IC exchangers in both

stationary and mobile phases.[22-26] The resorcinarenes are a recently developed class of macrocyclic compounds used as ion exchangers and our previous research on resorcinarene stationary phases confirms their usefulness as separators in IC systems.[25,27-30] Synthesizing these compounds with long alkyl chains facilitates their adherence to the packing resin. The upper rim of the resorcinarene structure can be functionalized with carboxylic groups, which can act as ion exchangers (Figure 1). The resorcinarene tetramer brings the carboxylic acid groups in close proximity to work in a cooperative manner during analyte binding.

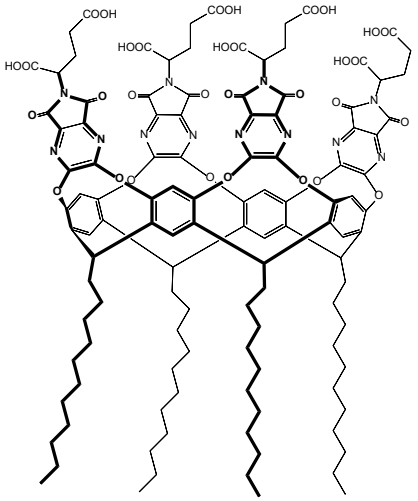

Figure 1 Glutamic acid resorcinarene with undecyl groups (GUA).

We have designed a new stationary phase containing resorcinarene sites to be used to separate a guanidine family of pharmaceutical contaminants.[31,32] The group of interest includes: guanidine (G), methylguanidine (MG), 1,1-dimethylbiguanide (DMG), agmatine (AGM), guanidinobenzoic acid (GBA) and cimetidine (CIM) (Figure 2). These all have the guanidine subunit in common, but vary in structure ranging from the very polar guanidine to the alkyl

containing cimetidine. This range of structures provides the opportunity to test the range of application of this new stationary phase. These guanidine compounds have antacid properties due to their basicity and have a wide range of pharmaceutical applications. For example, dimethylbiguanide is an oral antidiabetic drug, agmatine has been given as a dietary supplement and guanidine benzoic acid has a biological role in the body's guanidine cycle. Cimetidine is a histamine H (2)-receptor antagonist that inhibits stomach acid production. The excretion of such drugs to urine ultimately is the source of apparent contaminants in surface water. The EPA has called such contaminants as cimetidine "contaminants of emerging concern" and investigation into their detection and removal is underway.[1-3,32,34]

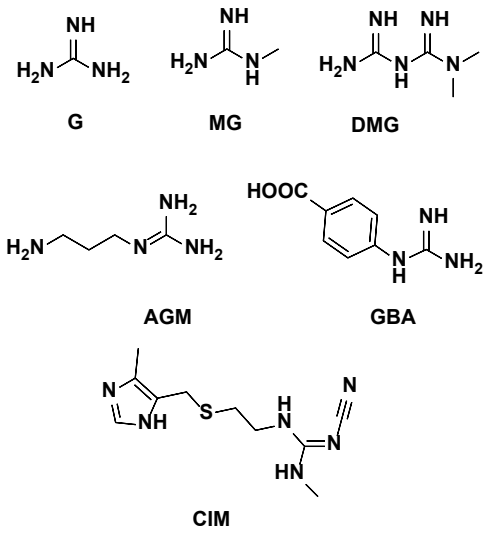

Figure 2 Guanidine compounds: guanidine (G), methylguanidine (MG), 1,1-dimethylbiguanide (DMG), agmatine (AGM), guanidine benzoic acid (GBA), cimetidine (CIM).

Sensitive and selective methods to determine trace amounts of guanidine compounds and others like them in the environment as well as in bio-fluids would help detect illness.[35] Yet these

compounds often suffer from the absence of chromophoric or flourophoric groups, which would render them not detectable by photosensitive methods. Indeed, chromatography is the most common analysis method due to established advantages over enzymatic and spectrochemical methods.[36] The use of derivatizing reagents in the form of post or pre- column reagents is a common way of detecting these compounds, although derivatization has apparent limitations.[37-39] The use of IC with suppressed conductivity, IPAD or UV-vis detection provides a relatively simple and low-cost technique for identification and quantification of these analytes with direct detection and no need for pre- or post-column derivatizing steps.[35]

In this manuscript we present research on a new stationary phase used to detect and quantify guanidine compounds by IC. As far as we know, this is the first report of guanidine compounds analyzed in surface waters using IC techniques. The new column packing material contains resorcinarene-based molecules functionalized with glutamic acid groups (GUA, Figure 1). Isocratic and multi-step gradient elution with methylsulfonic acid (MSA) as eluent proved to separate all of the guanidine compounds with good peak resolution. Even for lake, river and marsh water, with matrix peaks introduced by these water sources, the limits of detection and quantification were in the μg L^{-1} range. Three methods of detection, electrochemical (IPAD), conductivity detection (CD), and UV-vis, were employed and IPAD was found to work best for all of the compounds, although UV-vis was very sensitive for cimetidine. This direct detection of low ppm amounts of guanidine contaminants in environmental waters with easy sample preparation provides a simple yet reliable method for determination of these contaminants.

2. Experimental

2.1 Reagents

All reagents, including methanesulfonic acid (MSA), 50% NaOH solution, and guanidine compounds were analytical grade and obtained from commercial suppliers. All eluents and standards were prepared using Milli-Q (MQ) water of 18 Megaohm/cm resistivity. A solution of 1 M sodium hydroxide was used as the post column additive for IPAD detection. GUA was prepared by following the same procedure used to synthesize a similar compound.[28] Thermo Scientific (Sunnyvale, CA) provided the 4.6 μm particle size 55% cross-linked styrene-divinylbenzene polymeric macroporous resin.

2.2 GUA column preparation

Columns were prepared by the method described previously.[27] For example, 0.050 g of GUA and 1.5 g of resin were dispersed in 25 mL of methanol. The slurry was dried at room temperature. The dry powder was grinded with a mortar and pestle for 4 hours while 30 mL of deionized water was added slowly; the slurry was then packed into a 3 × 150 mm black PEEK column at 60 ºC and 4000 psi for 10-15 minutes. The columns were preconditioned with 1 mM MSA for 10 min at a flow rate of 0.8 mL/min before using for separations. The column void volume is 0.66 mL, with a void time of 2.2 min and a flow rate of 0.30 mL/min. Divinylbenzene macroporous resin (surface area of 350 m^2/g) was used for column preparation. Given the length (3 nm) and width (1 nm) of the GUA molecule and the amount of the resin used for each column, the resin could accommodate on its surface a maximum of 6.0×10^{-5} mol (0.117 g) of GUA. Thus, there is more than sufficient surface area on the resin particles to accommodate all of the GUA used, with less than half of the resin surface area occupied. Conductivity detection was

preceded by treatment with a CSRS 4 mm suppressor. The operating condition was AutoSuppression mode.

2.3 Analyte preparation

Guanidine stock solutions were prepared at 300 mg L^{-1} in deionized water and stored in the refrigerators at 4 °C. The environmental water samples were collected from the Provo River, Utah Lake and marsh water by Utah Lake and kept in plastic bottles in the refrigerator at 4 °C. The environmental water was filtered through cellulose filter paper (pore size 0.015-12 μm) to remove dirt and suspended particles and then centrifuged at 4000 rpm for 5 min. The centrifuged water was filtered through a 0.25 μm mesh Thermo Scientific Nalgene syringe filter, which is a surfactant-free cellulose acetate filter. Weak cation exchange solid phase extraction (WCX-SPE) material was used to remove the anionic species from the water. The WCX-SPE was first washed with deionized water under positive pressure airflow and then a 12 mL water sample was run through the WCX-SPE without positive pressure. The analytes were collected from the WCX-SPE by running 12 mL of 50 mM MSA through the WCX-SPE.

To determine the detectability of low levels of analytes, environmental water samples were spiked with the guanidine compounds. The apparent recoveries were obtained using calibration curves in the range of 0.05 - 0.8 mg L^{-1}. River water samples were spiked with 12 mg L^{-1} of analyte and 10 mL of water was filtered and loaded on SPE. The SPE was washed with 10 mL of 50 mM MSA, which was analyzed with an electrochemical detector. The apparent recoveries were calculated with the equation $R = (Xa_{exp}/Xa_{theor})\ 100\%$, where R is recovery, Xa_{exp} is the value experimentally obtained and Xa_{theor} is the known or theoretical value.[40] The apparent recoveries averaged over 4 times and relative standard deviations (RSD) were: G 96 (3.3), MG 90 (1.2), DMG 88 (0.2), AGM 85 (2.3), GBA 86 (2.2), and CIM 81 (1.1). To prepare

the spiked water samples, a 100 mg L^{-1} stock solution of analytes was first diluted to 3.50 mg L^{-1}, then to 600 μg L^{-1} or 300 μg L^{-1}, and finally diluted with environmental water to 75 or 150 μg L^{-1}.

2.4 Instrumentation

The ICS-5000^{+} Ion Chromatography system (Thermo Scientific) was used in this work. The system was equipped with a DP-5000^{+} gradient pump, a DC-5000 detector compartment with conductivity cell and IPAD cell, and an ASAP automated sampler. The Chromeleon® 7 software was used for system control and data processing. The CERS 500 (4 mm) self-regenerating suppressor at 40 mA was used for suppressed conductivity detection. A 5 μL sample injection volume was used throughout. Post-column addition of 1 M NaOH was delivered to a mixing tee at a flow rate of 0.5-0.6 ml/min to increase the eluent pH for detection by IPAD. A 125 μL knitted reaction coil was installed between the mixing tee and electrochemical cell to insure enough time for sodium hydroxide to mix with analyte. The IPAD cell consisted of a disposable Au working electrode, a titanium counter electrode, and a pH-Ag/AgCl combination reference electrode. The electrochemical waveform used for IPAD was based off one previously used to detect biogenic amines.[12] It was 0.13 V from 0.00 s to 0.04 s, 0.33 V from 0.05 s to 0.21 s, 0.55 V from 0.22 s to 0.46 s, 0.33 V from 0.47 s to 0.56 s, -1.67 V from 0.57 s to 0.58 s, and 0.93 V from 0.59 s to 0.60 s. Data was collected at a frequency of 1.67 Hz for IPAD and 5 Hz for the conductivity detector.

A PDA UV–vis detector with a combined deuterium/tungsten lamp and 10 mm cell was attached to the column outlet and placed in line with suppressed conductivity detector. The optimum detection wavelength was 200 nm, which most of the guanidine compounds showed the

highest sensitivity. The IPAD set-up was a little different since it required a post column reagent to provide a basic solution for the Au electrode.

2.5 Limits of detection and precision

To obtain the linear range of guanidine compounds for IPAD, suppressed conductivity and UV-vis detectors, the correlation between peak area and concentration was identified. Two sets of calibration curves were prepared for each of the guanidine analytes in deionized water using five increasing concentrations in the range of 0.10 - 20 and 0.05 - 0.80 mg L^{-1}. The analytes were measured separately three times. The limits of detection (LODs) and limits of quantification (LOQs) were calculated for each detector based on the slopes of the calibration curves using the equation LOD = 3.3(SD/S) and LOQ = 10(SD/S), where SD is the standard deviation and S is the slope of the line of the calibration equation. Replicate injections of solutions containing G (8.3 ppm), MG (8.3 ppm), CIM (8.3 ppm), of DMG (16.6 ppm), AGM (16.6 ppm) and GBA (16.6 ppm) were performed to measure retention times and peak area precisions. The replicate injection precisions were evaluated for IPAD, CD, and UV-vis detection by performing 4 consecutive injections of each analyte.

3. Results and discussion

3.1 Separators

The eight carboxylic acid groups from each GUA are positioned around one face of a resorcinarene (Figure 1). These carboxylic acid groups provide hydrogen bonding sites at low pH and anionic binding sites at neutral and high pH, while the benzyl groups of the cavitand provide for nonpolar interactions. The long alkyl groups on the lower rim of the cavitands are for absorption of the cavitands to the polystyrene column packing material. IR investigation of the

packing material showed a peak at 1700 cm^{-1}correlating to the carboxylic acid group of the resorcinarene, which was not present in pure resin. SEM characterization of the material showed that some of the 4.6 μm beads had been crushed during the grinding process.[27] Total porosity of the GUA column was 63% and the dynamic binding capacity of the packed column was 12 mM/column for GBA.

3.2 Isocratic elution in water

Separation of the guanidine compounds (G, MG, DMG, AGM, GBA, CIM) with the GUA column was first attempted by isocratic elution using 1, 2, 3, 4, 5.5, 6, 8, and 10 mM MSA and a flow rate of 0.8 mL/min. The compound retention times (min) with 1 mM MSA were 2.27 (G), 2.87 (MG), 9.37 (DMG), and 18.37 (AGM). GBA and CIM did not elute from the column with 1 mM MSA (Figure 3). Increasing the concentration of MSA to 2 mM led to reduced retention times (min) of 1.67 (G), 1.97 (MG), 4.32 (DMG), 5.55 (AGM) and elution of GBA at 11.4 min. It took 6 mM MSA to elute CIM in 35 min., but at this and higher MSA concentrations, the first four analytes began to coelute.

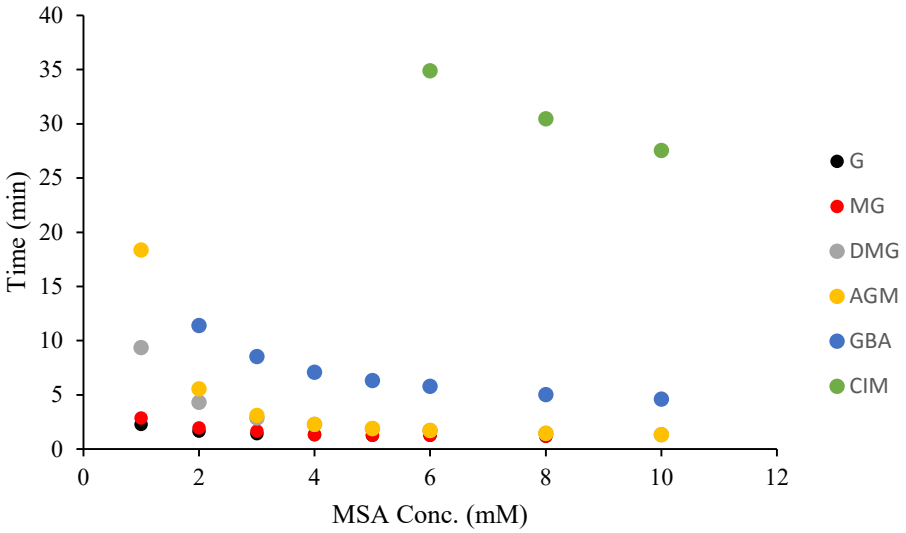

Figure 3 Effect of MSA concentration on the retention time of the guanidine compounds with the GUA column.

The order of analyte elution can be attributed to the analyte charge, solvated volume, size, and presence of hydrophobic groups. Guanidine has the highest charge density of the analytes, and thus maintains its hydration sphere, resulting in less attraction to the column active sites and a shorter retention time. Compared to guanidine, methyl guanidine and dimethylbiguanide are larger and have alkyl groups, which results in them having slower mass transfer than guanidine and longer retention times. Agmatine is dicationic in solution, is larger in size and has alkyl groups, features which lengthen its retention time. Guanidine benzoic acid, has a phenyl group, which results in slower mass transfer and a longer retention time. Cimetidine, the largest and most hydrophobic member of the group, eluted last due to slow mass transfer rate and stronger absorption to the hydrophobic polystyrene resin.

We have observed by NMR that the carboxylate groups of a similar resorcinarene interacted with the amine groups of various benzyl amines.[28] We also observed that the

resorcinarene more strongly bound amine than did the monomeric analog. Thus, for GUA the carboxylic acid groups are proposed to be the sites of interaction with the analytes and specifically the guanidine groups of the analytes. With another resorcinarene, this one containing four cyclen groups attached to the upper rim of the resorcinarene, we observed that the resorcinarene efficiently separate anions while a compound with a single cyclen did not.[41] We propose the carboxylic acids of GUA are also working in a cooperative manner to bind analytes

3.3 Gradient elution with MSA in water

Multi-step gradient elution resulted in the best resolution of the analytes in the shortest time (Figure 4). The best separation was achieved with a flow rate of 0.8 mL/min using 1 mM MSA for 5 min, 2 mM for 5 min, 3 mM for 5 min, and 25 mM for 30 min. The elution order was the same as that found in the isocratic runs and the conditions with IPAD were a little different than the other two detection methods due to the post column reagent system. The peak resolution factors for the peak pairs in this order were 1.3, 5.5, 1.0, 1.4, and 6.6 using IPAD. The presence of MSA as eluent in high concentrations caused an increase in baseline, attributed to the trace electrocatalytic activity of MSA on the surface of gold working electrode. As seen in Table 1, the chromatographic parameters for the separation of guanidine compounds on the GUA column gave plate numbers from 3 to 10 thousand N/m. Replicate injections of solutions containing 8.3 mg L^{-1} of G, MG, and CIM, and 16.6 mg L^{-1} of DMG, AGM and GBA were performed to measure retention times and peak area precisions. RSDs for the retention time and peak area of the replicate injections with multi-step gradient elution of MSA and IPAD were 4.29 and 4.30%, respectively.

Without GUA on the packing material and under the same conditions, no retention was seen for G, MG, DMG, and AGM. GBA was slightly retained and CIM was significant retained,

coming off at 24 min. Thus, GUA is critical for analyte separation, but as seen with CIM retention, the hydrophobic resin also plays a role in retention. The GUA molecules create cation exchange sites, which work in conjunction with the hydrophobic resin to allow analyte separation under low concentrations of MSA.

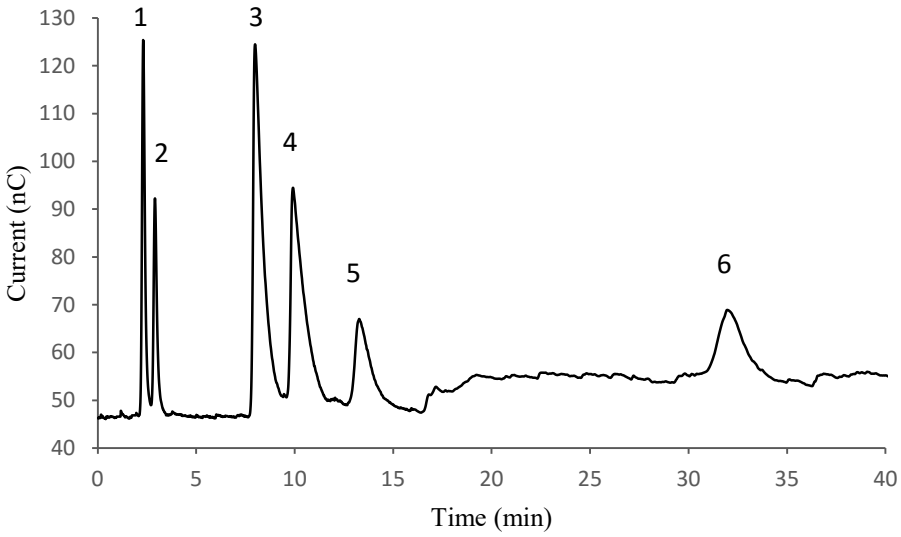

Figure 4 Separation of guanidine compounds with GUA column and IPAD. Peak assignment: 1-G, 2-MG, 3-DMG, 4-Agm, 5-GBA, 6-Cim. Conditions: flow rate 0.8 ml/min. Gradient, 1mM MSA for 5 min, 2 mM for 5 min, 3 mM for 5 min, 25 mM for 30 min. Analyte concentrations (mg L^{-1}): G and MG (8.3); DMG, AGM and GBA (16.6); CIM (8.3). Peak resolutions (Rs): Rs1 = 1.3, Rs2 = 5.5, Rs3 = 1.0, Rs4 = 1.42, Rs5 = 6.6.

Table 1 Chromatographic parameters for the determination of guanidine compounds by step gradient ion chromatography with GUA columns

	IPAD			CD			UV		
Analyte	t_R (min)	Half-peak width (min)	Plates number (N/m)	t_R (min)	Half-peak width (min)	Plates number (N/m)	t_R (min)	Half-peak width (min)	Plates number (N/m)
G	2.3	0.27	4000	8.7	0.403	20000	8.4	0.33	33000
MG	2.9	0.29	6000	9.9	0.51	16000	9.5	0.46	19000
DMG	8.1	0.82	4000	21.3	0.85	26000	22.7	1.33	13000
AGM	9.8	1.2	3000	23.3	1.49	11000	-	-	-
GBA	13.3	1.26	5000	27.2	1.95	8000	27.4	1.48	15000
CIM	31.8	2.07	10000	-	-	-	50.6	1.9	30000

Conductivity detection is one of the most commonly available detection methods in analyzing ionic water contaminants and was also investigated as a possible detection method in this work. The use of modest amounts of MSA and no organic solvent allowed us to use conductivity suppressed detector. The cation suppressor led to low noise levels and improved the methods' sensitivity for guanidine compounds in the acidic solvent. Five of the six guanidine compounds were detected, but cimetidine was not (Figure 5). The separation was carried out at flow rate 0.5 mL/min and the best applied multi-step gradient was 1mM MSA for 5 min, 2 mM for 5 min, 3 mM for 5 min, 4 mM for 5 min, 5 mM for 5 min, 6 mM for 5 min, and 25 mM for 20 min. The chromatographic parameters for the separation of guanidine compounds on the GUA column with this gradient gave plate numbers greater than electrochemical detection and from 32 to 105 hundred thousand N/m (Table 1). The peak resolution factors were good at 1.6, 9.9, 1.0, and 1.2. The calculated RSDs for the retention times and peak areas of the replicate injections with suppressed conductivity detection were 2.39 and 2.20 %, respectively.

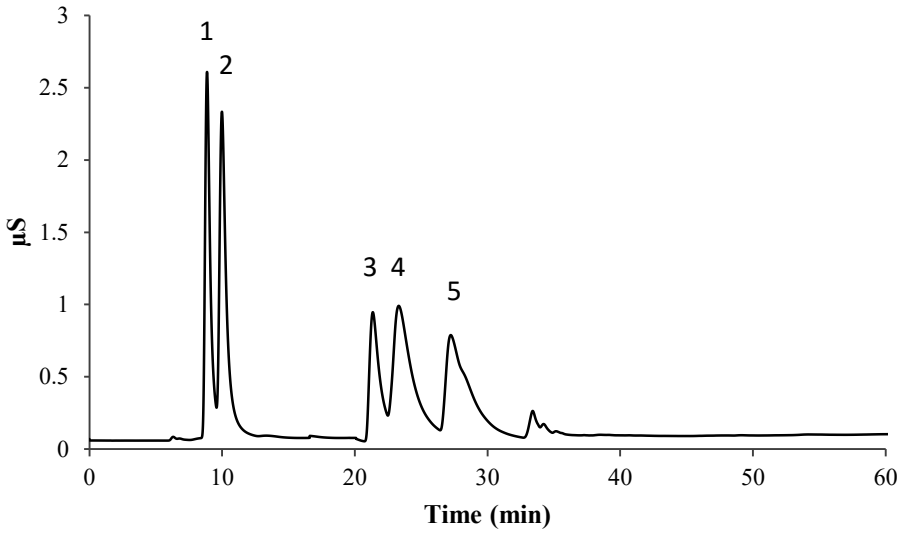

Figure 5 Separation of guanidine compounds with GUA column and CD. Peak assignments: 1-G, 2-MG, 3-DMG, 4-Agm, 5-GBA. Conditions: flow rate 0.5 ml/min. Gradient:1mM MSA for 5 min, 2 mM for 5 min, 3 mM for 5 min, 4 mM for 5 min, 5 mM for 5 min, 6 mM for 5 min, 25 mM for 20 min. Analyte concentration (mg L^{-1}): G and MG (8.3); DMG, AGM, GBA and CIM (16.6). Peak resolutions (Rs): Rs1 = 1.6, Rs2 = 9.9, Rs3 = 1.0, Rs4 = 1.2.

UV-vis detection is the most universal detection method in chromatography systems and was also used with the guanidine compounds in this work. A short wavelength of 200 nm was used to excite the guanidine compounds in an attempt to detect as many compounds as possible. Five of the six compounds were detected by UV-vis (the exception was agmatine) and one of the five (guanidine) was very weak (Figure 6). Agmatine does not absorb at 200 nm and was thus not detected. The separation flow rate was 0.5 mL/min and the gradient elution was the same as suppressed conductivity separation. The obtained peak resolution factors were 1.7, 13.3, 2.0, and 8.1. The chromatographic parameters gave plate numbers from 13 to 30 hundred thousand N/m and especially high for cimetidine (Table 1). Replicate injections were performed to measure retention times and peak area precisions. The obtained RSDs for the retention times and peak

areas with gradient elution of MSA and UV-vis was 3.21 and 2.21%, respectively. The RSDs were low for all of the detection methods.

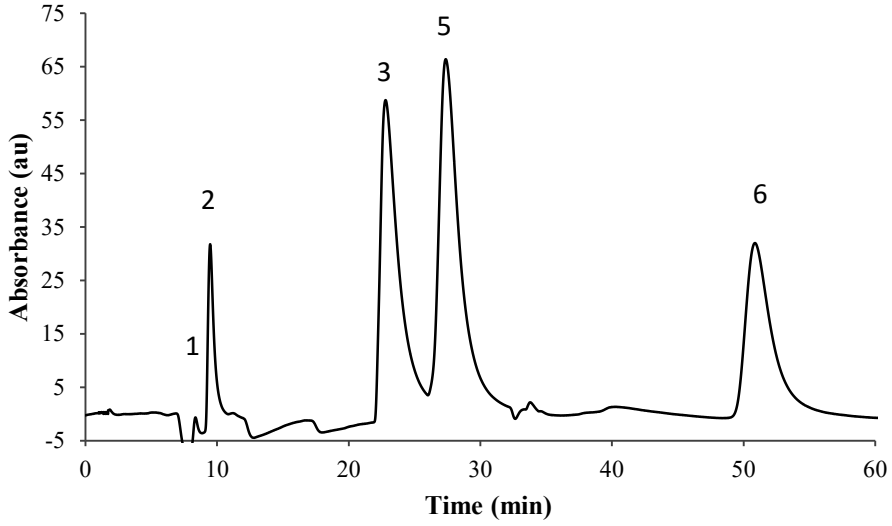

Figure 6 Separation of guanidine compounds with GUA column and UV-vis detection. Peak assignments: 1-G, 2-MG, 3-DMG, 5-GBA, 6-CIM. Conditions: flow rate 0.5 ml/min. Gradient: 1mM MSA for 5 min, 2 mM for 5 min, 3 mM for 5 min, 4 mM for 5 min, 5 mM for 5 min, 6 mM for 5 min, 25 mM for 20 min. Initial concentrations (mg L^{-1}): G and MG (8.3); DMG, AGM, GBA and CIM (16.6). Peak resolutions (Rs): Rs1 = 1.7, Rs2 = 13.3, Rs3 = 2.0, Rs4 = 8.1.

Limits of detection and quantification were calculated for each detection method and found to be very good and in the μg L^{-1} range (Table 2). The limits of detection were the smallest for electrochemical detection and ranged from 6–32 μg L^{-1} for G, MG, DMG, AGM, and CIM. The detection limit for GBA was a little greater at 76 μg L^{-1}. The limits of detection for conductivity were a little lower in the 1.7 to 8.2 μg L^{-1} range, except for CIM which couldn't be detectable with CD. UV-vis detection proved to be very good for cimetidine (5.1 μg L^{-1}), while it was comparable to the other methods for the other analytes, except, as stated before, for

arginine and guanidine. Comparing the three methods, IPAD was the best for detecting all six of the analytes due to the guanidine subunit being able to be oxidized on the gold electrode with the correct applied waveform and basic conditions provided by sodium hydroxide through the post column reactor.

Table 2 Limits of detection (LOD) and quantification (LOQ) of guanidine compounds with IPAD, CD and UV-vis detection at room temperature with MSA

Analyte	IPAD		CD		UV-vis	
	LOD (μg L^{-1})	**LOQ** (μg L^{-1})	**LOD** (μg L^{-1})	**LOQ** (μg L^{-1})	**LOD** (μg L^{-1})	**LOQ** (μg L^{-1})
G	6	20	1.7	5.7	66	220
MG	5.0	17	8.2	27	24	82
DMG	32	110	15	52	11	34
AGM	8.6	29	1.7	5.7	ND	ND
GBA	76	250	5.7	19	34	110
CIM	8.3	28	ND	ND	5.1	17

ND, not detected.

3.4 Analysis of guanidine compounds in river, lake and marsh water

After noting the efficient separation of the guanidine compounds in pure water with the GUA column, we evaluated the application of the technique to surface water sources, i.e. river, lake and marsh. The presence of organic and bioorganic compounds, such as humic substances and a variety of minerals makes natural water sources a complicated matrix to detect and separate very small concentrations of the pharmaceutical analyte.

None of the analytes was detected in the sampled river water under gradient conditions, although there were large matrix peaks (Figure 7). However, low levels of the analytes were detected when river water was spiked with 75 μg L^{-1} of each analyte and the multi-step gradient was composed of 1 mM MSA for 5 min, 2 mM for 5 min, 3 mM for 5 min, 4 mM for 5 min, 5 mM for 5 min, 6 mM for 5 min, 7 mM for 5 min, 8 mM for 5 min, and 25 mM for 20 min (Figure 7). Due to matrix peaks the run conditions and gradient were different from those used with pure water. Since electrochemical detection was able to detect all 6 guanidine compounds in water, we chose this detection method to analyze the surface water samples. The elution order of the analytes was the same as it was in pure water. The apparent recoveries of the analytes through the SPE filtration were high and ranged from 80 to 96%. The G was the highest and the CIM was the lowest due to their hydrophobic nature and retention on SPE.

As shown by the chromatograms, the matrix compounds affect analyte resolution. The chromatograms show three prominent matrix peaks at 2.5, 16 and 19 minutes in all of the water sources. The major ions in these water sources are: HCO_3^- (260 mg/L), SO_4^{2-} (40 mg/L)$^-$, Cl^- (15 mg/L), Ca^{2+} (55 mg/L), Mg^{2+} (15 mg/L), K^+ (3 mg/L), and Na^+ (10 mg/L) [42] and the biochemical oxygen demand BOD_5 equals 0.28 – 0.5 mg/L.[43] The major anions in the waters would not be appreciably retained on the column and indeed we saw that Cl^- and SO_4^{-2} eluted from the column at the same time as the first matrix peaks. Thus, we propose the matrix peak at 2.5 min is due to anions. The use of SPE significantly improved the signal to noise ratio due to the elimination of anionic species. The main cations in the water sources would be retained on the column, elute with the analytes, and could cause analyte separation problems. Under the IPAD conditions used, the reduction of the cations in this list is not feasible, since they have more negative reduction potentials than the applied electrode potential of -1.67 to + 0.55 V. Although the cations might

affect baseline noise, they do not give rise to the matrix peaks we observe. The compounds responsible for the matrix peaks at 16 and 19 minutes are being retained on the column and elute with the organic-based analytes. Therefore, it is likely that these matrix peaks are due to organic-based cations, maybe even ones that contain amine groups.

After noting the ability of the GUA column to separate low concentrations of analytes, a comparison between it and a commercial column was made. All six analytes were detected using the Dionex IonPac CS-17 analytical column (Figure 24, appendix), however there were differences. The biggest difference in the chromatograms was the baseline noise increased due to the greater MSA concentrations required to remove the analytes from the commercial column. A second difference was the signal from GBA was weaker and broader. Also, although the peak for MG was still weak, it now came close to the matrix peaks.

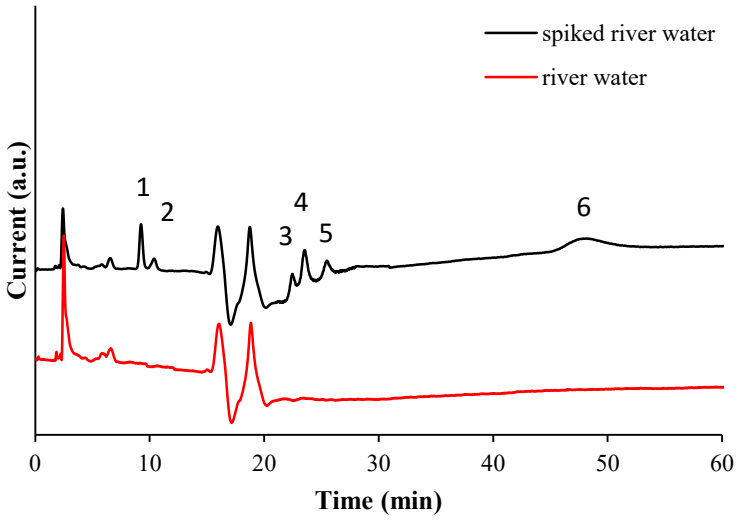

Figure 7 Separation of guanidine compounds in river water with GUA column and IPAD. Peak assignments: 1-G, 2-MG, 3-DMG, 4-Agm, 5-GBA and 6- CIM. Conditions: flow rate 0.6 ml/min. Gradient: 1mM MSA for 5 min, 2 mM for 5 min, 3 mM for 5 min, 4 mM for 5 min, 5 mM for 5 min, 6 mM for 5 min, 7 mM for 5 min, 8 mM for 5 min, 25 mM for 20 min. Analyte concentrations equal 75 µg L^{-1}.

Lake water samples had similar matrix peaks to river water and were also void of the 6 guanidine analytes. Using the same gradient as for river water, the low levels of analytes (150 µg L^{-1}) were able to be separated in spiked samples of lake water even with the presence of matrix peaks (Figure 8). The detectable levels of analytes are a little higher than they were for river water due to the stronger matrix peaks in these sources. The elution order was the same as it was for river water samples and ppb levels of analyte were detected. As with the river water, the lake water was filtered before being introduced into the instrument.

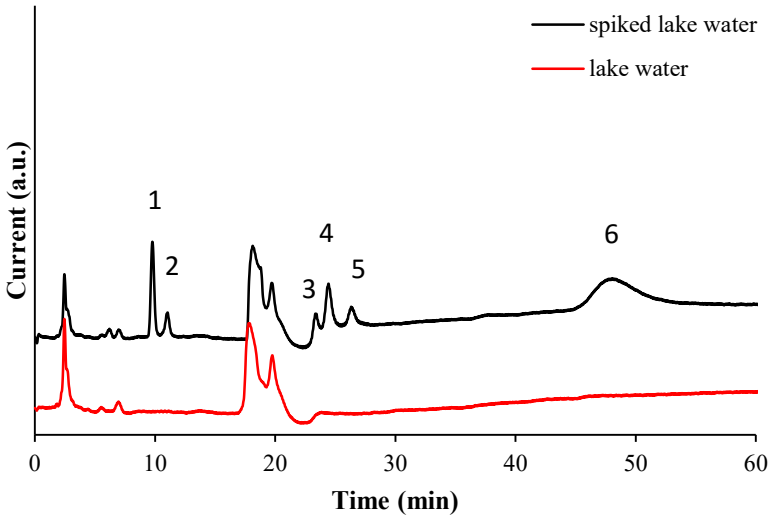

Figure 8 Separation of guanidine compounds in lake water with GUA column and IPAD. Peak assignments: 1-G, 2-MG, 3-DMG, 4-Agm, 5-GBA and 6-CIM. Conditions: flow rate 0.6 ml/min. Gradient: 1mM MSA for 5 min, 2 mM for 5 min, 3 mM for 5 min, 4 mM for 5 min, 5 mM for 5 min, 6 mM for 5 min, 7 mM for 5 min, 8 mM for 5 min, 25 mM for 20 min. Analyte concentrations equal 150 µg L^{-1}.

The marsh water showed a similar set of matrix peaks and was also not contaminated with any of the guanidine compounds. Low levels (µg L^{-1}) of the six guanidine compounds were detected and quantified in spiked marsh water samples using the same flow rate and gradient elution of MSA (Figure 9). The GUA column is able to separate the analytes in the marsh water even with the presences of matrix ions that come with the water.

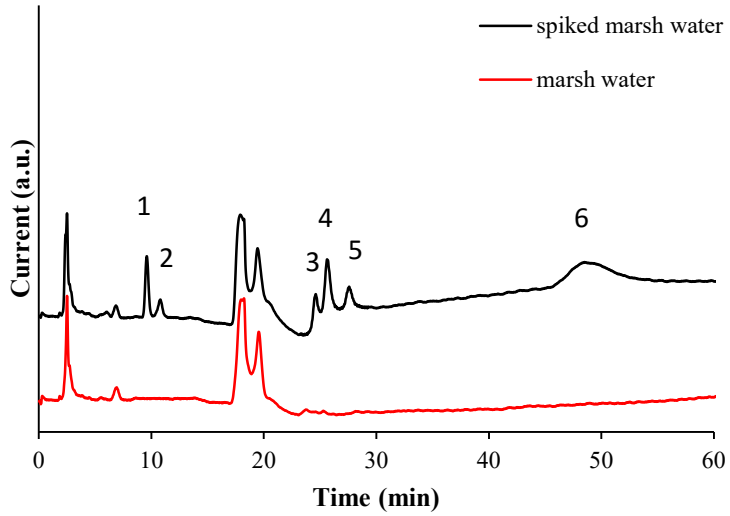

Figure 9 Separation of guanidine compounds in marsh water with GUA column and IPAD. Peak assignments: 1-G, 2-MG, 3-DMG, 4-Agm, 5-GBA and 6- CIM. Conditions: flow rate 0.6 ml/min. Gradient: 1mM MSA for 5 min, 2 mM for 5 min, 3 mM for 5 min, 4 mM for 5 min, 5 mM for 5 min, 6 mM for 5 min, 7 mM for 5 min, 8 mM for 5 min, 25 mM for 20 min. Analyte concentrations equal 150 µg L^{-1}.

4. Conclusions

The new GUA solid phase material effectively separated six different guanidine-containing compounds in pure water samples. Multi-step gradient elution with MSA was required to obtain good separations of analytes and matrix ions on the GUA column. Detection was found to be practical with IPAD, CD and UV-vis detection, with IPAD best in terms of the number of analytes detected. The new column material also effectively separated low levels of analytes in different environmental water sources, including river, lake, and marsh. The quantification of these analytes in the µg L^{-1} range by this IC method, means this method is as good or better than other chromatography and mass spectrometry methods.[44,45] However, with simple sample preparation, this IC method has advantages over other methods. The GUA

packing material used in IC systems gives a new option to separate pharmaceuticals and will lead to further research on other resorcinarene compounds with the potential for greater selectivity.

References

1 N. Bolong, A. F. Ismail, M. R. Salim and T. Matsuura, *Desalination*, 2009, **239**, 229–246.

2 M. J. Focazio, D. W. Kolpin, K. K. Barnes, E. T. Furlong, M. T. Meyer, S. D. Zaugg, L. B. Barber and M. E. Thurman, *Sci. Total Environ.*, 2008, **402**, 201–16.

3 S. Gonzalez and M. Petrovic, *Trends Anal. Chem.*, 2003, **22**, 685–696.

4 J. L. Domingo, *J. Chromatogr. A*, 2004, **1054**, 327–334.

5. S. Lee, D. Jung, Y. Kho, K. Ji, P. Kim, B. Ahn and K. Choi, *Chemosphere*, 2015, **135**, 208–16.

6 P. D. Hoppe, E. J. Rosi-Marshall and H. a. Bechtold, *Freshw. Sci.*, 2012, **31**, 379–388.

7 P. E. Grimmett and J. W. Munch, *Anal. Methods*, 2013, **2**, 151–163.

8 K. K. Barnes, D. W. Kolpin, E. T. Furlong, S. D. Zaugg, M. T. Meyer and L. B. Barber, *Sci. Total Environ.*, 2008, **402**, 192–200.

9 M. J. Benotti, R. A. Trenholm, B. J. Vanderford, J. C. Holady, B. D. Stanford and S. A. Snyder, *Environ. Sci. Technol.*, 2009, **43**, 597–603.

10 R. Katherine, J. Jeffrey and C. Paul, *Environ. Toxicol. Chemsirty*, 2008, **27**, 1721–1727.

11 J. M. Levengood and D. J. Schaeffer, *Ecotoxicology*, 2011, **20**, 1411–21.

12 L. Bhattacharyya and J. S. Rohrer, *Application of Ion Chromatography for Phamaceutical and Biological Products*, John Wiley & Sons. Inc., Hoboken, New Jersey, 2012.

13 A. Chalgeri and H. S. I. Tan, *J. Pharm. Biomed. Anal.*, 1996, **14**, 835.

14 N. Karu, J. P. Hutchinson, G. W. Dicinoski, M. Hanna-Brown, K. Srinivasan, C. Pohl and P. R. Haddad, *J. Chromatogr. A*, 2012, **1253**, 44–51.

15 G. a. Zachariadis, A. I. Lyratzi and J. A. Stratis, *Cent. Eur. J. Chem.*, 2011, **9**, 941–947.

16 M. C. Bruzzoniti, R. M. De Carlo, S. Fiorilli, B. Onida and C. Sarzanini, *J. Chromatogr. A*, 2009, **1216**, 5540–7.

17 A. I. Elefterov, M. G. Kolpachnikova, P. N. Nesterenko and O. A. Shpigun, *J. Chromatogr. A*, 1997, **769**, 179–188.

18 N. H. Evans, H. Rahman, J. J. Davis and P. D. Beer, *Anal. Bioanal. Chem.*, 2012, **402**, 1739–48.

19 M. Rey and C. Pohl, *Dionex Corp.*, 2003, **997**, 199–206.

20 E. Sugrue, P. N. Nesterenko and B. Paull, *J. Chromatogr. A*, 2005, **1075**, 167–175.

21 J. Weiss and D. Jensen, *Anal. Bioanal. Chem.*, 2003, **375**, 81–98.

22 M. C. Bruzzoniti, R. M. De Carlo, K. Horvath, D. Perrachon, A. Prelle, R. Tófalvi, C. Sarzanini and P. Hajós, *J. Chromatogr. A*, 2008, **1187**, 188–96.

23 J. D. Lamb, D. Simpson, B. D. Jensen, J. S. Gardner and Q. P. Peterson, *J. Chromatogr. A*, 2006, **1118**, 100–5.

24 Y. Kitamaki and T. Takeuchi, *Anal. Sci.*, 2004, **20**, 1399–402.

25 J. Wang, R. G. Harrison and J. D. Lamb, *J. Chromatogr. Sci.*, 2009, **47**, 510–5.

26 M. Wössner and K. Ballschmiter, *Fresenius. J. Anal. Chem.*, 2000, **366**, 346–50.

27 T. Panahi, D. J. Weaver, J. D. Lamb and R. G. Harrison, *J. Chromatogr. A*, 2015, **1376**, 105–111.

28 N. Li, F. Yang, H. A. Stock, D. V Dearden, J. D. Lamb and R. G. Harrison, *Org. Biomol. Chem.*, 2012, **10**, 7392–401.

29 N. Li, L. J. Allen, R. G. Harrison and J. D. Lamb, *Analyst*, 2013, **138**, 1467–74.

30 J. D. Lamb, C. A. Morris, J. N. West, K. T. Morris and R. G. Harrison, *J. Memb. Sci.*, 2008, **321**, 15–21.

31 F. Saczewski and Ł. Balewski, *Expert Opin. Ther. Pat.*, 2009, **19**, 1417–48.

32 J. D. Van den Berg, L. a Smets, M. Rutgers, A. Grummels, R. Fokkens, P. Jonkergouw and H. van Rooij, *Cancer Chemother. Pharmacol.*, 1997, **40**, 131–7.

33 A. Note, *EPA Method 538*, 2012, 7.

34 S. D. Richardson, *Anal. Chem.*, 2003, **75**, 2831–2857.

35 L. Bhattacharyya, *Application of Ion Chromatography for Pharmaceutical and Biological Products*, Rockville, MD, 2012.

36 J. Baranowska, I. Magiera, and S. Baranowski, *J. Chromatogr. B Anal. Technol. Biomed. Life Sci.*, 2013.

37 V. K. Boppana, G. R. Rhodes and D. P. Brooks, *Anal. Biochem.*, 1990, **184**, 213–8.

38 R. Gatti and M. G. Gioia, *J. Pharm. Biomed. Anal.*, 2008, **48**, 754–9.

39 R. Gatti and M. G. Gioia, *J. Pharm. Biomed. Anal.*, 2006, **42**, 11–6.

40 D. T. Burns, K. Danzer and A. Townshend, *Pure Appl. Chem*., 2002, **74**, 2201–2205.

41 J. Wang, R. G. Harrison and J. D. Lamb, *J. Chromatogr. Sci.*, 2009, **47**, 510–5.

42 B. Borup, G. K. Liljenquist, W. Miller, and G. P. Williams, *Envir. Sci. Technol.* 2012, **1**, 9-14.

43 J. L. Crawford, *Effects of Inorganic Nutrients and dissolved Organic Carbon on Oxygen Demand in Select Rivers in Northern Utah*, 2013, All Graduate Theses and Dissertations. Paper 1959.

44 T. Hanai, Y. Inamaoto, and S. Inamoto, *J. Chromatogr. B*, 2000, **747**, 23-128.

45 T. Niwa, *J. Chromatogr. B,* 2009, **877**, 2600-2606.

Chapter 5 Conclusion and Perspective

Deep chiral cavitands were synthesized and characterized with different techniques and have the tetramer structure of the cavitand. Glutamic ester and acid cavitands were fully characterized with NMR, mass spectroscopy, DLS, SEM, and TEM techniques. A series of amine guests with different substituent groups were used to analyze the binding strength and chiral recognition of GMA in DMSO. The comparison of binding constant between GMA and PGA showed the importance of tetramer structure in enhancing the binding strength between amines and host molecules. The greatest chiral discrimination was observed for secondary amines. DLS analysis showed the presence of agglomeration for ester and acid derivatives. The stimuli for reducing agglomerations were found to be concentration, pH, and temperature.

In addition, GUA was adsorbed onto 55% cross-linked styrene-divinylbenzene resin to prepare new stationary phases for ion chromatography (IC) columns. These new IC columns successfully separated uremic toxins in water and urine. Three and four step gradient elutions were necessary to obtain good separation of the analytes from each other and matric components. Even in the presence of urine matrix, uremic toxin concentrations were detected in the biological relevant range (ppb) with the new columns using PAD. The newly designed IC columns also effectively separated six different guanidine-containing compounds in pure water samples. Detection was found to be practical with IPAD, CD and UV-vis detection, with IPAD best in terms of the number of analytes detected. The new column material also effectively separated low levels of analytes in different environmental water sources, including river, lake, and marsh.

Based on the experimental results that I have obtained, I propose several future research projects which build on these results:

1. The GUE ligand showed a vase-like structure with well-defined ^{1}H NMR spectra in d_6-benzene. A hydrophobic pocket with a chiral opening can create asymmetric resorcinarene-based cavitands for chiral discrimination. The GUE ligand should be investigated more as asymmetric carrier for small chiral molecules.
2. As mentioned, the self-assembly feature of the resorcinarene molecules can result in them forming aggregates and several factors affect this process including concentration, pH, and temperature. The self-assembly and pH-responsive behavior of GUA can efficiently encapsulate drugs and release it. This is an area which can be widely used in drug delivery systems and needs more investigation.
3. Another class of cavitands which has been recently designed and synthesized in our group, is pillararenes. This class of cavitand can be modified with various substituents on their upper and lower rims to provide specific functionality and selectivity. Recent studies show the great potential of pillararenes in host-guest interactions.[1–3] The adsorbance of pillararene derivatives onto styrene-divinylbenzene resin can introduce new stationary phases to ion chromatography columns.
4. The presence of chiral moieties in the GUA column provides stereoselectivity for chiral analytes. Therefore, more investigation is required for achieving a chiral separation on the **GUA** column.

References

(1) Jie, K.; Zhou, Y.; Yao, Y.; Huang, F. *Chem. Soc. Rev.* **2015**, *44*, 3568–3587.

(2) Duan, Q.; Cao, Y.; Li, Y.; Hu, X.; Xiao, T.; Lin, C.; Pan, Y.; Wang, L. *J. Am. Chem. Soc.* **2013**, *135* (28), 10542–10549.

(3) Cao, Y.; Hu, X. Y.; Li, Y.; Zou, X.; Xiong, S.; Lin, C.; Shen, Y. Z.; Wang, L. *J. Am. Chem. Soc.* **2014**, *136* (30), 10762–10769.

Chapter 6 Appendix

1. Characterization of Dimethyl 2-(2,3-dichloro-5,7-dioxo-5,7-dihydro-6H-pyrrolo[3,4-b]pyrazin-6-yl)pentanedioate (GPy)

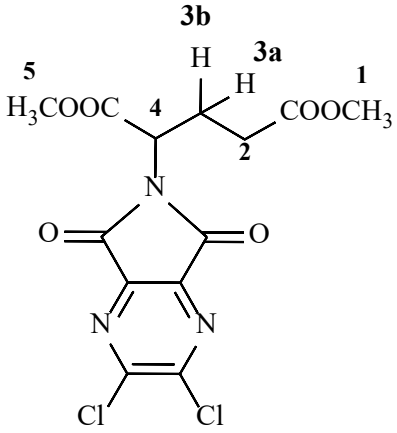

Figure 1 The structure of **GPy**

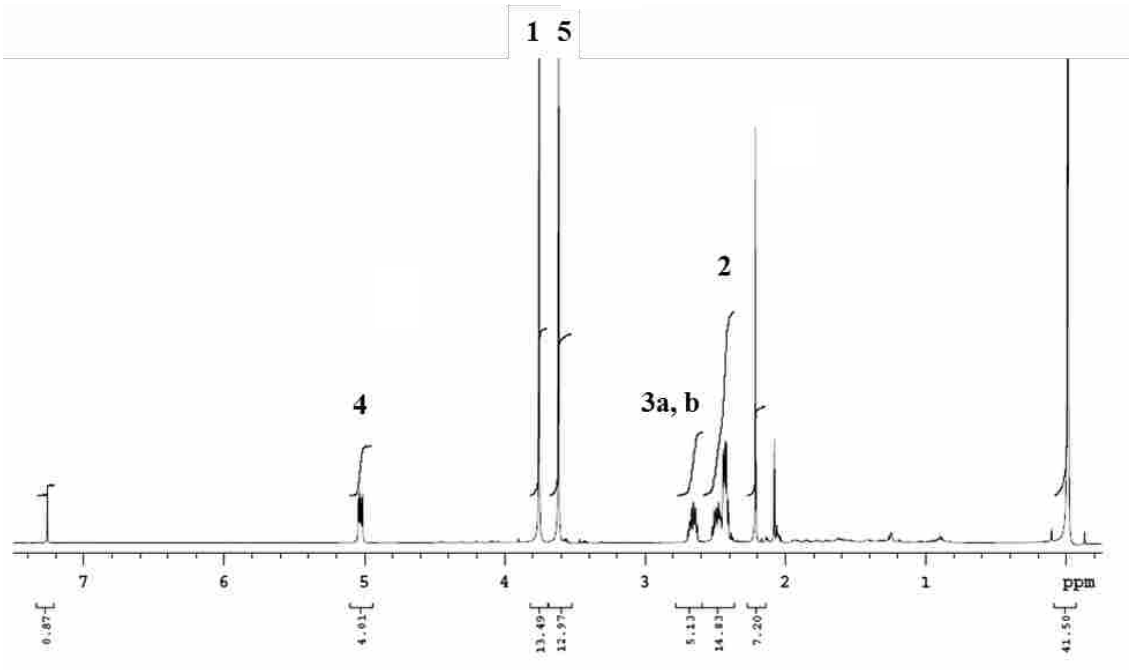

Figure 2 ^{1}H NMR of **GPy** in $CDCl_3$.

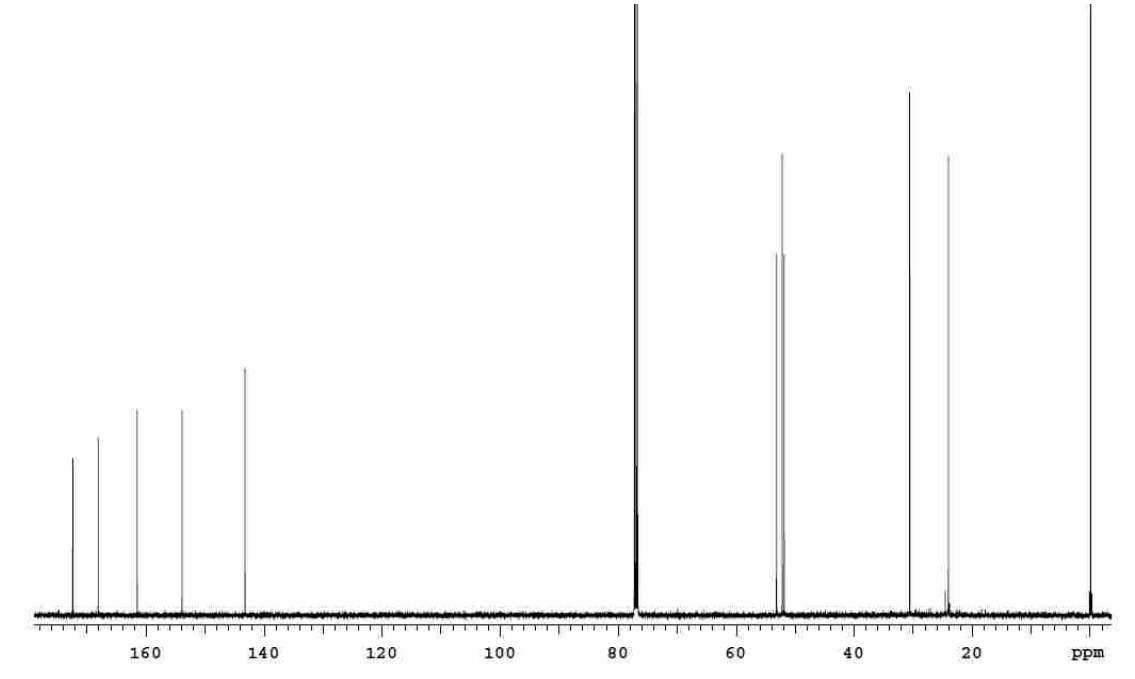

Figure 3 ^{13}C NMR of **GPy** in $CDCl_3$.

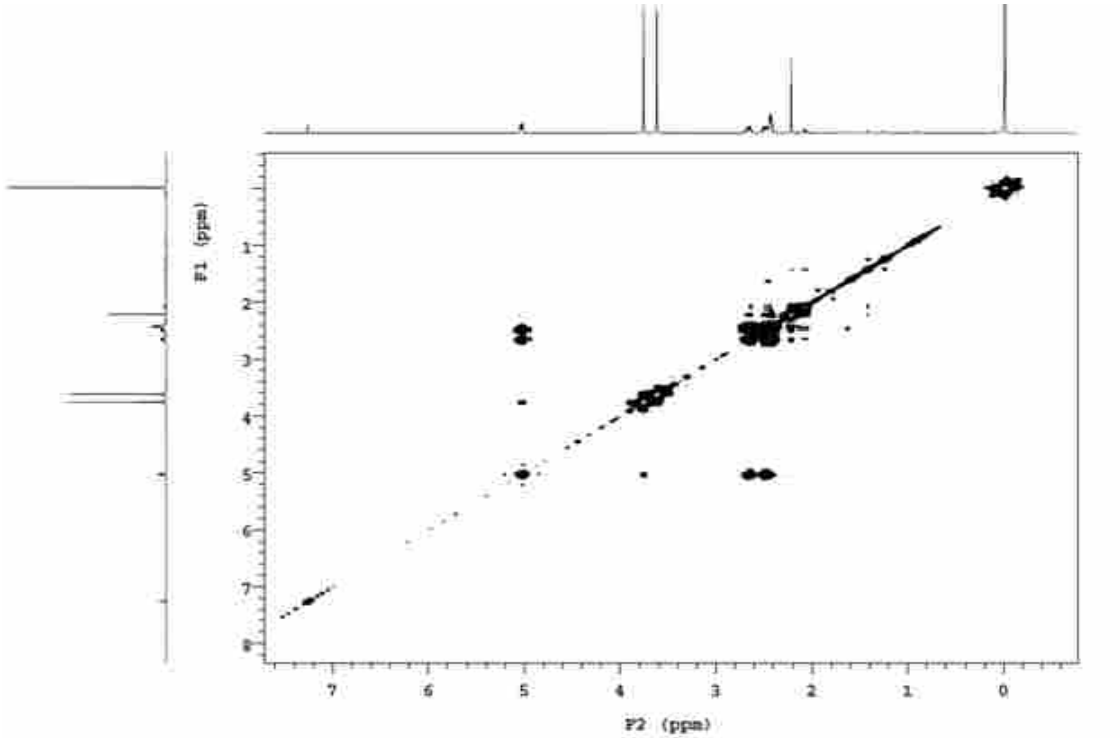

Figure 4 COSY NMR of **GPy** in $CDCl_3$.

2. Characterization of GME and GMA

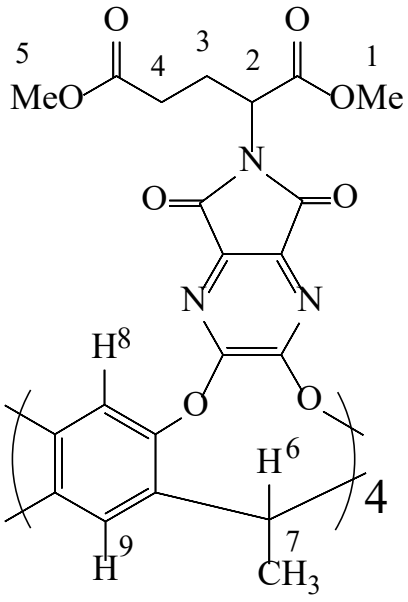

Figure 5 Structure of **GME**.

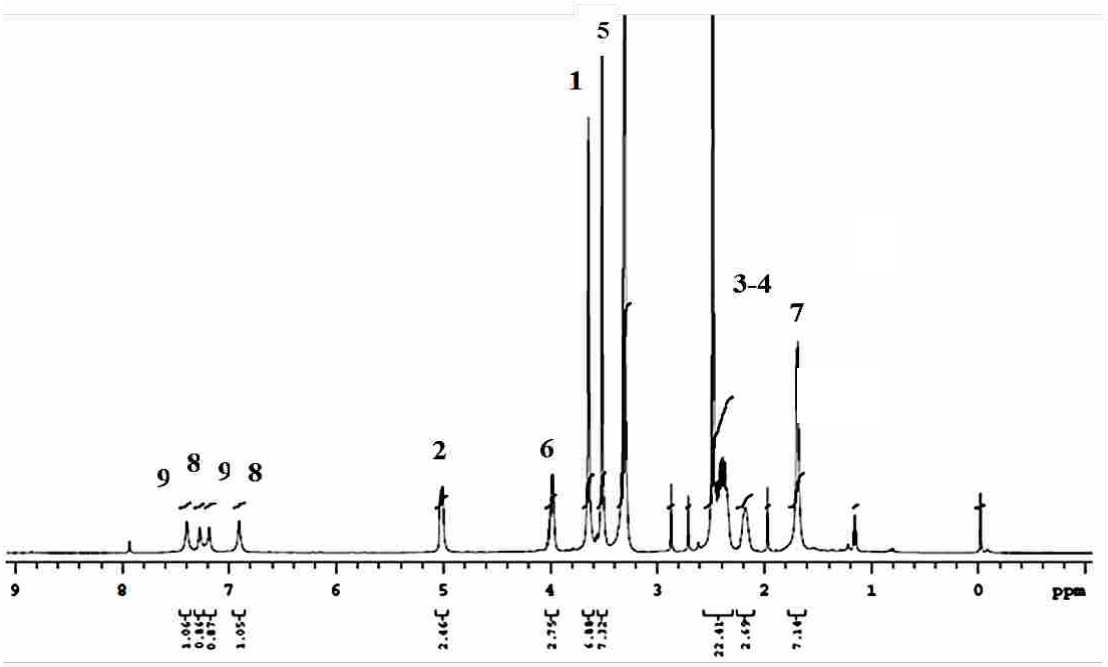

Figure 6 ^{1}H NMR of **GME** in d_6-DMSO.

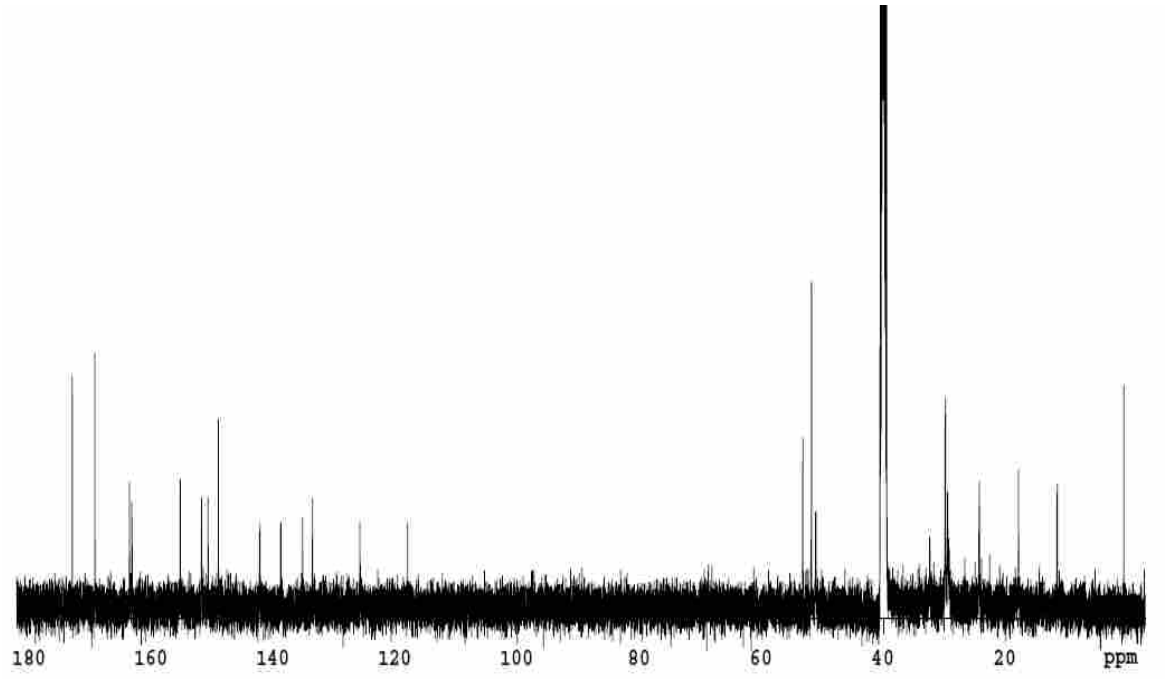

Figure 7 ^{13}C NMR of **GME** in d_6-DMSO.

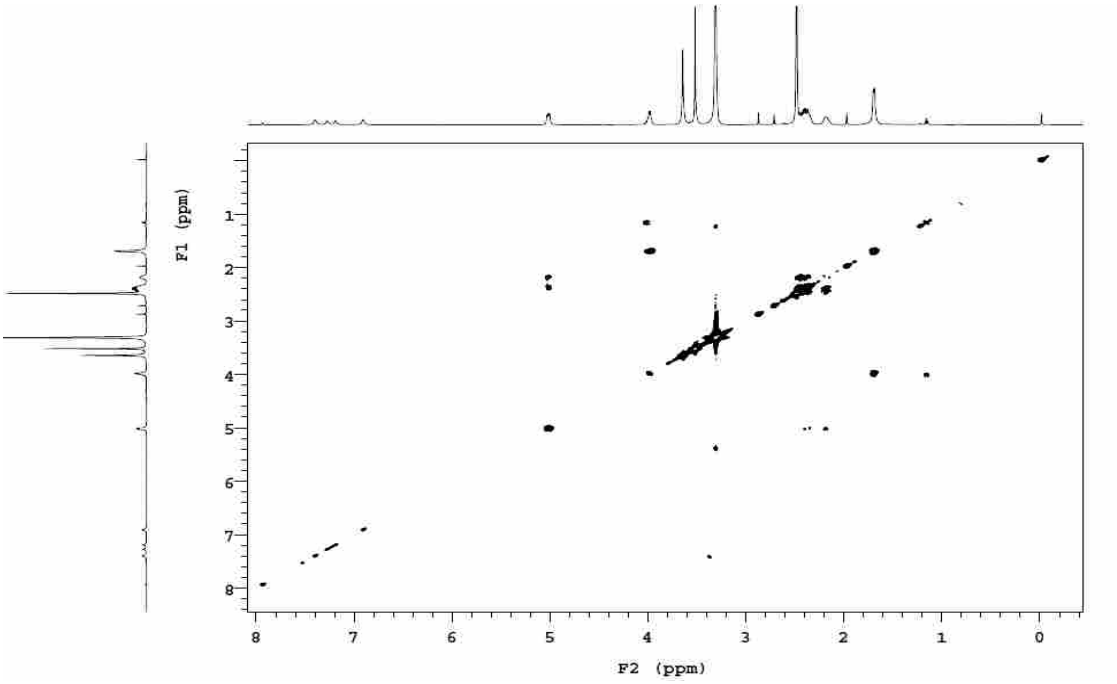

Figure 8 COSY NMR of **GME** in d_6-DMSO.

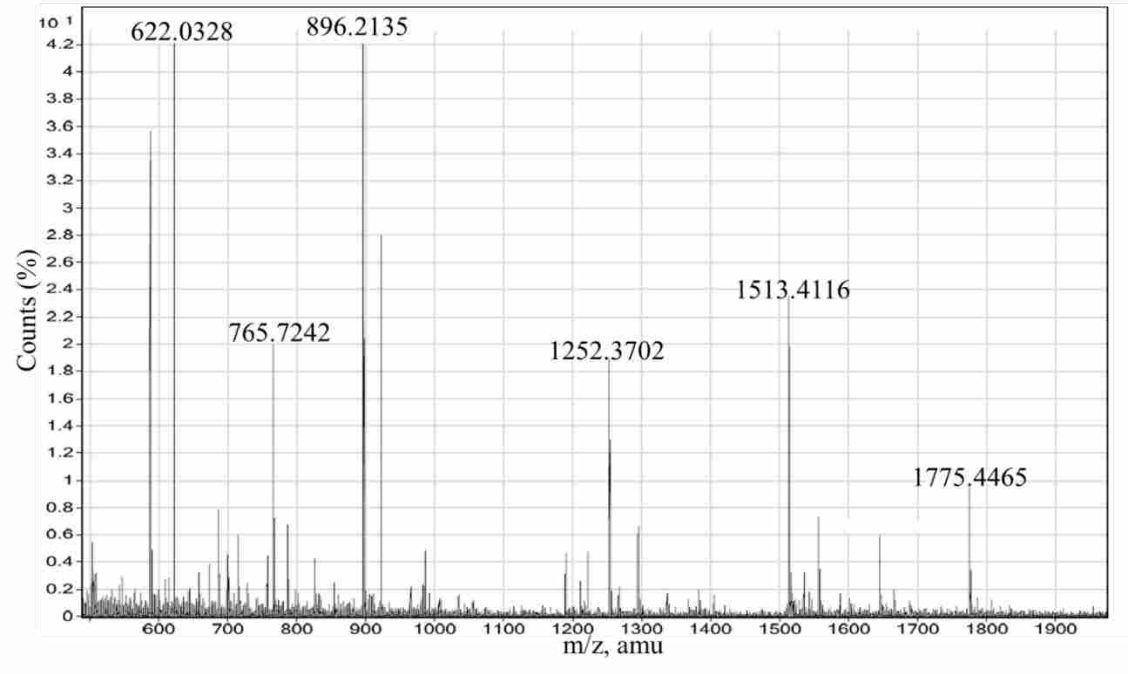

Figure 9 HRMS (ESI) of **GME**, calculated for $[M + H_2O + H]^+$ 1775.5350, found 1775.4465 in acetone.

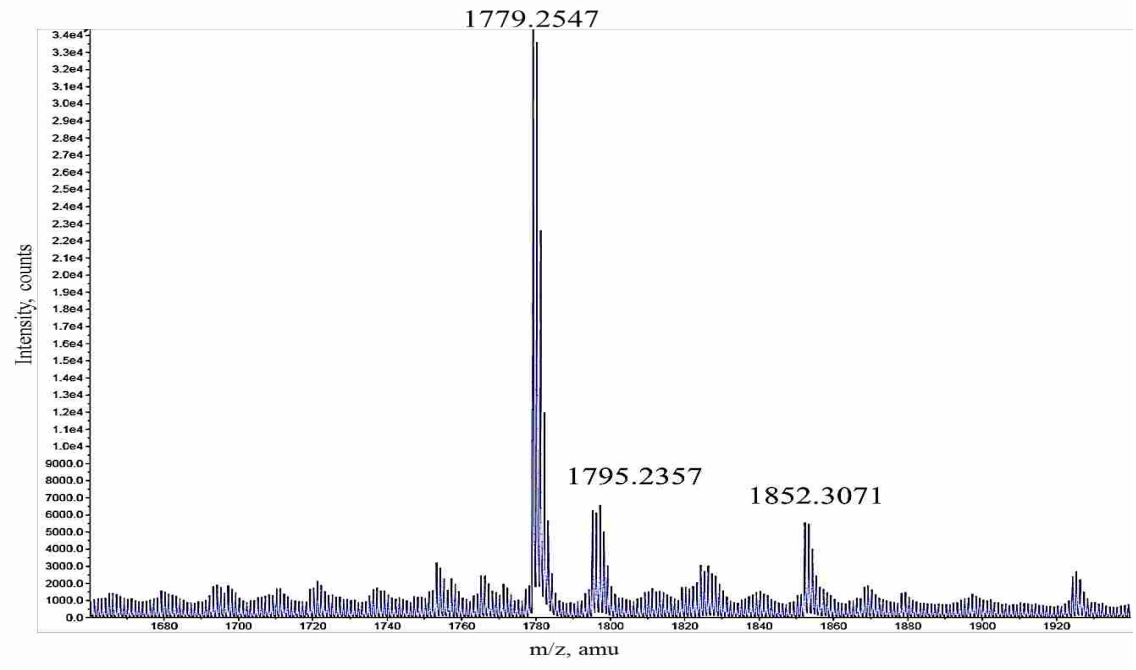

Figure 10 HRMS (MALDI) of **GME**, for $[M + Na]^+$ 1779.3935, found 1779.2547.

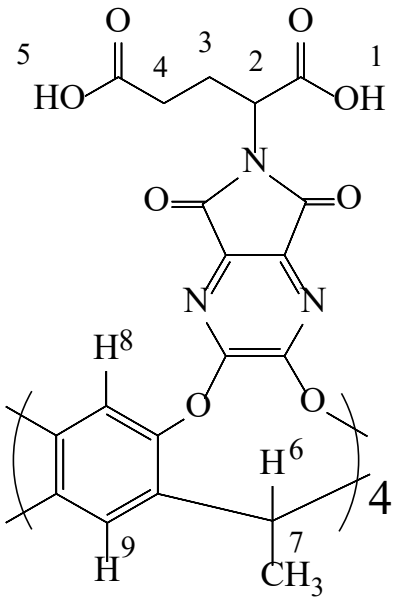

Figure 11 Structure of **GMA**.

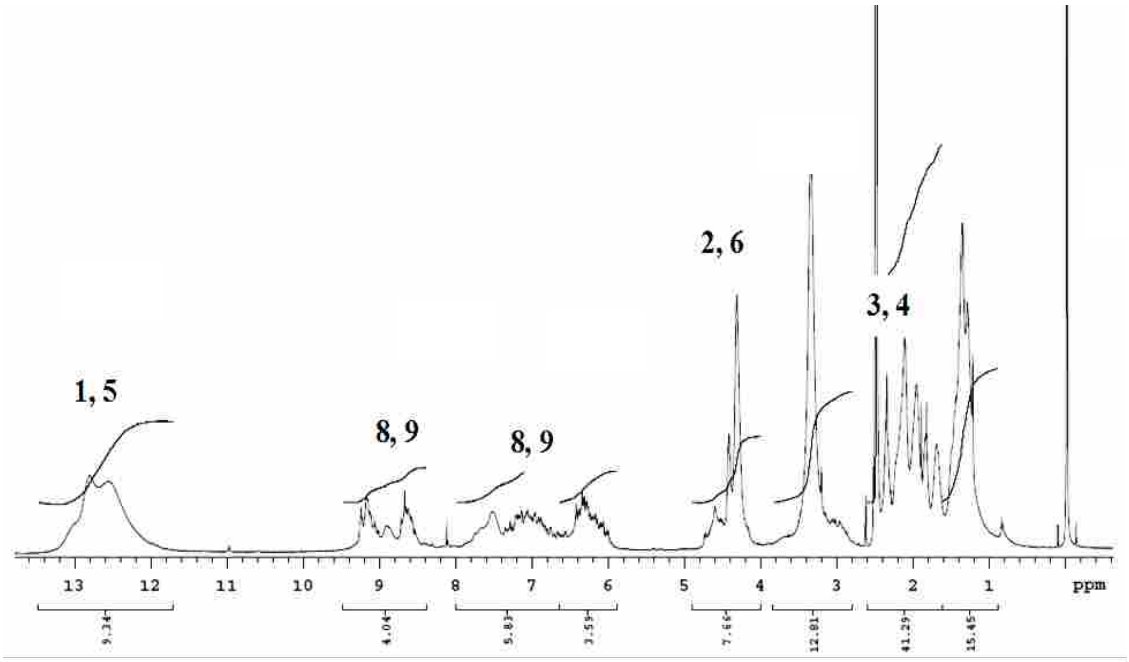

Figure 12 ^{1}H NMR of **GMA** in d_6-DMSO.

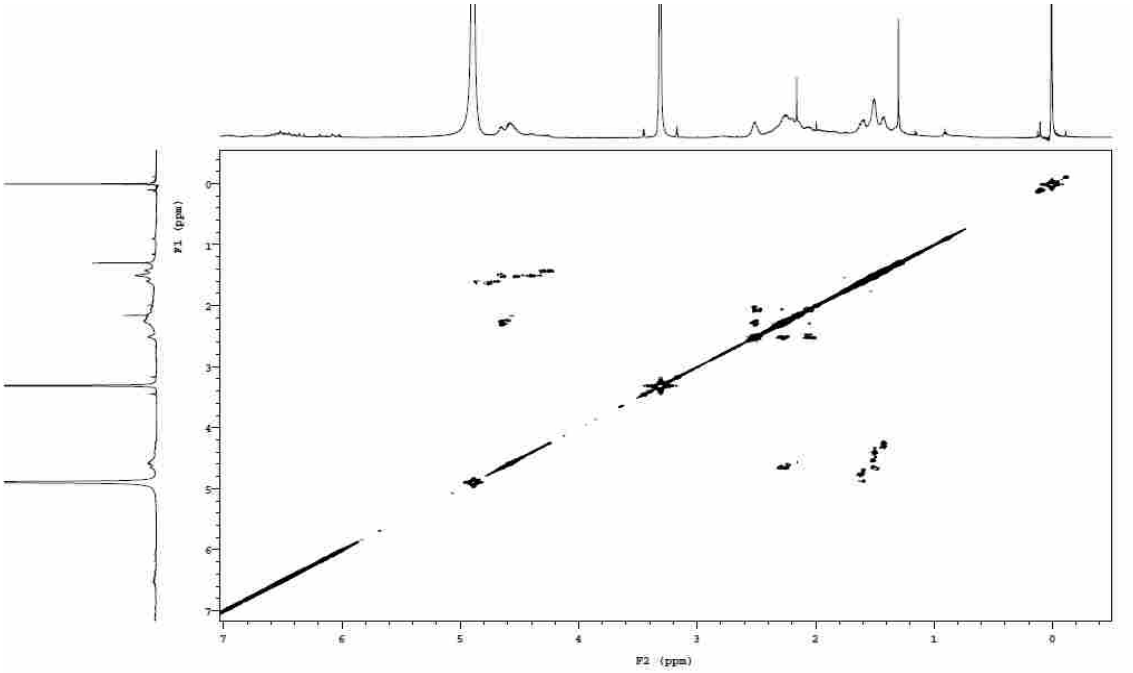

Figure 13 COSY NMR of **GMA** in d_6-DMSO.

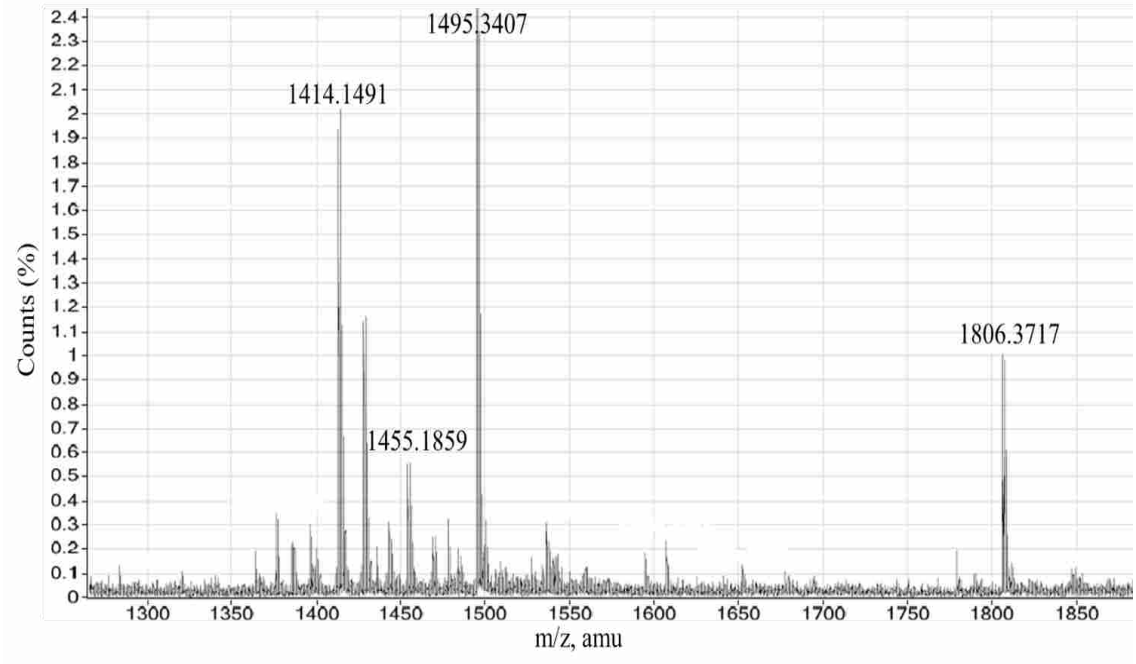

Figure 14 HRMS (ESI) of **GMA** calculated for $[M + 9H_2O + H]^+$ 1806.3877, found 1806.3717.

3. Characterization of GUE and GUA

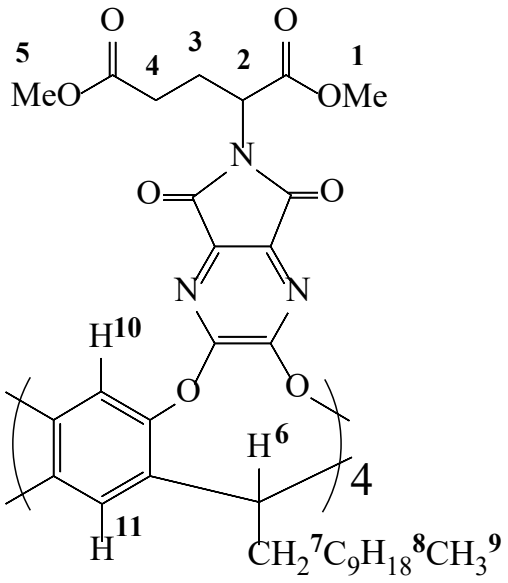

Figure 15 Structure of **GUE**.

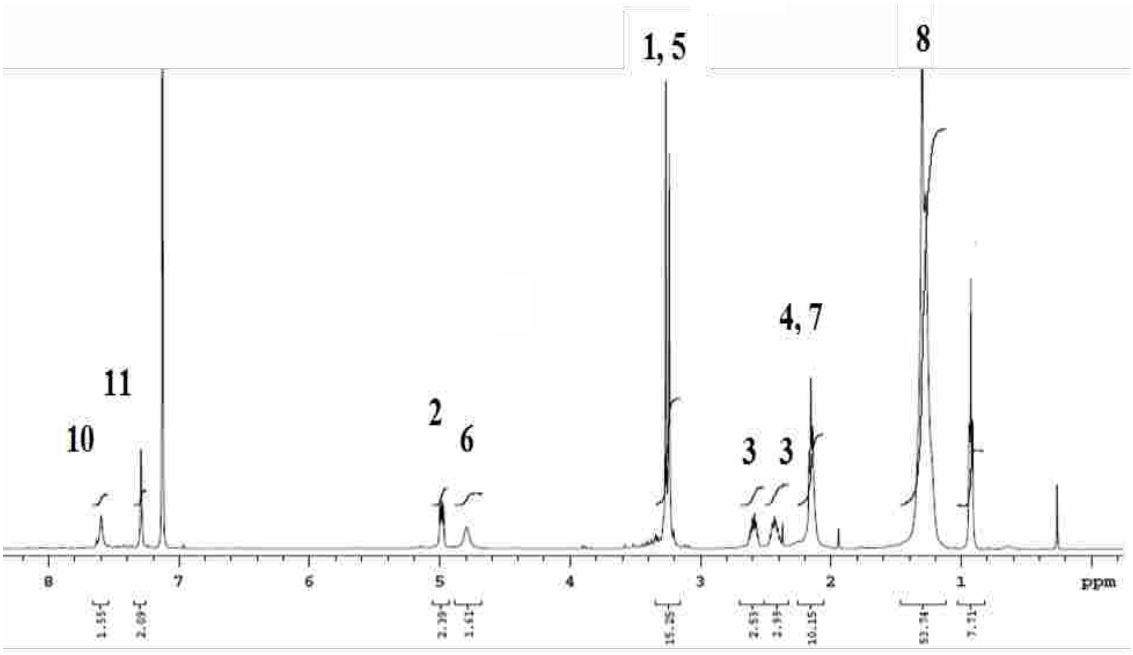

Figure 16 ^{1}H NMR of **GUE** in d_6-C_6H_6.

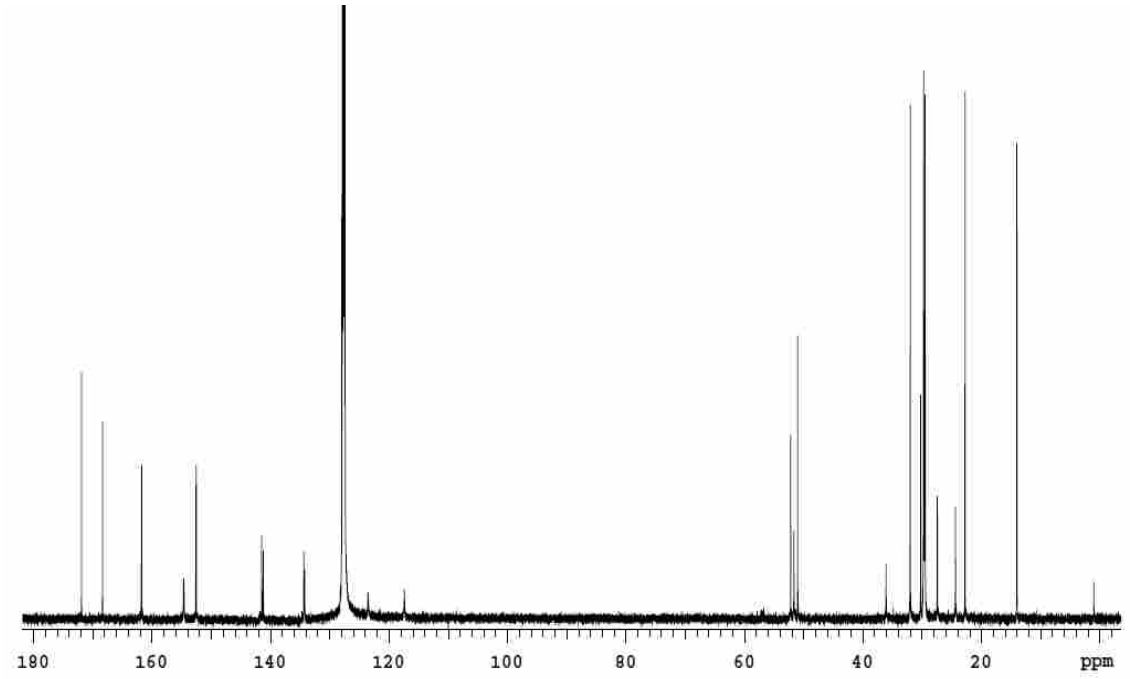

Figure 17 ^{13}C NMR of **GUE** in d_6-C_6H_6.

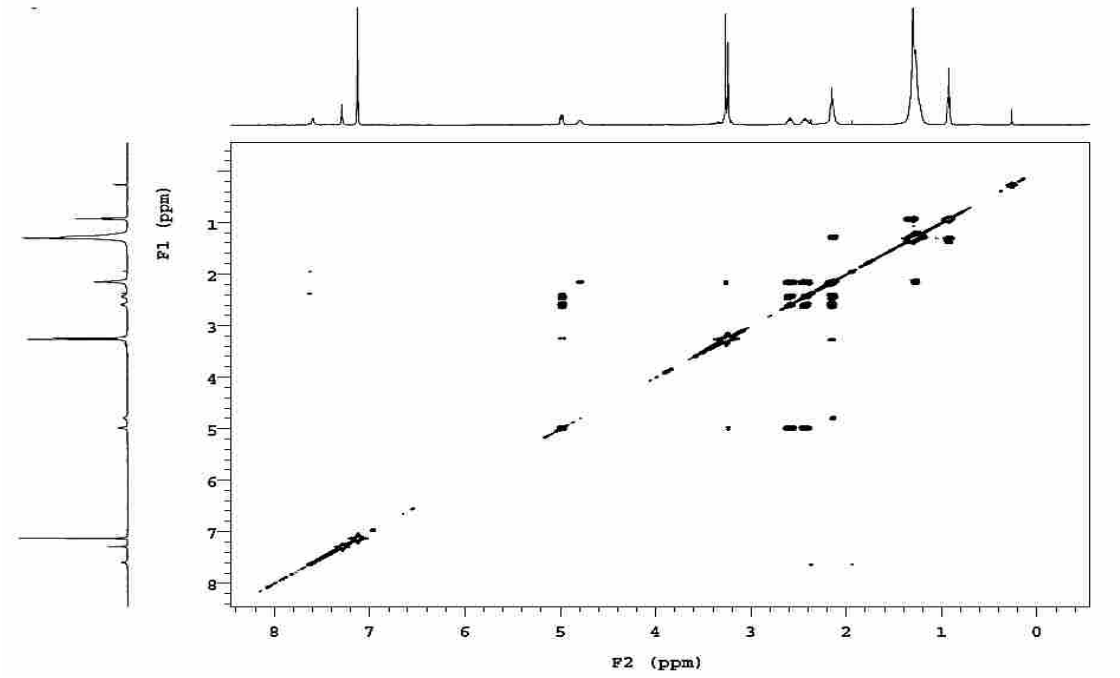

Figure 18 COSY NMR of **GUE** in d_6-C_6H_6.

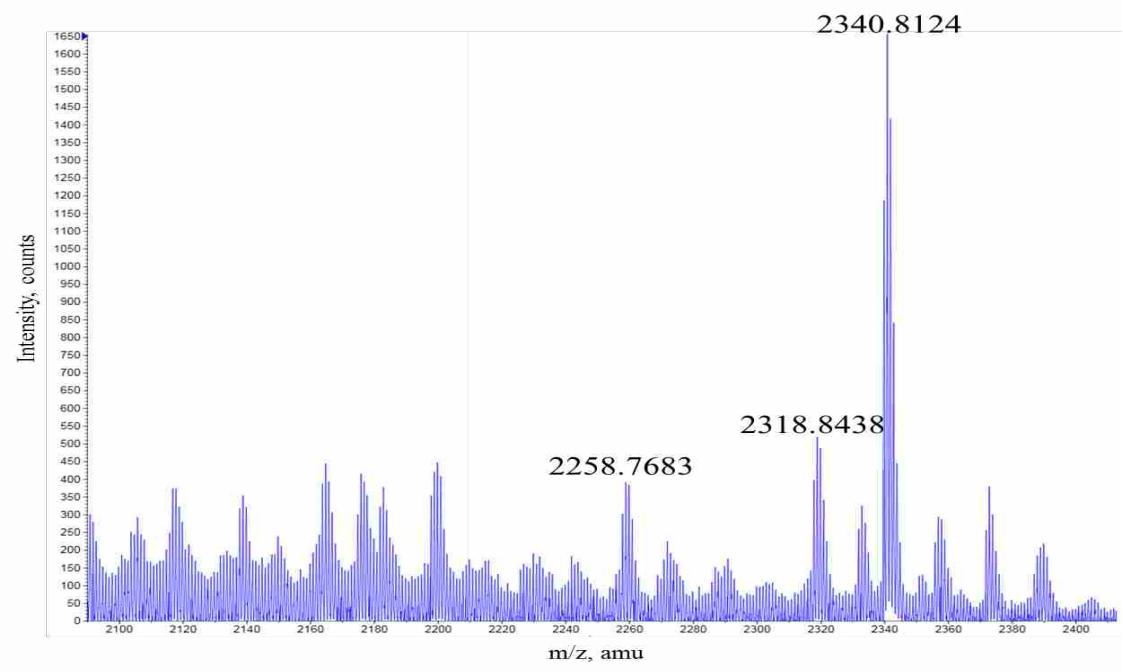

Figure 19 HRMS (MALDI) of **GUE** calculated for $[M + Na]^+$ 2340.0215, found 2340.8124.

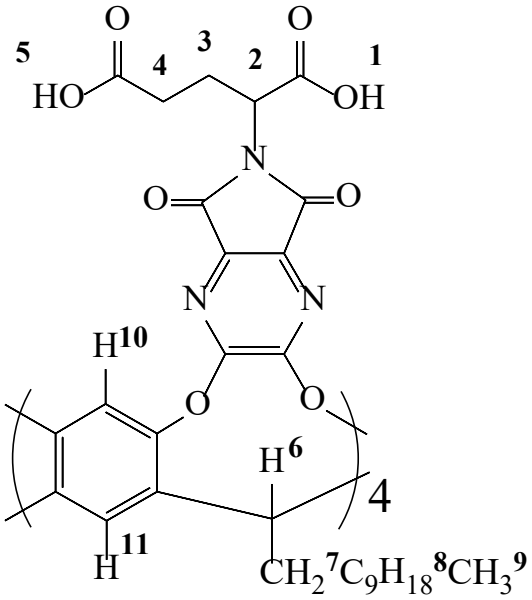

Figure 20 Structure of **GUA**.

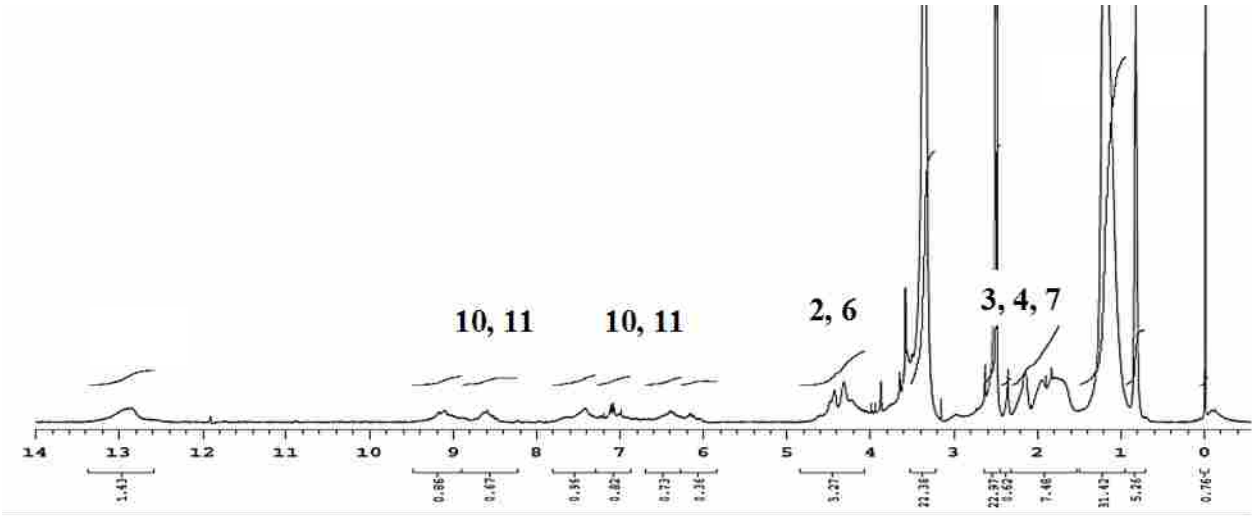

Figure 21 ^{1}H NMR of **GUA** in d_6-DMSO.

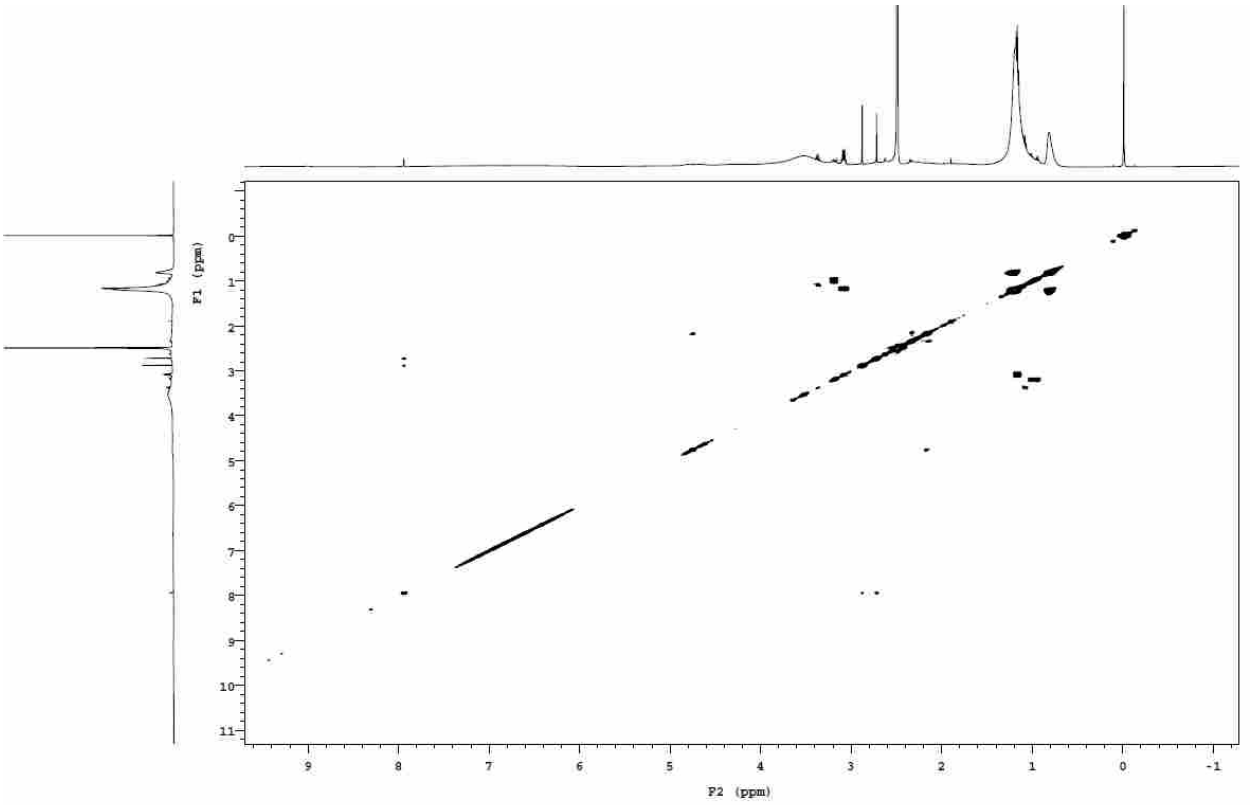

Figure 22 COSY NMR of **GUA** in d_6-DMSO.

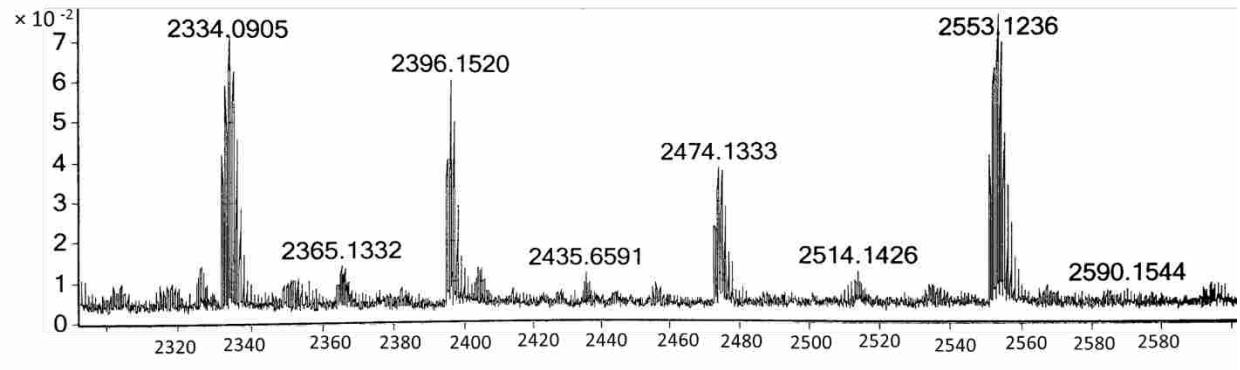

Figure 23 HRMS (ESI) of **GUA** calculated for $[M + 9H_2O + H]^+$ 2368.0055, found 2368.0144.

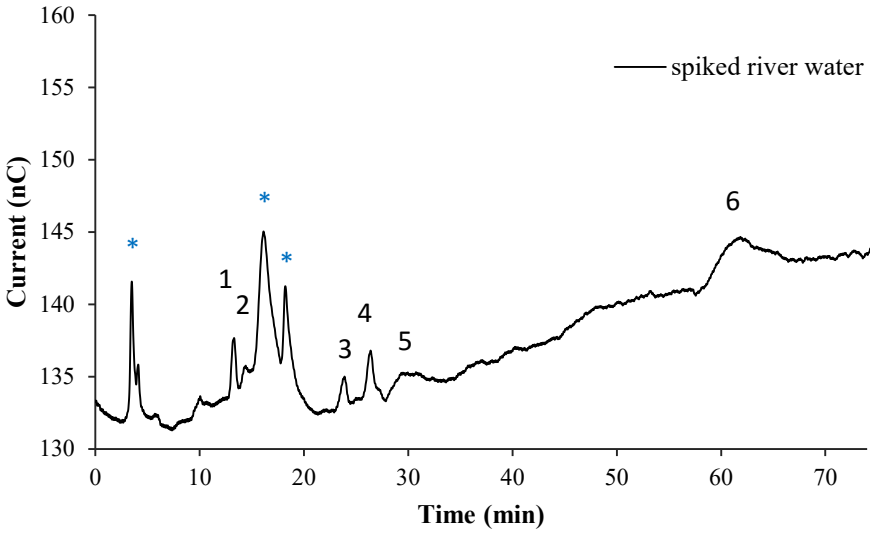

Figure 24 Separation of guanidine derivatives in river water. Peak assignments:1-G, 2-MG, 3-DMG, 4-Agm, 5-GBA and 6- CIM (* matrix peaks). Dionex IonPac CS17 analytical column (4 x 250 mm) and IPAD were used. Conditions: flow rate 0.6 ml/min, column equilibrated 10 min with 3 mM MSA before injection. 0-3 min 3mM MSA, 3-5 min 5 mM, 5-7min 7 mM, 7-9 min 9 mM, 9-11 min 10 mM, 11-13 min 11 mM, 13-15 min 13 mM, 15-17 min 14 mM, 17-19 min 15 mM, 19-21 min 17 mM, 21-23 min 19 mM, 23-30 min 20 mM, 30-40 min 22 mM, 40-70 min 25 mM. Analyte concentrations equal to 75 µg/L.

Table 3 Calibration curves data obtained with ED detection at room temperature with MSA.

Concentration range 1-20 mg/L			Concentration range 0.05-0.85 mg/L			
Analyte	Linear equation	R^2	Linear equation	R^2	LOD (µg/L)	LOQ (µg/L)
G	y = 0.248x - 0.132	0.99	$y = 2.00\times10^{-4}x + 0.00340$	0.99	1.7	5.7
MG	y = 0.196x - 0.0697	0.99	$y = 2.00\times10^{-4}x - 0.00170$	0.99	8.2	27
DMG	y = 0.125x + 0.0005	0.99	$y = 8.00\times10^{-5}x + 0.0299$	0.99	15	52
AGM	y = 0.212x - 0.0419	0.99	$y = 1.00\times10^{-4}x + 0.00360$	0.99	1.7	5.7
GBA	y = 0.0931x - 0.00740	0.99	$y = 8.00\times10^{-5}x + 0.000300$	0.98	5.7	19

a: relative standard deviation was obtained for 3 replications of each experiment

Table 4 Calibration curves data obtained with CD detection at room temperature with MSA.

Concentration range 1-20 mg/L			Concentration range 0.05-0.85 mg/L			
Analyte	Linear equation	R^2	Linear equation	R^2	LOD (µg/L)	LOQ (µg/L)
G	y = 0.248x - 0.132	0.99	$y = 2.00\times10^{-4}x + 0.00340$	0.99	1.7	5.7
MG	y = 0.196x - 0.0697	0.99	$y = 2.00\times10^{-4}x - 0.00170$	0.99	8.2	27
DMG	y = 0.125x + 0.0005	0.99	$y = 8.00\times10^{-5}x + 0.0299$	0.99	15	52
AGM	y = 0.212x - 0.0419	0.99	$y = 1.00\times10^{-4}x + 0.00360$	0.99	1.7	5.7
GBA	y = 0.0931x - 0.00740	0.99	$y = 8.00\times10^{-5}x + 0.000300$	0.98	5.7	19

a: relative standard deviation was obtained for 3 replications of each experiment

Table 5 Calibration curves data obtained with UV-Vis detection at room temperature with MSA.

Concentration range 1-20 mg/L			Concentration range 0.05-0.85 mg/L			
Analyte	Linear equation	R^2	Linear equation	R^2	LOD (µg/L)	LOQ (µg/L)
G	$y = 0.233x - 0.00260$	0.99	$y = 2.00\times10^{-4}x + 0.0122$	0.99	66	220
MG	$y = 1.03x - 0.949$	0.99	$y = 2\times10^{-4}x + 0.00930$	0.99	24	82
DMG	$y = 0.122x + 0.0366$	0.99	$y = 9.00\times10^{-5}x + 0.0358$	0.99	11	34
GBA	$y = 0.0912x - 0.0341$	0.99	$y = 9.00\times10^{-5}x - 0.00460$	0.98	34	110
CIM	$y = 2.29x + 3.15$	0.99	$y = 758\times10^{-4}x + 4.69$	0.98	5.1	17

a: relative standard deviation was obtained for 3 replications of each experiment